Title	A New Nonblocking Optical Switching System for All-Optical Communication Networks
Author(s)	Md.Mamun-ur-Rashid, Khandker
Citation	
Issue Date	2003-09
Type	Thesis or Dissertation
Text version	author
URL	http://hdl.handle.net/10119/946
Rights	
Description	Supervisor:堀口 進，情報科学研究科，博士

A New Nonblocking Optical Switching System for All-optical Communication Networks

by

Md. Mamun-ur-Rashid Khandker

submitted to
Japan Advanced Institute of Science and Technology
in partial fulfillment of the requirements
for the degree of
Doctor of Philosophy

Supervisor: Professor Susumu Horiguchi

School of Information Science
Japan Advanced Institute of Science and Technology

September, 2003

Abstract

Future communication networks will demand a huge bandwidth that cannot be handled by electronic communication networks. However, optics as a carrier of information can handle this huge bandwidth. The major obstacle in this regard is a suitable switching system that can efficiently route optical signals. An all-optical switch networks, in which data remains in the optical domain throughout its journey from source to destination, is central to such switching systems. The present trend to merely embed the optical signal into the existing electronic switch networks cannot achieve the goal of having a huge-capacity switching system because of the different physical properties of optics. Existing switching systems do not scale well for large number of ports when optics is considered as the carrier of information. There are two major problems, namely crosstalk and path-dependent-signal loss, that need to be addressed while designing a switch network with guided-wave technology. Because of stringent bit error- rate requirement of optical transmission facilities, elimination of crosstalk has become an important issue for making optical networks work properly. It is also difficult to handle the path-dependent-signal loss and delay in the optical domain with such a high bit rate - especially if the variation is large. Another practical problem is the cost, since the optical components are very expensive. That is why an all-optical switch network needs to be customized according to different cost-performance requirement of different switching systems.

In this dissertation, an all-optical switching system is proposed in which a new optical switch network will be used in conjunction with an efficient routing technique. The switch network is strictly nonblocking and, theoretically has no path-dependent loss and delay. In addition, it provides constant first-order crosstalk and, therefore scales well. The switch network is constructed by using independent building blocks recursively. Thus, by choosing appropriate building blocks, it can be customized according to the cost-performance requirement of a system . Also proposed are 3×3 and 4×4 wide-sense nonblocking networks as building blocks with novel routing algorithms. Proposed *Distributed Control Routing*, in which *Header* is transmitted through a separate control plane, ensures that *data* remains in the optical domain from source to destination. This switching system can easily be implemented using present technological knowledge.

Acknowledgments

I would like to express my deepest gratitude to my advisor, Professor Susumu Horiguchi, for his support, encouragement, invaluable guidance throughout the course of this work, and most of all for being a good friend. His dedication, prudence, and work of ethics have been a constant source of inspiration. Without his patience and understanding in difficult times, it would most probably not be possible to complete this work.

Many thanks to Professor Hong Shen, my sub-theme supervisor, along with Dr. Xiaohong Jiang, for their constructive criticism and useful discussions which improved my understanding of a problem using mathematics.

I would also like to give a special thank to Professor Teruo Matsuzawa for being my co-supervisor. I must express my gratitude to Associate Professor Toru Abe, Associate Professor Kunihito Yamamori of Miyazaki University, along with Mr. Toshiyuki Asano, and Dr. Yasuyuki Miura of CRL for their relentless help in my early days of Japan. This acknowledgement cannot be a complete one without mentioning the names of Dr. Ryoko Hayashi, and the ever smiling guy, Dr. Masaru Fukushi. They are really assets of this lab. I would also like to thank Associate Professor Yasushi Inoguchi.

The International Student Section of JAIST deserves a big THANK from me. They have duely justified the name by their attainments and deeds.

I owe to the people of Japan who are the tax payers, and whose contribution made it possible for the Japanese government to offer me the *Monbusho Scholarship*. Whatever I have contributed in my Ph. D. work is for them, by them. Whatever good things I have achieved credit goes to them, and whatever I couldn't is my inability, my responsibility.

I owe to my friends and fellows here in Japan who always helped me to their best, and made my life easier.

Along the way, innumerable people either directly or indirectly have provided me knowledge, experience and support. I would like to thank them all.

I am grateful to my wife as well as my children who sometimes have sacrificed their personal likings for me, for my work, and have given me the fullest support.

My parents who have the dream to see me as "Dr. Mamun" will definitely be the happiest persons. Thumbs up to them.

You may wonder how come I became such a lucky person — everything clicked so well! I really believe that I got such a friendly environment because there was a hidden gesture of the almighty Allah. I am really grateful for His mercy.

Contents

List of Figures

Chapter 1

Introduction

1.1 Background

Optical network has become a promising candidate to meet the increasing demands for high channel bandwidth and low communication latency of high-performance computing/communication applications. Switching systems are central components in communications networks. First, they allow a reduction in overall costs by reducing the number and/or cost of transmission links required to enable a given population of users to communicate. Second, they enable heterogeneity among terminals and transmission links, by providing a variety of interface types. Although switching systems have a long history, the introduction of optical signals as the carrier of information has made the researcher rethink on the architecture of the switching systems. Merely embedding the optics in the present electronic switch networks cannot achieve the goal of having a high performance switching system.

Switching systems have two main parts - switch networks and switching algorithm. There are two major problems, namely, crosstalk and signal loss, need to be addressed while designing an optical switch networks with guided-wave technology [1, 2, 3, 4, 5]. Guided-wave technology provides high switching speed, which is also essential for future all-optical switch networks. Lithium Niobate directional couplers can have switching speeds from hundreds of picoseconds to tens of nanoseconds [6, 7]. Conversely, switching speed is of the order of millisecond in the case of mirror-based technology (like MEMs). Another problem is path-dependent path-loss and delay [1]. This problem is serious when the difference of length between longest path and shortest path is large. It is difficult to adjust the gain and the delay of the optical signal in such high bit-rate.

The switching technique in optical switching systems needs special attention. Electronic centralized switching and self-routing technique both fail to cope with the high-speed optics. In case of centralized switching, packets arrived at all inputs are converted into electronic domain and a central-control takes decisions about how to set up paths for all connections. The delay due to conversion of packets and setting up paths is not accepted. The delay also increases as the size of the network increases. On the other hand, packets in self-routing technique contain header and data together. To set up connections, packets need to be converted into electronic domain in all stages of the switch networks. This also causes huge delay. Even if only header is converted into electrical domain, optical data must be delayed appropriately in every stages of the switch network for setting up connections. By now, all-optical self-routing is not possible because optical buffers are not available.

The contribution of this research is a complete new switching system comprised of an optical switch networks with an efficient switching technique - that shows the best-known results. We propose a strictly nonblocking optical switch network, which is constructed by recursive usage of smaller building blocks. The building blocks are independent. They have their own architecture and routing strategies. Any $N \times M$ network can be constructed by building blocks of size $n \times m$. The delay, loss and crosstalk are not path dependent. The delay and the loss are of the $O(\log_2 N)$ and the crosstalk is almost constant, and equal to that of the building block. Although the switch network is strictly nonblocking, the loss, crosstalk and blocking property of the network is bounded by the building blocks, and therefore, scales well. In other words, the cost and performance can be customized by choosing appropriate building blocks.

The concept of building blocks is central to our switch networks. Thus we propose small wide-sense nonblocking (hereafter WSNB) switches as the building blocks with novel routing algorithms. These wide-sense nonblocking networks can establish any new connection without interrupting existing connection like a strictly nonblocking network. Proposed 3×3 WSNB network requires only 4 switching elements - so far the fewest known number. These building blocks drastically reduce the hardware cost of the target network. Results with 4×4 WSNB networks [8] have also been presented in this dissertation. We have also shown how the proposed recursive networks are used in Clos networks to reduce the hardware cost.

Last but not the least, we have introduced a new routing technique, called distributed control routing, which is a combination of centralized-routing and self-routing. In distributed control routing, header is converted into electronic domain only once when it is in the input of the switching system, routed through the network using self-routing algorithm, and appears at the output. Meanwhile, the header generates control signals to the corresponding optical switching elements along the path. Data will be transmitted in circuit switching fashion. An appropriate amount of delay is inserted between data and header to let the switches change their states accordingly. If t_C is the time required to convert optical header into electronic signal, t_S is the time required to setup the state of a switching element and t_P is the time for electronic signal to cross one stage then total delay of data is, $\triangle T = t_C + t_S + O(t_P \log_2 N)$ unlike self-routing, in which

$\triangle T = O((2t_C + t_S)\ \log_2 N)$. In self-routing switch-setup-delays are additive; here they are not. This ensures that data remains in the optical domain from input to output and the delay is similar to the best achievable delay of an electronic signal routing.

1.2 Outline of The Thesis

Chapter 2 explains the necessity of optical signal as the carrier of information. Available and proposed optical devices essential for understanding problems in optical communication networks have also been described.

Chapter 3 addresses the problems with designing all-optical switching system. We focus on switch networks and their routing algorithms.

Chapter 4 proposes a new nonblocking optical switching system. *Recursive Networks* has been proposed for this switching system. Then, *Generalized Recursive networks*, which do not have the limitation of being square networks, have been discussed.

Chapter 5 presents building block structures for Generalized Recursive Networks. Two wide-sense nonblocking networks consisting of fewest known switching elements have been described.

Chapter 6 describes the *Distributed Control Routing* mechanism for routing signals in Generalized Recursive networks.

Chapter 7 evaluates our switching system and presents comparisons with other existing networks.

Chapter 8 shows conclusion and mentions future research opportunities on this topic.

Chapter 2

Optics and Electronic Signals

2.1 Differences and Advantages of Optics over Electronics

The physics of optical and electrical approaches to interconnection are different in any ways. Optics arguably has many potential benefits to offer, and only a few of these have been exploited so far. Notable prior discussions of optics for interconnections and reasons for it include Goodman et al. [9] and the comparison of optical and electrical interconnects by Fledman et al.[10] and [11]. In practice, in both the electrical and optical cases, it is electromagnetic waves that carry the signals (Figure 2.1). It is not electron or other

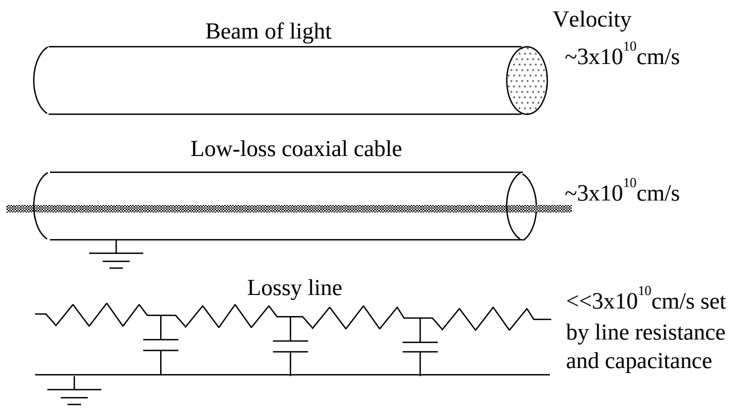

Figure 2.1: Electrical and optical signals in dielectric medium

charge carriers that carry the signals in wires, rather it is electromagnetic waves. That means, the signal do not propagate at the electron velocity ($\sim 10^6 m/s$). In typical electrical cables, the signals move essentially at the velocity of light (or somewhat smaller if the cables are filled with dielectric). We refer to such cables as "LC" lines below. In fact, signals typically travel slightly slower in optical fibers than they do in coaxial cables because the dielectric used in cables has a lower dielectric constant than glass. The real and important basic differences between optical and electrical physics for the purposes of interconnecting electronics can be summed up as in Figure 2.2. The three differences,

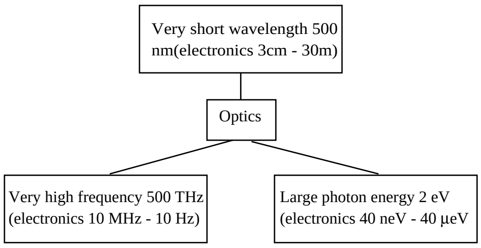

Figure 2.2: Fundamental differences between optics and electronics for communication, expressed in terms of wavelength, frequency and photon energy.

the shorter wavelength, the higher (carrier) frequency, and the larger photon energy, are all aspects of the same difference, since choice of any one of wavelength, frequency, or photon energy uniquely determines the other two. (Wavelength $\lambda = \frac{c}{\nu}$, where c is the velocity of light, and ν is the frequency; photon energy (in the convenient energy units of electron-volts)$E = \frac{h\nu}{e}$ where h is Planck's constant and e is the electronic charge.) For the electrical case, we have shown numbers for photon energies and electromagnetic wavelengths corresponding to a typical practical range of clock frequencies for electronic digital systems, 10 MHz to 10 GHz. In some cases, it is somewhat arbitrary whether consequences are ascribed to the high frequency or to the short wavelength, though the consequences of the large photon energy are clearly distinct.

2.1.1 High Frequency of Light

In electrical interconnections, we generally work at “base band”, i.e., we typically do not use a ”carrier”, but simply turn the voltage on and off. Converting the information so that it modulates a high-frequency (e.g., microwave) electrical carrier is usually sufficiently cumbersome although is used for telecommunications. In optics, on the other hand, we are generally modulating a very high frequency carrier. The high frequency of light has several consequences.

Absence of signal loss and distortion

The carrier frequency of light is very high compared to any frequency at which we can modulate. As a result, modulating the light beam makes essentially no difference to the propagation of light. Only over large distances in fibers do we see dispersive effects resulting from high speed modulation, and optics has negligible additional propagation loss from large bandwidth signals. By contrast, electrical interconnections have very substantial problems of signal distortion at high modulation frequencies [12, 13, 14, 15]. The problems of loss and distortion in electrical lines lead to several difficulties in system design, including the following two specific consequences.

i) Difficulty of "high aspect ratio" architectures

It has recently been realized [12, 13, 14, 15] that there is a relatively general formula for characterizing the number of bits per second, B, that can be sent down simple electrical interconnects given the ISI (inter-symbol-interference) from frequency-dependent loss and distortion. This limit is set only by the ratio of the length l to the cross-sectional dimension $\sqrt{A}$ of the interconnect wiring - the "aspect ratio" of the interconnection (see Figure 2.3). (A is the total cross-sectional area of the wiring). The limit is approximately $B \sim \frac{B_o A}{l^2}$ bits/s, with $B_o \sim 10^{15}$ (bit/s) for high performance strip lines and cables, $\sim 10^{16}$ for small on-chip lines, and $\sim 10^{17} - 10^{18}$ for equalized lines. Such a limit will certainly become a

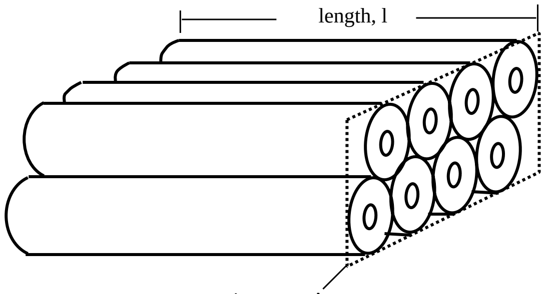

Figure 2.3: Illustration of the "aspect ratio = $\frac{l}{\sqrt{A}}$" of a set of electrical cables.

problem as machines approach Tb/s information bandwidths, and is already easily seen as a practical limit on sending signals down long cables, for example. This limit is scale-invariant - that is, neither growing or shrinking the size of the system substantially changes the number of bits that can be sent - because it only depends on the ratio of length and cross-sectional size. Optical interconnections, however, simply do not have this "aspect ratio" problem at all. First, as mentioned above, they do not have modulation-frequency-dependent loss, e.g., changing the modulation frequency of a signal on a light beam from 1 MHz to 1 GHz makes no difference to the loss experienced by the signal. Second, the loss in optical fibers can be extremely low in absolute magnitude, e.g., 0.2 dB/km in fiber used for long distance communications, leading to negligible distance dependent loss over the scale of interconnect distances. Third, pulse dispersion, though it does exist in optical fiber, is relatively weak compared to metallic cable, and can be compensated anyway. In typical (uncompensated) long-distance fiber, there is essentially zero pulse dispersion at about 1.3 microns wavelength, and at 1.5 microns wavelength (where the loss is minimum), the dispersion is about 15 ps for every nanometer of modulation wavelength bandwidth (corresponding to about 130 GHz of frequency bandwidth) and every kilometer of length. This means, for example, less than 1/10 of a clock period of dispersion for a 6 GHz bandwidth signal over 1 km fiber length. Fourth, optical fiber can be very small in diameter (e.g., 125 microns). As a result, the optical interconnections can readily exceed the bit rate capacity of simple electrical interconnects by at least 9 orders of magnitude for the same cross-sectional area and length [12].

ii) Signal and clock timing

A signal propagating down an electrical line may start out with sharply rising and falling "edges", but these will gradually lengthen from the loss-related distortion discussed above. This "softening" of the edges makes precise extraction of timing information progressively more difficult. This can be a significant problem, for example, when trying to communicate the system clock signal. One source of variability in both loss and signal rise and fall time is the temperature dependence of the resistivity of the metals used as conductors in electrical wiring. For both copper and aluminum, for example, the resistance of a line changes at a fractional rate of about $0.004/^oC$, leading to a 40% change over a 100^oC range. The delay on an RC line and the rise time on an LC line are both simply proportional to the resistivity in the line. By contrast, optical systems have relatively little problem with such variations. There is some variation in the propagation speed of signals with temperature in optical fiber because of the change of refractive index with temperature, which is $\sim -10^{-5}/^oC$. For a 10 m optical fiber cable, the corresponding change in delay over a 100^oC temperature range is only about 30 ps (about 0.07% of the propagation delay).

Absence of frequency dependent crosstalk

Electrical wires become increasingly good antennas at high frequencies, both for transmitting and receiving. This is true whether we consider true electromagnetic transmission and reception, or simply capacitive coupling between lines. Again, because of the high carrier frequency of optics, it essentially makes no difference to any cross-talk in optics what the modulation frequency is, so there is essentially no frequency-dependent cross-talk with optics, a significant feature for high-speed, dense interconnections.

Impedance matching using resonant transformers

There are several differences between optics and electronics as far as impedance matching is concerned. One particular feature of impedance matching with optics results from the fact that optical signals have very small modulation bandwidth compared to the optical carrier frequency; the impedance matching necessary in optics, for example as a light beam has to transition from propagating in air to propagating in a semiconductor or in glass, can be handled relatively effectively using a very simple resonant impedance transformer. The "resonant impedance transformer" in the optical case is an antireflection coating. The classic simple anti-reflection coating is a dielectric layer a quarter wavelength thick, with a refractive index that is the geometric mean of the indices being matched. A simple passive electrical impedance transformer will not work well with broadband modulation, and certainly does not work with "baseband" (i.e., no carrier) modulation that is normal in simple digital electrical interconnections; unencoded digital logic signals may go down nearly to d.c. in their frequency spectrum because they may have arbitrarily long strings of "zeros" or of "ones".

Use of short optical pulses

It is relatively straightforward in optics to generate short optical pulses. The technique of "mode-locking" of lasers can give a repetitive stream of pulses, with pulse lengths in the range of $\sim$ 100 ps to $\sim$ 10 fs, and pulse repetition rates of $\sim$ 100 MHz to $\sim$ 100 GHz. The possibility of using short optical pulses creates some novel opportunities, even when the electronic devices in the rest of the system operate at speeds much longer than the pulse length. One use would be in clock distribution (a concept for which optics is interesting even without the use of short pulse lasers [16]. A central, mode-locked laser could serve as the system clock [17]. The short pulses arriving at clock receivers would give the best possible clock signal to the clock receiver; rather than a slowly rising clock "edge". Based on numbers discussed above, for example, it would appear to be possible to distribute clock signals with less than 30 ps variation over a $100^o C$ temperature range in a system of the order of 10 m in size using optical fiber. The use of output modulators with short optical pulses has two benefits. The first benefit is in the performance of the interconnect link [18, 19, 20, 21]. At the receiver end, the receiver is driven by an impulse, which will generally give much better performance out of the receiver than if it is driven by the usual slowly rising and falling signals [21]. At the transmitter end, we need only drive optical power through the output modulator when it has completed its transition to its desired output state [20]. This gives the most efficient use of optical power since no optical power is wasted driving the modulator while it is still transitioning from one state to another. The second benefit is that the use of short pulses with output modulators can eliminate signal skew. If all of the output signals are read out based on the same short pulse optical clock source, they can all be read out synchronously. Another possibility with short pulse systems is the use of ultrafast devices for time-multiplexing an interconnect for higher capacity. This is currently not yet practical for interconnects, but devices operating on picosecond or faster time scales are feasible in the laboratory [22, 23], and do represent a longer term possibility for the use of optics.

Wavelength division multiplexing

The very high carrier frequency of light also allows the use of multiple different frequency carriers on the same light beam or in the same optical fiber. (In the terminology of optics, it is more common to refer to the carriers as being on different wavelengths rather than on different frequencies, hence the term “wavelength-division multiplexing”.) There is no problem in principle with the use of multiple wavelengths in optics, and laboratory techniques exist for combining and separating them. At the time of writing, various techniques are being developed that may allow practical use of this concept in applications, and the technique is in use in long-distance communications systems. Such wavelength-division multiplexing could increase the capacity of the interconnection system or reduce the amount of cabling required in the system. For example, it could allow interconnection between two-dimensional arrays of devices using only one-dimensional arrays of optical fibers; one-dimensional fiber arrays are currently much easier to align and connectorize.

We will discuss WDM system in more detail later in this chapter.

2.1.2 Short Wavelength of Light

The short wavelength of light leads to the following consequences.

Low-loss dielectric waveguides and optical components

In electrical interconnections, the wavelength corresponding to the frequency of the signal is generally large compared to the cross-sectional size of the wiring that must route the signals within the system. In optics, however, because the wavelength of light is so small, the structures that guide the optical waves can be made larger in cross-sectional dimensions than the optical wavelength (e.g., a 10 micron diameter core in a single mode optical fiber is much larger than the approximately 1 micron wavelength of light). In general, waves are confined and guided using boundaries between materials. At or near the boundary with the guiding material, the guiding material responds sufficiently strongly to the incident wave amplitude to reflect the wave in the desired direction. When a wave is incident on a dielectric material, small oscillatory currents can flow, essentially without loss, as temporary, small distortions (or polarizations) of the electron clouds in the material. Such effects are strong enough to confine waves in dielectric waveguides (such as optical fiber) that are large compared to a wavelength. As a result, we can have extremely low loss propagation of signals in optical fiber, and we can also make low-loss lenses and other optical components that route optical signals in free space. But for the base-band electrical case, where waves must be confined and directed over dimensions small compared to the wavelength, only conducting materials can in practice provide enough current response for the guiding. Conventional conducting materials are lossy, leading to high loss in electrical lines. The loss is usually frequency dependent because of the skin effect, and so also leads to pulse dispersion. Even superconductors, though technically loss-less conductors at d.c., can have significant loss when carrying high frequency signals because the inductive voltage (which unavoidably appears across the line when currents are changing) leads to conventional, lossy conduction as a parasitic process.

Free-space multi-channel imaging interconnects

In electrical systems it is usually unthinkable not to control carefully the information path from source to destination using a waveguide. Certain exceptions exist, where we may make a few wireless connections through free space, but for interconnections at any significant density such free space electrical interconnections are impractical. One reason for this impracticality is fundamentally that the wavelengths of the electrically-driven signals are too long. The laws of diffraction tell us that it is difficult to focus a wave to a dimension smaller than a wavelength. Hence, we could not focus two interconnecting "beams" to different points on a chip or board, allowing us only one interconnection. It is difficult to design antennas that have a broad enough bandwidth to operate with base band modulation (including operating down to d.c.). Free space electrical interconnections could also be very sensitive to cross-talk and to picking up extraneous signals. In optics, by contrast, it is routine simultaneously to image multiple sources on one plane to multiple receivers on another (Figure 2.4). The fundamental reason that makes this possible is the short wavelength of light; even with relatively simple optics, it is possible to image thousands of outputs on one surface to thousands of inputs on another, with spot sizes on the order of several (e.g., 10) wavelengths in size. Optics therefore allows very large

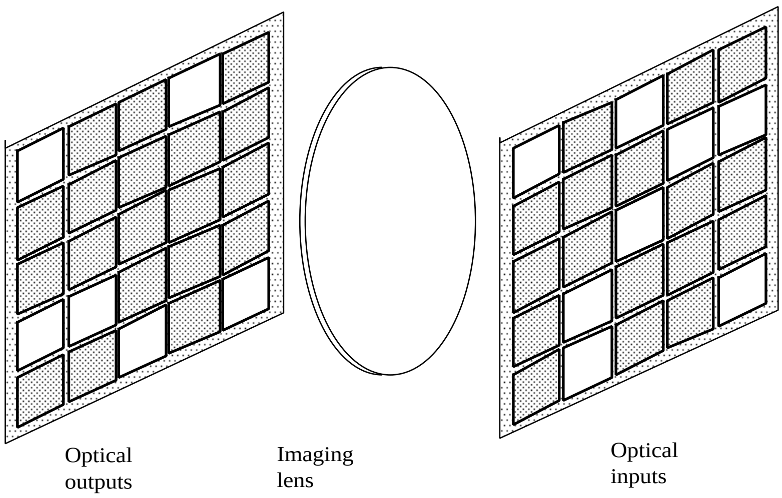

Figure 2.4: Concept of imaging arrays of outputs on one plane to arrays of inputs on another.

numbers of connections from one plane to another through "free space". Another related consequence is that it is possible to make very global interconnect topologies (such as so-called "perfect shuffles" [24], crossover networks [25], Banyans [26], and sliding Banyans [27]) in which many of the "beams" cross through one another. It is also worth noting that free space interconnections need not actually be in open space; they could take place essentially entirely within solid, rigid glass structures, for example. In free space, light beams can pass through one another with no interference of any kind.

Beamsplitters without back reflection

It is very often desirable to be able to make multiple connections to a given signal line so that the same data can be made available to multiple parts of a system. Once we are working at clock frequencies sufficiently high that the wavelength associated with the clock frequency is comparable to or smaller than the size of the system (e.g., the length of the backplane), we cannot, however, neglect wave reflections. Any simple attempt to plug in additional connections leads to wave reflections from the connection. In free space optics, however, it is straightforward to use a beamsplitter to split out any fraction of the beam without any back reflections (though, of course, the power transmitted through the beam splitter is reduced accordingly). One reason why this works is that the physical processes that divide the beam (usually partial wave reflection off of an interface) effectively divide both the electric and magnetic components of the wave by the same factor, retaining the correct impedance ratio between them; no back reflected wave is required to satisfy boundary conditions. In principle, this kind of perfect beamsplitting is also possible in certain kinds of waveguides, both optical and microwave.

Fan-in

A problem that is shared by both electrical and optical connections is the difficulty of combining independent signals without fundamental loss. In both the electrical and optical cases, it is difficult to combine N channels to one input without sustaining a $1/N$ power loss. In electrical systems, it is therefore usual to perform the fan-in logically rather than physically, sending each input channel to a separate logical gate input, and rather than trying to perform a simple "wired-OR" function physically without logic gates. It is indeed possible to combine N inputs without power loss into one photodetector, for example by bringing the N beams at N distinct angles or onto N distinct positions on the photodetector. The catch is that the photodetector then needs to be N times larger in area than it would have to be for only one beam. The larger detector area required for "loss-less" beam combination tends to reduce the electrical response of the detector proportionately also. Consequently, the voltage induced on the photodetector for a given input beam power (and hence photodetector current) will also be reduced. Hence, there is little or no benefit in terms of useful power transfer efficiency by trying to use a larger photodetector with "loss-less" beam combination. It is, or course, quite legal to combine different wavelengths without loss since the different frequencies represent different physical modes, and use of such wavelength techniques is a possible advantage of optics.

2.1.3 Large Photon Energy of Light

The most important single physical consequence of the large photon energy in optics is that, for essentially all of the situations of importance here, light is generated and detected quantum mechanically, whereas electrical signals use classical generation and detection. For example, detection of light in practice involves counting photons, not measuring electric field amplitudes. A typical semiconductor photodiode will generate one electron of current for every absorbed photon, with the electron of current resulting from the quantummechanical absorption of a photon to create an electron-hole pair. Similarly, a relatively efficient laser diode will generate one photon for every few electrons passed through the diode, with each photon resulting from the recombination of an electron and a hole. In contrast, electrical signals are carried on voltages or currents, which effectively are respectively the statistical average potential energies and flow rates of classical "gasses" of electrons. Changes of these average potentials or flow rates at the receiving device cause changes of average potentials or flow rates in "gasses" of electrons inside the receiving device. The fact that the photon energy of light is so large has two specific consequences for optical interconnections

Voltage isolation

Detecting photons allows us to generate currents and voltages without any direct electrical connection with the light source, yet still with a band width that extends down to d.c. as required for logical interconnections. This already solves an important problem in electrical systems, and is exploited extensively in so-called "opto-isolators", which usually contain a light-emitting diode (connected to the "transmitting" circuit) and a photodiode (connected to the "receiving" circuit).

Quantum impedance conversion

As discussed above, essentially all electrical signal lines have both high capacitance per unit length (1 - 3 pF/cm), and low impedance (30 - 100 ohms). This creates a problem for electronic circuits, illustrated in Figure 2.5. Use of optical emitters or modulators and photodiodes fundamentally enables us to avoid the problems of the low impedance of electrical transmission lines [28], as illustrated in Figure 2.6. The reason why optics can avoid the low impedance problem is that the voltage generated in a photodetector bears no particular relation to the classical "voltage" in the light beam. It is quite possible, for example, to generate 1 V in a photodetector from a light beam with 600 microvolts of classical voltage - a consequence, fundamentally, of the photoelectric effect. The emergence of quantum well modulator technology has, however, led to quite practical low power optical output devices that can demonstrably send digital signals from chip to chip

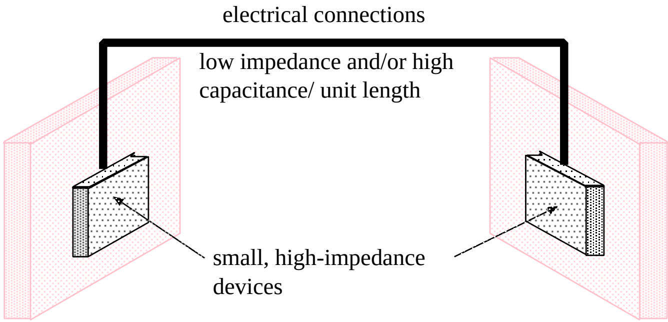

Figure 2.5: A small, high impedance, low power electronic device that wishes to communicate to another similar device, for example on another chip, is forced to use an electrical line with low-impedance and/or high capacitance per unit length. Line drivers with low output impedance and high power dissipation are the typical solution.

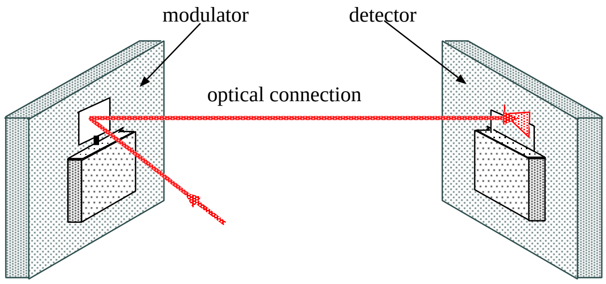

Figure 2.6: Optical devices can effectively match the impedances between the electronic logic devices because they use quantum detection and generation. The photodiode generates one electron of current for every absorbed photon. Electroabsorptive modulators tend to pass one electron of current for every photon modulated. Efficient laser diodes would also emit one photon for every electron of current in principle.

with substantially less power (e.g., < 6 mW total dissipation at 375 Mb/s) than electrical connections [29]. This feature of optics is likely to be particularly important for large arrays of optical inputs and outputs, and may allow much larger amounts of information to be sent on and off chips optically than is practical electrically. One recent study [30] has predicted (implicitly using the benefits of quantum impedance conversion) that dense optical interconnections directly in and out of silicon chips will have an interconnect capacity that will be able to track the ability of advancing silicon technology to perform logic operations, and to achieve information flows exceeding 1 - 10 Tb/s on and off a single silicon chip.

2.2 Optical Devices

Optical devices include optical amplifier, attenuator, connector, tunable laser and filter, wavelength mux/demux, switching elements optical cross-connect (OXC) etc.

Semiconductor optical technology is emerging as a leading technology for building high-speed systems. Based on this technology a number of high-speed optical devices such as optical bidirectinal couplers, self-electrooptic effect devices (SEEDs), optoelectronic intefrated circuits and interference filters using logic etalons (OLEs) have been experimentally demonstrated. These devices can provide extremely high data rates and a very large number of parallel channels.

2.2.1 Switching Optical Signals

The equipment available for switching optical signals today is of the hybrid optical-electronic-optical (O-E-O) type, which is expensive to build, integrate and maintain. As a result, these switches have not been widely deployed. O-E-O switches separate incoming optical signal into individual wavelengths (optical demultiplexing), convert each wavelength into a single high-speed electronic data stream, and demultiplex the high-speed streams into many low-speed channels. They then route each channel path digitally, combining (multiplexing) groups of low-speed channels into high-speed streams and modulating each high-speed stream onto an optical wavelength. Finally, through optical (wavelength-division) multiplexing, they place many of the optical wavelengths onto an optical fiber. Since there is no optical path from input to output, these switches are called "opaque". The advantages of this approach are powerful. Since each data stream has been converted to electronic form, each stream can be monitored and dynamically routed independent of all the others. But the drawbacks are equally formidable. Not only are O-E-O switches expensive, they also incapable of handling signals that do not conform to standard data rates and formats. They consume kilowatts of power. And, although an O-E-O switch can route individual packets, it requires a variable amount of time to read and interpret a received packet's header information, and then to deliver the packet to the correct output channel. Thus the result is a delay, or latency, that can range from microsecond to hundreds of milliseconds. This variable delay may constitute a fatal shortcoming in the future, when even real-time traffic like voice and video will be carried over packet-switched networks. Certainly it can be devastating to streaming multimedia communications. What the communication industry is crying out for are all-optical (also called photonic, or transparent) switches in which data remains in the optical domain from source to destination. Several approaches are being explored for making the necessary devices. These include array of tiny movable mirrors, known as microelectromechanical systems, or MEMS, and units based on liquid crystals, optical waveguide technology, total internal reflection etc.

Bulk optics

The most mature approach available is precision bulk optics, which creates robust connections. The technology takes many forms - for example, having a motor nove a precision mirror surface to direct an input light beam from one output to another. Examples are lucent technologies' original direct beam-steering technology, DiCon Fiberoptics' moving prisms, and Lightpath Technologies' rotary switches. These switches have low loss, reflection and crosstalk because they rely on highly mature manufacturing techniques. But they are too expensive, too large, and too slow.

Mach-Zehnder interferometers

Mach-Zehnder Interferometers (MZIs) form the next most mature O-O-O switching technology. The MZI method splits incoming light into two beams, routing each beam along a different path, and then recombining them to form two outputs. If the phase is varied on one of the two paths by changing the speed of the light along the path, the fraction of the input light sent to each of the outputs can be controlled. Changing the phase from 0 to 180 degrees shifts all the light from one output pot to the other. The speed of light along a path can be changed by having the path traverse a material in which the speed of light is a function of temperature or the strength of an applied electric field. Varying the temperature or the field strength creates what are known, respectively, as *thermo-optic* or *electro-optic* switches. Advantages are: reliable, fast and integrates well with others functions. Example: JDS Uniphase's PIRI subsidiary, a 2×2 switch. Drawbacks: The paths must be fairly long - on the order of a centimeter - because the speed of light can be changed only slightly (less than 0.01%) by reasonable changes in electric field strength or temperature. This size constraint restricts the technology's scalability, limiting it to about 40 ports. The fundamental operation principle also limits the isolation and crosstalk performance for wide-band channels because the two paths will cancel perfectly only at a single wavelength, and modulating a carrier broadens its spectrum - the higher the modulation rate, the broader the spectral line.

Directional couplers

Directional couplers (DCs) are built on waveguide technology. DC consists of two waveguides placed very close together for a length L [31]. The overlap of the evanescent fields of the two waveguides causes light energy to exchange between them with a coupling coefficient per unit length k, where k is a function of the waveguide dimensions and parameters, the spacing between them, and the wavelength of the light. Complete light transfer is accomplished when the waveguides are fully phase matched, which means $\triangle\beta = \beta_1 - \beta_2 = 0$. The propagation constant for a given waveguide can be written as $\beta = \frac{2\pi N}{\lambda}$ where N is the effective refractive index of the guide mode and λ is the free-space optical wavelength [32]. In addition, the interaction length has to satisfy the condition $L = (2n+1)l$, where n is an integer, and l is the coupling length. A switch can be constructed by inducing a phase mismatch $\triangle\beta$ between the waveguides as shown in Figure 2.7. The

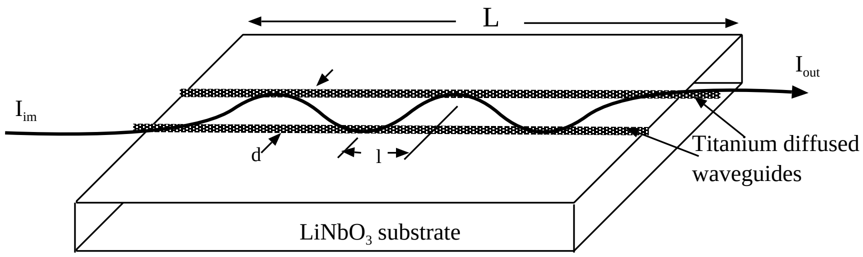

Figure 2.7: Illustration of the optical energy from one waveguide to the other. Here $\frac{L}{l} = 5$.

phase mismatch can be induced electrically by fabricating the Directional Coupler on an electro-optic material, like LiNbO3 [32]. Optical switching of the Directional Coupler is also possible through the free-carrier induced changes in the index of refraction and through semiconductor electron-hole pair generation. However, it is virtually impossible to construct a directional coupler switch/modulator with sufficient tolerance to eliminate the crosstalk completely. This limits the ultimate size of the switch networks to be fabricated on a single topology. The strength of Directional couplers is their ability to control extremely high bit-rate information. Also has got importance for suitability in integrated circuit fabrication. The implementation of large space switch requires the interconnection of many such Directional Couplers.

i) Current System Design Constraints

The purpose of this section is to outline the main issues that need to be addresses when a switching system is based on Ti:LiNbO3 Directional Couplers.

a) Voltage Requirements: Voltage is required to change the states of the switch. In practice, for a uniform dB switch there may be a low bias voltage required for the cross state. This cross state voltage can vary from 0 to $5V$ for a single-polarization device [33]. For a polarization independent device using a reversed $\triangle\beta$ electrode configuration, the cross state voltage can be as high as $\pm 25V$ [34]. For a single polarization devices the bar state voltage will be $\approx 15V$ if $L = l$ [33]. On the other hand, the polarization-independent devices require voltage as high as $100V$ [34]. One method that can be used to reduce the applied voltage is to increase the length L.

b) Switching efficiency: One of the most important parameters in the design of switching systems based on Directional Couplers is the switching efficiency. The switching efficiency is the magnitude of the ratio of the output power when the device is in the cross state to the output power when the device is in the bar state. Another commonly use term is crosstalk, which is the ratio of the power in the unselected waveguide over the total input power. At present the switching efficiencies for polarization-independent devices are smaller in magnitude that single-polarization devices. Sing-polarization devices have reported switching efficiency as large as 40 dB while polarization-independent devices have only achieved 25 dB.

c) Single-polarization versus Polarization-independent Devices: The advantage of polarization independent system is that standard single-mode fiber can be used. The major disadvantage of a polarization-independent system is that higher voltage is required for the Directional Coupler. When the high-speed switching is desired, it will be difficult to switch at these higher voltages. The advantages of a single-polarization system include lower voltages required for their operation, smaller bend radii (TM polarization), and a simple design and fabrication process which should allow for more optimization. The major disadvantage of single-polarization devices is that polarization-preserving fibers will be required [35].

d) Switching Speed: The switching speed of a Directional Coupler is limited by the capacitance of the electrodes. For the electrodes that have been described, the capacitance can be approximated to be $C = \epsilon L$ where $\epsilon_r \approx 35$ is the dielectric permittivity of the crystal [32]. Thus, the capacitance of these electrodes is on the order of 1 pF.

   Higher speed electrodes have been developed based on travelling wave electrodes that have successfully modulated optical signals at a rate of 14 GHz [6, 7].

e) Drift: One potential problem with $Ti : LiNbO_3$ directional couplers is that the output optical power can migrate from one waveguide to the other when a fixed voltage is placed on the electrodes. This migration of power is referred to as *drift* [36]. Devices with effective coatings of SiO_2, about 200nm in thickness, have been demonstrated with little or no drift.

f) Intercoupler Interference: Intercoupler interference occurs when two or more couplers are fabricated in such close proximity that a applied voltage on one devices can alter the transfer efficiency curves of the the other neighboring couplers. Proper ground plane layout can eliminate this potential problem.

g) Device Uniformity: It is desirable to have all the couplers on a substrate have the same characteristics. The tunability required for variations adds to the complexity of the electronics.

Microelectromechanical systems(MEMs)

MEMs are small mechanical devices built using semiconductor fabrication technologies that provide small size, precision, repeatability, and low cost in high volume. The simplest use a single microscopic moving mirror to redirect the light. This creates a single pole double throw (1×2) switch. These states can be implemented in two ways: by covering and uncovering the beam path using a sliding, fixed-orientation mirror or by swinging a tilting mirror between two precision angular stops. These switches can be arranged in a two dimensional array to form a matrix switch (Figure 2.8). The more challenging and complex implementation will be to build a 3-D switch. Limits to the scaling include the diameter of the mirrors and their maximum tilt angle. The mirror should be about 50% bigger than the optical beams to avoid excessive loss; and tilt is limited by both the method used to build the switch and the technique used to actuate the mirror. The main drawback is the switching time. The typical switching time for MEMs is 4ms.

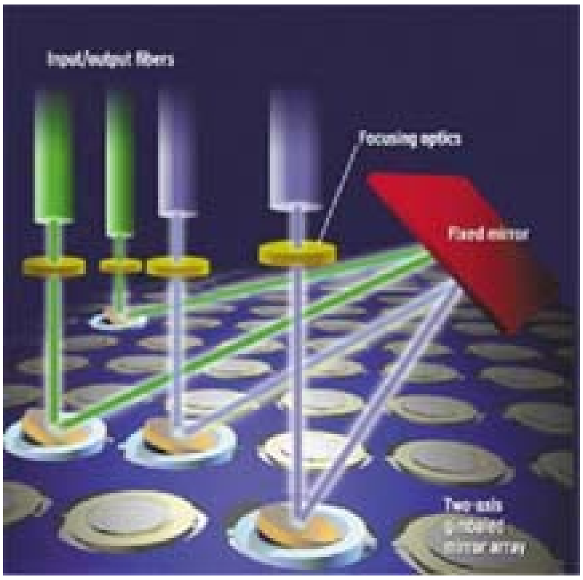

Figure 2.8: A two dimensional MEM structure

Multiple quantum-well switch (MQW)

By sandwiching a low bandgap material such as GaAs between two high bandgap material such as AlGaAs, a quantum well in the macroscopic level is formed. Electrons and holes in the material tend to become confined in the region of the low bandgap material where the potential energy is low. Light is absorbed when the photon creates an electron-hole pair bound together in an excitonic state. By switching on and off an electric field, the transparency of the quantum well can be modulated at that particular wavelength of light. This is called the quantum-confined Stark effect (QCSE). This electroabsorption effect is approximately 50 times larger than that of bulk semiconductors. Unlike switches made of $LiNbO_3$ technology, multiple quantum-well switches utilize orthogonally intersecting waveguides and have relatively small interaction regions. The MQW switch is comprised of two orthogonally intersecting quantum-well rib waveguides on a silicon substrate [47], as shown in Figure 2.9. Switching occurs within a nonlinear modulation region at the

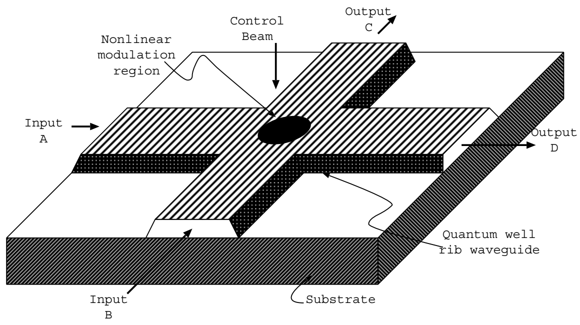

Figure 2.9: An MQW switch.

junction of the two waveguides. This modulation region is approximately the same size as the width of each of the two waveguides, approximately 5-mm to 10-mm [47, 48]. Switching function can be activated either optically or using electric field at the junction. Using MQW switches, it is reasonable to achieve a waveguide spacing, G, of 10 mm, which corresponds to approximately n=1,200 waveguides per layer.

Acousto-optic switch

An acousto-optic tunable filter is a four part device (2 inputs, 2 outputs) in which the coupling between the two inputs is responsive to the intensity and frequency of an acoustic wave impressed across its interaction region. A very important distinction between an AOTF and waveguide switch is that the coupling is wavelength-sensitive. To effect a certain coupling between applied signals at wavelength λ_A, an acoustic signal of a particular frequency (in the range of about 100 MHz) must be applied. To simultaneously effect a degree of coupling between two signals each at a different wavelength λ_B, a second acoustic signal at an appropriate frequency can also be applied. Thus the AOTF behaves like several independent lithium niobate switches all running in parallel, each responsive to a different wavelength of the incident light.

2.2.2 Optical Amplifiers

Linear optical amplifiers

A device that can be used to overcome the losses associated with optically transparent or relational devices is the linear optical amplifier. These devices amplify signals by adding more photons of the same polarization, frequency, and direction (stimulated emission) to the photons entering the devices.

An schematic diagram of a semiconductor laser amplifier is shown in Figure 2.10 with the active region of width W, thickness d, and length L stippled. Among many options the three main amplifying structures are ‘Travelling wave (TW) amplifiers’, ‘Near travelling wave (NTW) amplifiers’ and ‘fabry-Perot (FP) amplifiers’. TW amplifier has

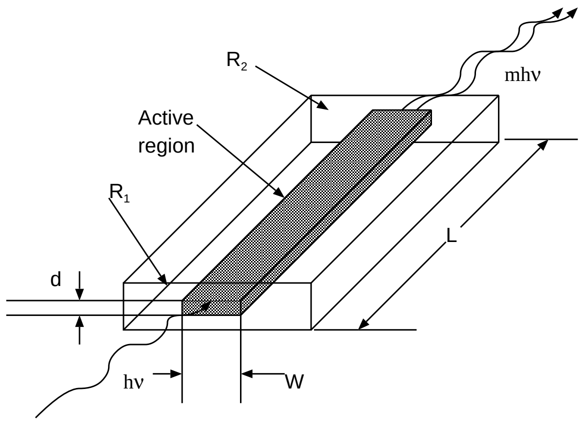

Figure 2.10: Semiconductor optical amplifier

the property that light entering the input facet will only pass through the active amplifying region once. An FP amplifier, on the other hand, allows light to enter the input facet and reflect between the two facet mirrors of the cavity (R_1 and R_2 of Figure 2.10), thus forming multiple paths through the active region. Finally, the NTW amplifier is a practical approximation to the TW amplifier limited by the antireflection (AR) coating that can be grown on the input and output facets of the device. When AR coatings are applied, the operating current is generally higher than the originally threshold current. Thus, if a semiconductor laser designed to lase at $1.55 \mu m$ is given an AR coating on both facets to convert it to an NTW SOA, the peak wavelength of the SOA gain passband will be shorter than the $1.55 \mu m$ wavelength at which the device was designed to lase. Although the TW amplifiers appear to have the most promise as optical amplifiers, they have their own problems. First because of their large bandwidth and spontaneous emission shot noise they have a large output noise power [37].

The advantage of FP amplifier is that the cavity gain, which is the input/output gain of the FP amplifier, can be much higher than the single pass gain. One weakness of the FP amplifier is the narrow passband that are a result of the resonance of the cavity. This narrowband transmission makes the device very sensitive to fluctuations in the bias current, temperature, and the signal polarization. Lithium Niobate based Fary-Perot resonator can be used as optical bistable devices.

Recently, Linear Optical Amplifier (LOA) has been available with impressive capacity. For example, in March 2002, Genoa Corporation has produced the G110 and G212 Linear Optical Amplifiers with a range of gains from 10 to 25 dB for use in C-Band, single- and multi-channel (DWDM) applications [38]. Its gain is fully controllable over the range of 15 to 25 dB. Both linear optical amplifiers are designed for single- or multi-wavelength applications of any data rate up to and beyond 40 Gbps. SOAs are typically constructed in a small package, and they work for 1310 nm and 1550 nm systems. In addition, they transmit bidirectionally, making the reduced size of the device an advantage over regenerators of EDFAs. Modern optical networks utilize SOAs in the follow ways:

* *Power Boosters*: Many tunable laser designs output low optical power levels and must be immediately followed by an optical amplifier. (A power booster can use either an SOA or EDFA.)

* *In-Line Amplifier*: Allows signals to be amplified within the signal path.

* *Wavelength Conversion*: Involves changing the wavelength of an optical signal.

* *Receiver Preamplifier*: SOAs can be placed in front of detectors to enhance sensitivity.

Erbium-dopped fiber Amplifiers

EDFAs allow information to be transmitted over longer distances without the need for conventional repeaters. The fiber is doped with erbium, a rare earth element, that has the appropriate energy levels in their atomic structures for amplifying light. EDFAs are designed to amplify light at 1550 nm. The device utilizes a 980 nm or 1480nm pump laser to inject energy into the doped fiber. When a weak signal at 1310 nm or 1550 nm enters the fiber, the light stimulates the rare earth atoms to release their stored energy as additional 1550 nm or 1310 nm light. This process continues as the signal passes down the fiber, growing stronger and stronger as it goes. Figure 2.11 shows a fully featured, dual pump EDFA that includes all of the common components of a modern EDFA. The input coupler, Coupler #1, allows the microcontroller to monitor the input

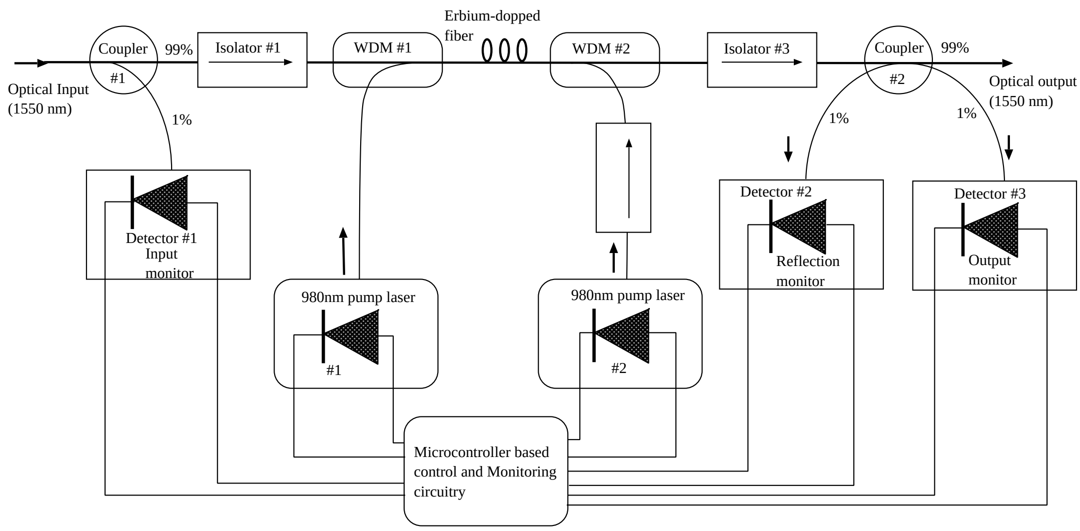

Figure 2.11: A block diagram of a modern dual pump EDFA

light via detector #1. The input isolator, isolator #1 is almost always present. WDM #1 is always present, and provides a means of injecting the 980 nm pump wavelength into the length of erbium-doped fiber. WDM #1 also allows the optical input signal to be coupled into the erbium-doped fiber with minimal optical loss. The erbium-doped optical fiber is usually tens of meters long. The 980 nm energy pumps the erbium atom into a slowly decaying, excited state. When energy in the 1550 nm band travels through the fiber it causes stimulated emission of radiation, much like in a laser, allowing the 1550 nm signal to gain strength. The erbium fiber has relatively high optical loss, so its length is optimized to provide maximum power output in the desired 1550 nm band. WDM #2 is present only in dual pumped EDFAs. It couples additional 980 nm energy from Pump Laser #2 into the other end of the erbium-doped fiber, increasing gain and output power. Isolator #3 is almost always present. Coupler #2 is optional and may have only one of the two ports shown or may be omitted altogether. The tap that goes to Detector #3 is used to monitor the optical output power. The tap that goes to Detector #2 is used to monitor reflections back into the EDFA. This feature can be used to detect if the connector on the optical output has been disconnected. This increases the backreflected signal, and the microcontrolled can set to disable the pump lasers in this event, providing a measure of safety for technicians working with EDFAs.

Photons amplify the signal avoiding almost all active components, a benefit of EDFAs. Since the output power of an EDFA can be large, any given system design can require fewer amplifiers. Yet another benefit of EDFAs is the data rate independence means that system upgrades only require changing the launch/receive terminals. The most basic EDFA design amplifies light over a narrow, 12 nm, band. Adding gain equalization filters can increase the band to more than 25 nm. Other exotic doped fibers increase the amplification band to 40 nm.

Raman optical amplifiers

Raman optical amplifiers differ in principle from EDFAs or conventional lasers in that they utilize stimulated Raman scattering (SRS) to create optical gain. Raman gain arises from the transfer of power from one optical beam to another that is downshifted in frequency by the energy of an optical phonon. By the early part of 2000s, almost every long-haul (typically defined 300 to 800 km) or ultralong-haul (typically defined above 800 km) fiber-optic transmission system uses Raman amplification. Raman amplifiers have some fundamental advantages. First, Raman gain exists in every fiber, which provides a cost-effective means of upgrading from the terminal ends. Second, the gain is nonresonant, which means that gain is available over the entire transparency region of the fiber ranging from approximately 0.3 to 2 m. A third advantage of Raman amplifiers is that the gain spectrum can be tailored by adjusting the pump wavelengths. For instance, multiple pump lines can be used to increase the optical bandwidth, and the pump distribution determines the gain flatness. Another advantage of Raman amplification is that it is a relatively broad-band amplifier with a bandwidth 5 THz, and the gain is reasonably flat over a wide wavelength range.

However, a number of challenges for Raman amplifiers pre-vented their earlier adoption. First, compared to the EDFAs, Raman amplifiers have relatively poor pumping efficiency at lower signal powers. Although a disadvantage, this lack of pump efficiency also makes gain clamping easier in Raman amplifiers. Second, Raman amplifiers require a longer gain fiber. However, this disadvantage can be mitigated by combining gain and the dispersion compensation in a single fiber. A third disadvantage of Raman amplifiers is a fast response time, which gives rise to new sources of noise, as further discussed below. Finally, there are concerns of nonlinear penalty in the amplifier for the WDM signal channels.

Figure 2.12 shows the typical transmit spectrum of a six channel DWDM system in the 1550 nm window. Notice that all six wavelengths have approximately the same amplitude. A Raman optical amplifier is little more than a high-power pump laser, and a WDM or

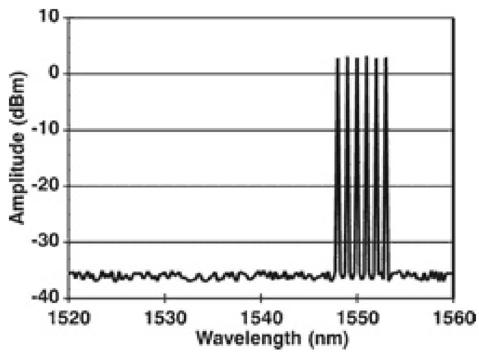

Figure 2.12: DWDM transmit spectrum with six wavelengths

Directional Coupler. The optical amplification can occur in the transmission fiber itself (DRA), distributed along the transmission path. Optical signals are amplified up to 10 dB in the network optical fiber. The Raman optical amplifiers have a wide gain bandwidth (up to 10 nm). They can use any installed transmission optical fiber. Consequently, they reduce the effective span loss to improve noise performance by boosting the optical signal in transit. They can be combined with EDFAs to expand optical gain flattened bandwidth.

Figure 2.13 shows the topology of a typical Raman optical amplifier. The pump laser and circulator comprise the two key elements of the Raman optical amplifier. The pump laser, in this case, has a wavelength of 1535 nm. The circulator provides a convenient means of injecting light backwards in to the transmission path with minimal optical loss.

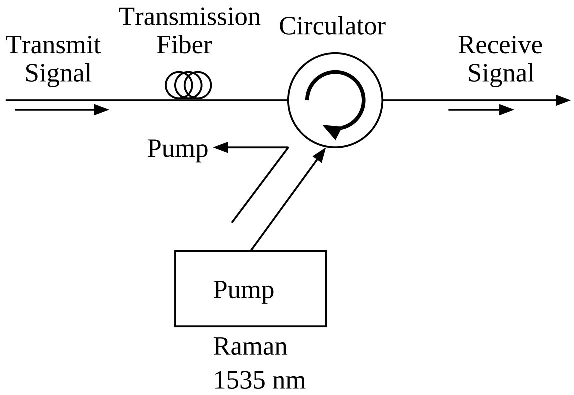

Figure 2.13: Typical raman amplifier configuration

Fiber optics connectors

Fiber optic connectors have traditionally been the biggest concern in using fiber optic systems. Fiber-to-fiber interconnection can consist of a splice, a permanent connection,

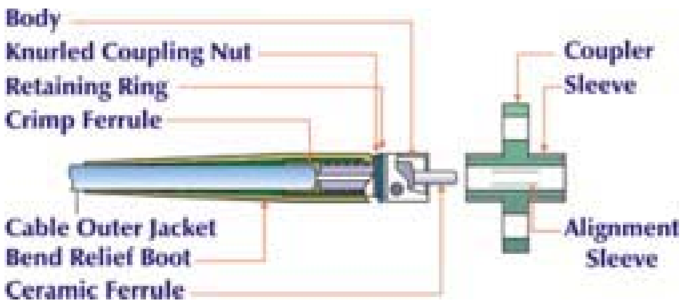

Figure 2.14: Parts of a fiber optic connector

or a connector, which differs from the splice in its ability to be disconnected and reconnected. Different connector types have different characteristics, different advantages and disadvantages, and different performance parameters. But all connectors have the same four basic components: a)The Ferrule, b)The Connector Body, c) The Cable, d) The Coupling Device. Insertion loss may vary from 0.2 dB to 1.0 dB. Installing fiber optics connectors involves cleaving, polishing, cleaning and handling. Single-mode fibers have cores that are only 8–9 μm in diameter. As a point of reference, a typical human hair is 50–75 μm in diameter, approximately 6–9 times larger! Dust particles can be 20 μm or larger in diameter. Dust particles smaller than 1 μm can be suspended almost indefinitely in the air. A 1 μm dust particle landing on the core of a single-mode fiber can cause up to 1 dB of loss. Larger dust particles (9 μm or larger) can completely obscure the core of a single-mode fiber. Fiber optic connectors need to be cleaned every time they are mated and unmated. There are many industry standards for fiber optic connectors as well as Bellcore standard.

2.2.3 Wavelength Division Multiplexing System

One of the most important achievements of optical networks is the capacity enhancement on a single physical link. This has been possible by wavelength division multiplexing. Wavelength-division multiplexing (WDM) is the transmission of many signals through a single optical fiber using different wavelengths, each of which carries a separate, independent signal. Each wavelength represents an optical channel, analogous to a radio or television channel transmitting at an assigned frequency. In dense WDM, wavelengths are closely spaced, commonly at intervals as small as 0.4 or 0.8 nm in the main telecommunications band near 1550 nm. The International Telecommunications Union (ITU) has specified a grid of standard frequencies separated by increments of 100 GHz (approximately 0.8 nm), referenced to a frequency of 193.1 THz (corresponding to a wavelength of 1552.52 nm). These wavelengths are in the "conventional" or C band of the erbium-doped fiber amplifier (EDFA) at 1530 to 1570 nm, and there is interest in expanding to other wavelengths. Other bands of interest are the "long" or L band (approximately 1570 to 1610 nm) and the "short" or S band (approximately 1490 to 1530 nm). The importance of DWDM is for exploiting the enormous capacity of optical fiber to carry information, which is nearly three orders of magnitude greater than the highest bit rates under development. DWDM also allows the capacity of installed optical fiber to be increased easily for meeting the rapid growth of the Internet and other data applications.

The basic approach is shown in Figure 2.15. Here each of three high-speed information sources modulates one of three laser diode optical transmitters, each diode producing light at a different wavelength. As shown, the modulation bandwidth of each source is smaller than the spacing between the optical wavelengths λ_1, λ_2 and λ_3 such that the modulated spectrum of the three signals do not overlap.These three signals are combined in an optical wavelength division multiplexer, a passive structure formed entirely out of glass and operates independently of the nature of the modulating signals. The combined signal is transmitted along a length of optical fiber. At the receiving end of the link, the combined signal is separated into three spectral components(λ_1, λ_2 and λ_3) by the wavelength demultiplexer, another all-optical passive device. Each of the spectrally separated signals is now detected by its own dedicated receiver. There are a number of techniques by

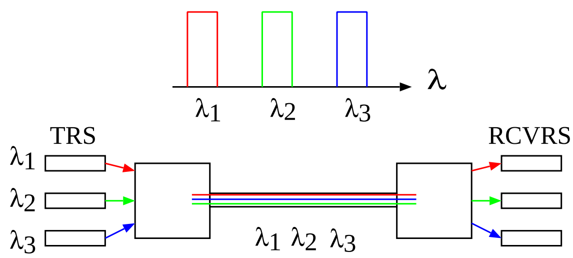

Figure 2.15: Principles of wavelength division multiplexing

which wavelength multiplexer and demultiplxer can be build. Microprism, Braggs grating, Acousto-optic tunable filters etc.

Fiber Bragg Gratings Commercially available fiber Bragg gratings have been important components for enabling WDM and optical networks. A fiber Bragg grating is a small section of fiber that has been modified to create periodic changes in the index of refraction. Depending on the space between the changes, a certain frequency of light – the Bragg resonance wavelength – is reflected back, while all other wavelengths pass through (see Figure 2.16). The wavelength-specific properties of the grating make fiber Bragg gratings useful in implementing optical add/drop multiplexers. Optical add/drop multiplexer (ADM) is an optical devices in which a particular channel and/or wavelength can be dropped for procesing and new channels and/or wavelengths can be added to the outgoing fibers. This device is now hybrid optoelectronic devise. All optical ADMs will soon be available. Bragg gratings also are being developed to aid in dispersion compensation and signal filtering as well.

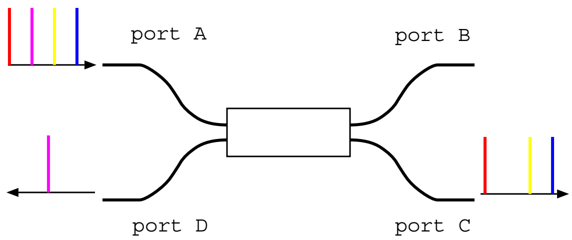

Figure 2.16: Fiber bragg grating technology: Optical A/D multiplexer

WDM system also requires wavelength conversion for reuse of wavelength. Opaque, digitally transparent or all-optical conversion techniques are envisaged. SOA based all-optical wavelength conversion using cross phase modulation principle has been proposed by Suzuki et. al. [39]. In [40] SOA based delay interferometer wavelength converter has been proposed. Wavelength conversion can be performed to any wavelength within approximately 30 nm around the SOA gain maximum. All-optical 3R regenerators have also been investigated recently [40]. Wave-mixing is also an option for achieving all-optical wavelength conversion.

2.2.4 Optical Cross-Connect

Efficient use of fiber facilities at the optical level obviously becomes critical as service providers begin to move wavelengths around the world. Routing and grooming are key areas that must be addressed. This is the function of the OXC. There are three generic optical cross-connect techniques: wavelength division multiplexing (WDM), space division multiplexing (SDM), and time division multiplexing (TDM). There are also proposed

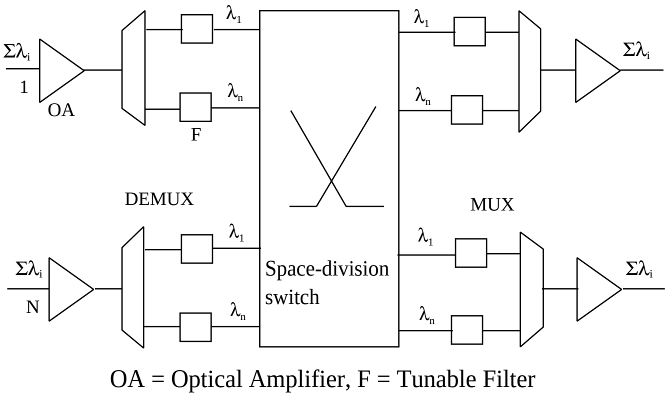

Figure 2.17: Optical cross-connect

systems on a combination of two of these techniques [49, 50, 51]. Time division technique may be appropriate to cross-connect at relatively low data rates. TDM has a limitation on signal formats. Other two multiplexing techniques have no limitations on signal formats and data rates. WDM technique has been extensively studied for optical cross-connects [52, 53, 54].

Figure 2.17 depicts the functional architecture of a reconfigurable *optical cross-connect*(OXC), also called a *wavelength-selective switch*. Each of the N input fibers carries n WDM channels. After demultiplexing, the nN individual channels are switched through a $nN \times nN$ space-division switch. The switch fabric permutes the nN channels. The nN output channels are then remultiplexed into output fibers.

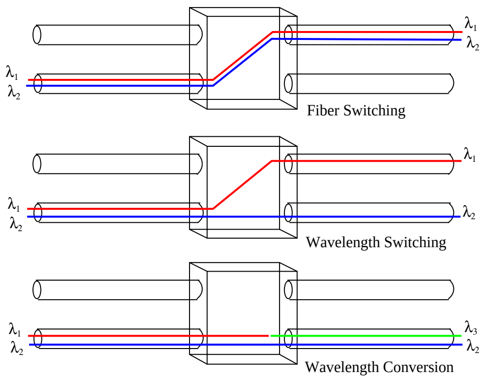

Figure 2.18: Three different wavelength routing in cross-connect

In the optical domain, where 80 optical channels can be transported on a single fiber, a network element is needed that can accept various wavelengths on input ports and route them to appropriate output ports in the network. To accomplish this, the OXC needs three building blocks (See Figure 2.18):

1. **fiber switching**-*the ability to route all of the wavelengths on an incoming fiber to a different outgoing fiber*

2. **wavelength switching**-*the ability to switch specific wavelengths from an incoming fiber to multiple outgoing fibers*

3. **wavelength conversion**-*the ability to take incoming wavelengths and convert them (on the fly) to another optical frequency on the outgoing port; this is necessary to achieve strictly nonblocking architectures when using wavelength switching*

2.2.5 Hybrid Router/OXC-centric Network Architecture

Figure 2.19 shows an architecture of the optical networks consists of multiple optical cross-connects (OXCs) interconnected via WDM links in a general mesh topology. The network model considered here consists of IP/LSR router attached to an optical core network. Each OXC can switch high-speed optical signals (e.g. OC-48, OC-192) from input ports to output ports. The switching fabric may be purely optical or electrical or a combination. The LSRs are clients of the optical network and are connected to their peers over switched optical paths (lightpaths) spanning potentially multiple OXCs. LSRs process traffic in the electrical domain (proposals on optical domain are also coming recently) on a packet by packet basis. OXC processing unit is one wavelength. In [45] Haraki et al. proposed all optical MPλS (multi protocol wavelength) switching. There, out of W wavelengths K are being used for addressing nodes in the network and rest $(W-K)$ are being used for data transfer. It is notable that while $(W-K)$ wavelengths are sending data, K address wavelengths remain idle. This may be considered as poor utilization of wavelengths. A lightpath is a fixe bandwidth connection between two network elements such as IP/LSR routers established via OXCs. Two IP/LSRs routers are logically connected to each other by a single-hop channel. This logical channel is the so-called lightpath – the connection is transparent to bit rates and formats. A continuous lightpath is a path that uses the same wavelength on all links along the whole route from source to destination.

The node may be implemented using a stand-alone router interfacing with the OXC through a defined interface, or it may be an integrated system, in which the router is a part of the OXC system [46].

These OXCs may be equipped with full wavelength conversion capability, limited wavelength conversion capability or even no wavelength conversion capability at all.

The request to setup a path can come either from a router or from an ATM switch connected to the OXCs. The request must identify the ingress and the egress OXCs between whom the lightpath has to be setup. Additionally it may include traffic related parameters such as bandwidth, reliability parameters and restoration options, and setup and holding priorities for the path. The lightpaths are provisioned by choosing a route through the network with sufficient available capacity. Protection is provided by reserving capacity on routes that are physically diverse from the primary ligthpath.

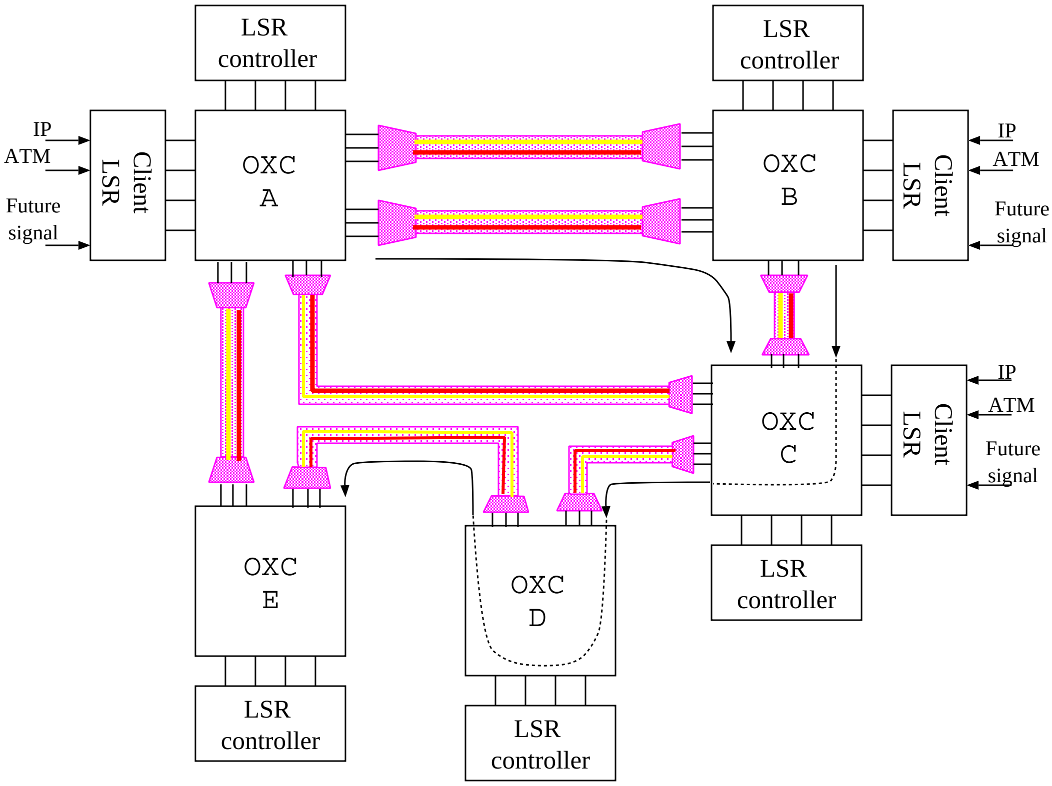

Figure 2.19: A hybrid router/OXC-centric architecture

There should be a mechanism to exchange control information between OXCs, and between OXCs and other LSRs. This can be accomplished by using either an in-band or an out-of-band signaling channel (i.e 1510 nm supervisory channel), using the same links that are used to carry data-plane traffic.

2.3 All-optical Networks

2.3.1 Devices

Optical packet switching provides a potential solution for the next generation optical networks. Its high-speed, protocol and bit rate transparency is ideal for different classes of traffic inside the network. With the advances in optoelectronics and silicon microfabrication, a number of key components necessary for a multi-function switch nodes are available. For example, tunable wavelength converter using semiconductor optical amplifier (SOA) and the MEMS based optical switch are actively been studied and are very promising to be commercialized before long.

In spite of the excitement of the advances in device and the advantages with optical packet switching, all-optical network remains a challenging topic. Without the powerful processing power and abundant storage in the electronic domain, the design of an optical packet switching router involves engineering efforts and genius. When optical signals travel along the fiber, not only the amplitude is attenuated but also the shape is distorted due to dispersion. Fiber nonlinearity and polarization dependence of components both contributes to a further degradation of the signal. To reshape and regenerate the signal all optically is still an active research. Also, information delivered at different wavelength will have different speed travelling inside fibers. The packets thus need to be re-clocked or re-aligned before information can be extracted for routing. Ideally, all the functions mentioned above, in addition to some other requirements imposed by the network architecture such as add-drop capability, would be provided at the switching nodes. Contention resolution for all-optical packet switching is an important problem because a fine method to implement optical buffer is not known. Delay loops cannot serve the purpose efficiently. Wavelength conversion and deflection routing are the two interesting methods to reduce the contention in the incoming packets. However, the number of wavelengths available in a router will determine the complexity of the design and thus the cost of the whole system.

The European KEOPS (Keys to Optical Packet Switching) project [85] proposed an all optical network having an optical packet layer in between the electronic switching layer, for example ATM, and the underlying optical backbone supported by WDM. This optical layer not only serves as the linkage between the terabit backbone and the sub-gigahertz electronic switching layer, its transparency in format and bit rate also helps to integrate different kind of services in the future network. Packets in this layer will be routed with optical cross-connect (OXC) within the switch.

Optical IP routers can be used as core routers in internet backbones. The inlets and outlets of a core router are optical fibers which operate in WDM mode with a number of wavelengths per fiber depending on the technology. More wavelengths per fiber could yield a higher degree of statistical multiplexing and lower blocking probability in the router. Nevertheless, problems such as all-optical synchronization, buffering, and node cascadability still need to be solved completely. The solutions available at the moment are far from field implementations.

Since the processing is in the electronic domain, end user need not to be in the optical domain. Moreover, the speed of optics is in no way higher than electromotive force. So, processing speed will not be higher even if we do it in optical domain. However, inherent parallelism of optical signal can result in higher speed of data transfer and processing.

2.3.2 Routing and Wavelength Assignment

Within an all-optical domain, wavelength conversion (changing the wavelength of a connection) is still expensive and not yet practical without an O/E/O conversion. Therefore it is important to understand the routing implications of limited (or no) wavelength conversion. This requires us to look at what is called the "Routing and Wavelength Assignment

(RWA) Problem": Given one or more connections that need to be established in an all-optical domain, determine the routes over which each connection should be routed and also assign each connection a color. If the routes are already known, the problem is called the "Wavelength Assignment (WA) Problem". The first-order implication for GMPLS is that in the absence of wavelength conversion, the necessity of finding a single wavelength that is available on all links introduces the need to either advertise detailed information on wavelength availability, which probably doesn't scale, or have some mechanism for probing potential routes with or without crankback to determine wavelength availability. Choosing the route first, and then the wavelength, may not yield acceptable utilization levels in mesh-type networks.

Bit transparent regenaration, retiming and reshaping (3R) of optical signal in all-optical domain is another problem that is under research.

2.3.3 Survivability

Survivability is another important research aspect in the photonic networks. Protection and Restoration schemes for Ring and Mesh type networks have been studied for quite a long time. However, irregular, arbitrarily connected networks have not been studied yet. Survivability issues in multicast environment must also be addressed considering the stringent delay requirement.

Another question is to be resolved. If we have optical buffer and processing in optical domain, does it mean that we well be able to achieve maximum throughput? It may or may not be. The large number of buffers along the connection means the large delay. Large delay is not desirable in an optimum network. The introduction of so called packet routing of electronic networks may result the same old problems of contention and delay in the optical networks. This author thinks that complete packet switching or complete circuit switching cannot utilize the advantage of the optical signal fully. Proportionate role of these two switching technique in the network and their co-existence can be an important research topic.

Chapter 3

Problems with Designing All-optical Switching Systems

Several dramatic advances in the optical-networking arena in recent years have emerged to set the foundation for the next-generation optical internet and to challenge both the traditional view of networking (routing,switching, provisioning,protection,and restoration)and the conventional approaches of networks design that have always addressed technology first and management second. The abundance of bandwidth propelled by the explosion of DWDM poses a new challenge to network architects -the new challenge is to managing the abundance of bandwidth. There is an attractive opportunity to evolve DWDM technology toward an optical networking infrastructure with transport,multiplexing switching, routing survivability,bandwidth provisioning and performance monitoring, supported at optical layer.

OXCs are considered to be one of the key component for all-optical networking. All optical links coming into a core node are terminated on an OXC. The cross-connect switches transit traffic (data destined for another core node) directly to outbound connections, while switching access traffic (data destined for this node) to ports connected to an access router. The granularity at which data can be switched is at the entire wavelength level. In the first chapter we have seen a block diagram (Figure 2.17) of an OXC where switching system plays very important role.

Switching system has a long history. Problems in designing an optical switching system has some major differences from their electronic counter part. The reasons of this difference is due to different physical property of optics. An optical switching system can best be represent by Figure 3.1. The two main parts of the switching system are a) switching networks and b) routing strategy. Although routing strategy depends on the switch architecture, it is also necessary to design a switch network so that the routing becomes easier and takes short time. We discuss problems with optical switch networks and routing through them.

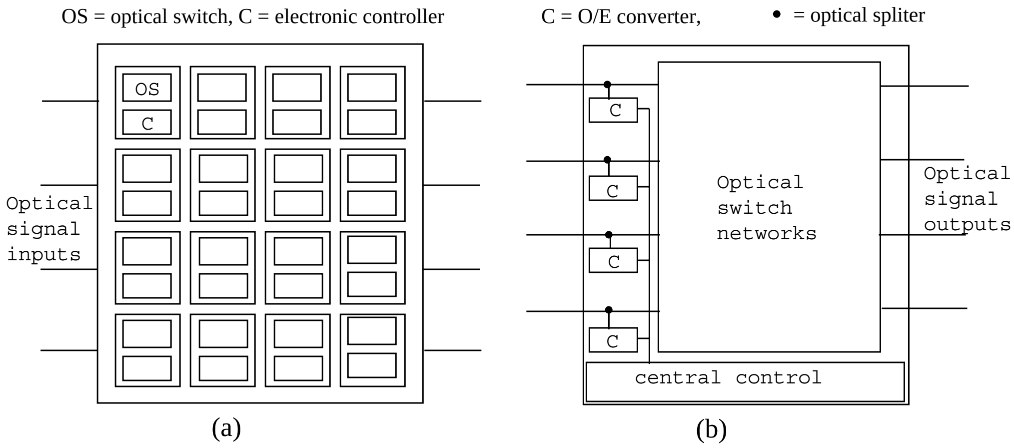

Figure 3.1: Block diagram of an optical switching system

3.1 Optical Switch Networks

There is a huge body of research concerning with the optical switch networks. They have dealt with four major problems – number of switches or switch count, delay, crossralk, signal loss and connectivity or blocking probability. Although signal loss is not a big deal now, path-dependent path-loss is a matter of concern. If signal loss varies to a great extent when the connection path changes, it would be difficult to control the gain in high speed, and make the system costly and complex. Connectivity provides a measure of the network's flexibility in terms of its ability to provide a desired signal path through the network. In general there are four different classes of network interconnection topologies: i) Strictly nonblocking, ii) Wide-sense nonblocking, iii) rearrangeably nonblocking, and iv) blocking networks.

Network complexity is proportional to the total number of switching elements required (or *switch count*) to implement the network. *Delay* is proportional to the *path length*. *Path length* refers to the total number of switching elements a signal passes through in order to traverse the network before reaching an output port. *Signal loss* is also dependent on path length. If two connections from an input to two different outputs have different path length then the signal loss is said to be *path-dependent*.

Definition 1 *The* total number of SEs *of a switching network is the number of switching elements required in the network. The* maximum signal loss *is given by the maximum number of* SE*s on a signal path. The* maximum crosstalk *is given by the maximum number of crosstalk* SE*s on a signal path, where a crosstalk* SE*, denoted by* CSE*, is an* SE *that carries signals at both of its two inputs at the same time.*

The path dependent path loss is defined as

$$PD_L = maximum\ signa\ loss - minimum\ signal\ loss$$

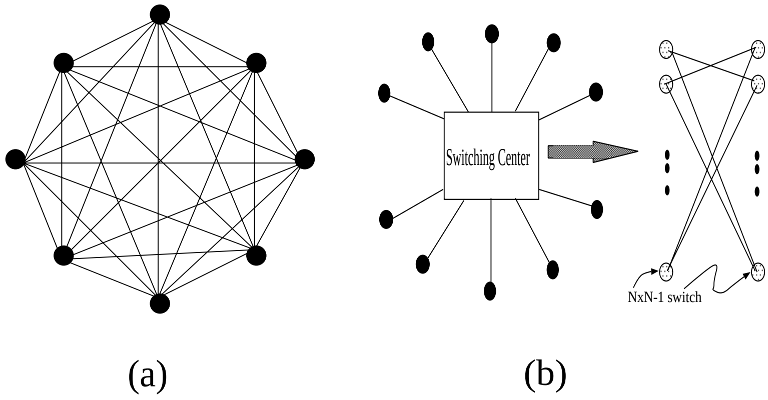

Figure 3.2: Direct, fully connected users

Crosstalk occurs when two optical paths (channels) carrying signals interact with each other. There are two ways in which optical paths can interact in a planar switching network. First, two optical channels on different waveguides cross each other in order to obtain a particular topology. We call this a *channel crossover*. Alternatively, two paths sharing a switching element will experience some undesired coupling from one path to the other. This is called *switch crossover* [41]. Experimental results reported in [42] showed that it is possible to make crosstalk from passive intersections of optical waveguides negligible. The switch crossover crosstalk can occur in several stages. But the first-order-crosstalk contributes major portion of the total crosstalk. We will discuss some important switch architectures using directional couplers only.

3.1.1 Strictly Nonblocking Networks

In a strictly nonblocking network, every input has a dedicate path through the network to each output. Thus in this class of network, any input can be routed to any unused output regardless of the way other input signals are routed. Electronic crossbar network is an examples of this class. However, optical crossbar networks are not strictly nonblocking, rather wide-sense nonblocking. Anyway, optical crossbar networks are widely used for their simple routing algorithm. Strictly nonblocking property is desirable for optical switching system to reduce the packet loss as there in no optical buffer available. N nodes can be interconnected as shown in Figure 3.2(a). This interconnection pattern in strictly nonblocking. This approach requires $N(N-1)/2$ fibers between the users, and clearly inefficient. Alternatively, we can use a switch consisting of $2N$ copy of $1 \times N - 1$ switches (Figure 3.2(b)). It is notable that optical switches are transparent from input to output. Thus a 1×2 switch can also be used as 2×1 switch. This is a significant difference from that of an electronic switch.

Router/selector switch

Figure 3.3(a) is an example of 4×4 router/selector strictly nonblocking switch implemented with 2×2 switching elements [43]. Since there is a dedicated path from any input to any output, existence of a connection between an idle input and an idle output does not depend on other connections. Advantages are simple routing, relatively low loss and zero low first-order crosstalk. The drawbacks of this network are high switch count ($2N(N-1)$ *SE*s) and non-customizable, i.e. if a network system wants to compromise with crosstalk and loss to reduce its hardware cost, we cannot do that with this network. The shape of the network is always square. For this reason it cannot be used in Clos network to reduce the switch complexity. In this network, routing is done by following the binary

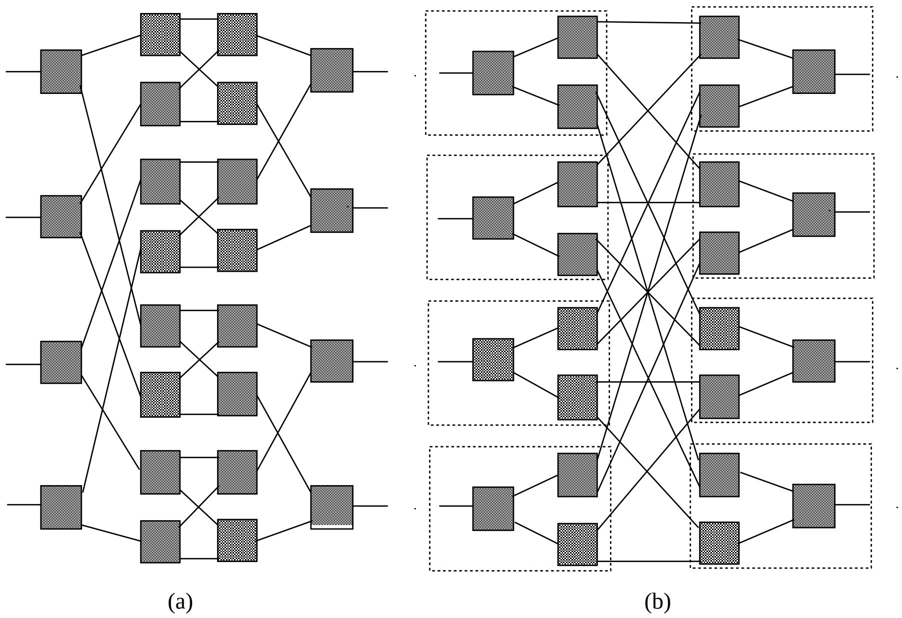

Figure 3.3: 4×4 router/selector switch network. (a) Single substrate version (b) Multisubstrate version

trees whose roots are the desired input and output. The leaves of the input tree and the leaves of the output tree will meet at exactly one link in the center of the network. The routing is simple – use only one path from input to output. The loss in router/selector architecture is nominally the same for all paths and is $L_T = 4L_F + 2(\log_2 N)L_C$ for the multiple-substrate version (see fig 3.3(b)) and $L_T = 2L_F + 2(\log_2 N)L_C$ for the single substrate version. If we ignore the higher order crosstalks ($\leq x_C^4$), then signal-to crosstalk ratio of a router/selector switch is as shown in equation (3.1).

$$SXR = 10\ \log_{10}\left[\frac{1}{(\log_2 N)x_C^2}\right] = -10\ \log_{10}[\log_2 N] - 2X_C \tag{3.1}$$

With the typical values of X_C and L_C a 16×16 router/selector switch results 54 dB SXR. The path-dependent-path loss is zero. The main drawback of this switch is the

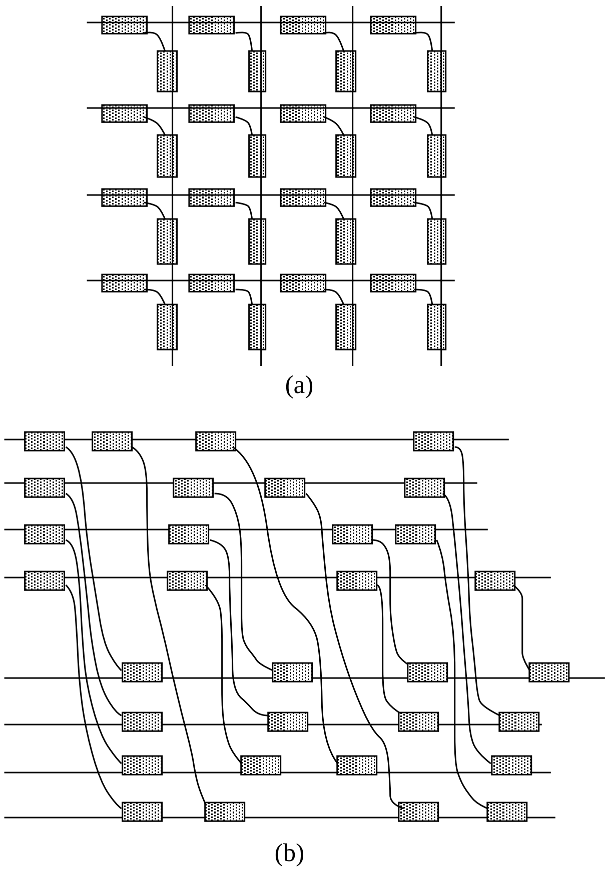

Figure 3.4: 4×4 double crossbar switch with Directional Couplers

switch count and non-customization. A system with moderate crosstalk constraint may want to reduce its hardware cost but router/selecter architecture cannot provide us this opportunity.

Double crossbar networks

Realizing the switch dimension limitations imposed by the cross talk, directional coupler switch architects proposed and build double crossbar networks as shown in Figure 3.4 [44]. There are $2N^2$ couplers are required for a switch of dimension N. The maximum signal loss is proportional to $2N$, or more exactly $L_T = 2L_F + 2NL_C$ dB. The first order crosstalk is zero. The path dependent path loss is

$$PD_L = 2N - 1 - N = N - 1 \tag{3.2}$$

The signal-to-crosstalk ratio is,

$$SXR = -2X_C - 10\log_{10}\left[\frac{1 - 10^{(1-N)L_C/10}}{10^{L_C/10} - 1}\right] dB \tag{3.3}$$

For typical values of X_C (-30 dB) and L_C (-0.5 dB) a 16×16 double crossbar switch network results 43.7 dB SXR, which is much better than simple crossbar switch. The

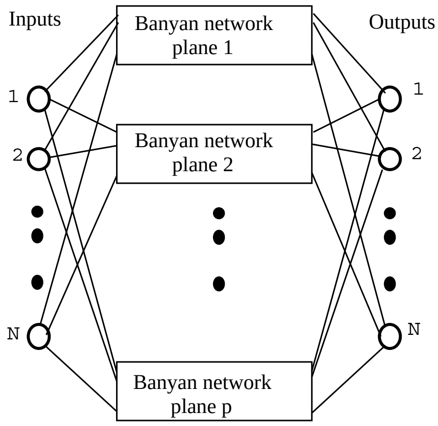

Figure 3.5: Multi-plane Banyan networks

double crossbar switch can have a size of 128 × 128 with SXR is 13 dB.

Multi-plane Banyan strictly nonblocking networks

By vertically stacking multiple copies (planes) of the Banyan-type networks, nonblocking network can be created [66] as shown in Figure 3.5. A switching network is strictly nonblocking if we can always set up a new connection without disturbing the existing ones [66, 68] and each connection has a dedicated path. The results [61] indicated that given the constraint of crosstalk-free, the hardware cost of a strictly nonblocking optical MIN will be high. Banyan-type networks have a unique path between an input-output pair, and this makes them blocking networks. Conventionally, blocking occurs when two connections intend to use the same link, in which case, one of them will be blocked. This is indicated as link-blocking. There is, however, another type of blocking in DC-based photonic switching systems. If adding the connection causes some paths — including the new one — to violate the crosstalk-free constraints, the connection cannot be added even if the path is available. We refer to this second type of blocking as crosstalk-blocking. By ensuring that only one signal passes through a switch at a time, the first order crosstalk can be eliminated and also the link-blocking constraint will not be violated, and this provides a cost-effective solution to both the crosstalk-blocking problem and the link-blocking problem.

All paths of a Banyan-type network have the same property in terms of blocking. To study the blocking probability, we can arbitrarily select an input and an output in a Banyan-type network and set up a connection between them. We call the path between the input-output pair the tagged path. The links and the *SE*'s along the path are called the tagged links and the tagged *SE*'s, respectively. The stages of *SE*'s are numbered from left (stage 1) to right (stage $\log_2 N$). For a tagged path, an input intersecting set I_i associated with stage i ($\forall\ 1 \leq i \leq \log_2 N$) is defined as the set of all inputs that intersect a tagged *SE* at stage i. Likewise, an output intersecting set O_i associated with stage i is the set of all outputs that intersect a tagged *SE* at stage $\log_2 N - i + 1$. For an $N \times N$ switch, we use the notation $B(p)$ to refer to a Banyan-type optical MIN that has p parallel planes and no crosstalk *SE*s along the path of each connection. An $N \times N$ B(p) network is strictly nonblocking if the following is true:

$$p \geq \begin{cases} 2\sqrt{N} - 1 & \text{if } \log_2 N \text{ even} \\ \frac{3}{2}\sqrt{2N} - 1 & \text{if } \log_2 N \text{ odd} \end{cases} \tag{3.4}$$

The result was obtained by using the idea of worst-case analysis, i.e. to find the maximum possible number of connections that will conflict the tagged path.

The signal-to-crosstalk ratio is calculated by considering the worst case scenario where each plane may have (N/2) connections but no signals intersect with the other signals at any couplers. However, each signal starts accumulating crosstalks from second stage up to last stage. The resulting equation is as shown in (3.5). Since every path traverses the same number of couplers, they suffers the same amount of loss, and the loss terms are cancelled out in the expression.

$$SXR = -2X_C - 10\log_{10}\left[\frac{\log_2 N(\log_2 N + 1)}{2}\right] \tag{3.5}$$

For 16×16 multi-plane Banyan optical switch network, the SXR is 50 dB. This suggests that SXR virtually does not impose any restriction on the size of switch networks.

M-plane banyan networks are customizable. The main problem with this networks is that it does not have routing algorithm. Although it is a strictly nonblocking in the sense that any free input can be connected to any free output but how an input signal is routed to the appropriate plane is not known. Plane selection algorithm will depend on the type of input/output switches.

Clos networks

C. Clos [70] showed that for networks of large enough dimension, strictly nonblocking networks could be constructed that uses fewer cross-points than the crossbar networks. Figure 3.6 shows a three stage Clos network. We assume the following labels to the parameters of this network. Let:

N = the number of inputs and outputs of the network

n = the number of inputs per switches in the input-stage(stage-1) and the number of outputs per switches in the output-stage(stage-3)

m = the number of switches in middle-stage(stage-2)

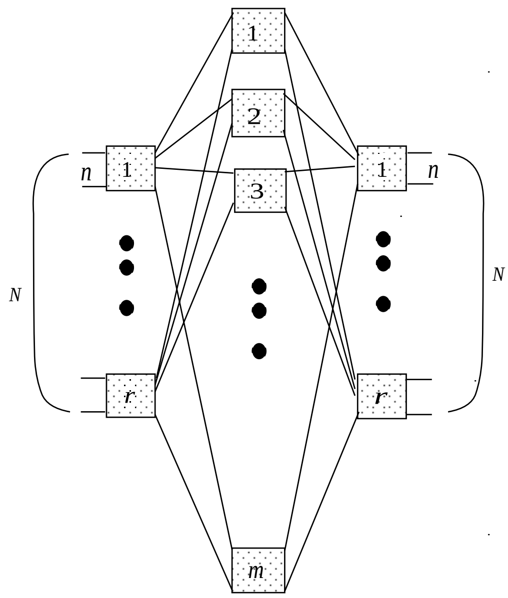

Figure 3.6: $N \times N$ three stage Clos network

r = number of switches in the input or output stages

Every switch in the input stage connects to every switch in middle-stage by exactly one link; mirror image of this connection pattern exists between middle-stage and output-stage. Select an arbitrary input i and output j. To ensure strictly nonblocking operation, we must guarantee that whatever other connections exist in the network, a connection can be made between input i and output j. Input i shares its input switch with $n-1$ other inputs, all of which may be connected to different output switches through different switches in the middle stage. Therefore, there must be at least $n-1$ middle-stage switches to satisfy these connections. Further, the switch output that j connects to has $n-1$ other outputs that may be connected to $n-1$ middle-stage switches other than those required by the $n-1$ input connections. Once the demand of the $n-1$ inputs and $n-1$ outputs are satisfied, there must still be one free center stage switch for the connection from i to j, so that total number of middle-stage switches required is

$$m = 2(n-1) + 1 = 2n - 1 \tag{3.6}$$

If we assume that each of switches (building blocks) in the Clos network is a crossbar switch, the total number of cross-points in the network is

$$T_N = (2n-1)(2nr + r^2) \tag{3.7}$$

The number of cross-points is optimized for $N = n^2$, then $r = n$ and equation (3.7) reduces to

$$T_N = 3N(2\sqrt{N} - 1) \tag{3.8}$$

The Clos networks requires fewer number of cross-points than original crossbar networks when $N \geq 25$.

The Clos structure itself does not have any path dependency because all paths have to cross the same three stages. But the Clos networks inherits path dependency from its building blocks – Crossbar networks.

3.1.2 Wide-sense Nonblocking Networks

The body of research available on wide-sense nonblocking networks is sparse because of the complexity of considering not only the number of possible interconnections but also the number of ways to arrive at these interconnection patterns. Like strictly nonblocking network, a network that is wide-sense nonblocking allows any input to be connected to any unused output. The difference between the two is that in wide-sense nonblocking network, while each input may have more than one paths to reach a particular outputs. Different connection can share a path i.e connections do not have any dedicated path. However, if a specified algorithm is followed, all of the desired interconnections can be established.

If we use 2×2 switches in the middle-stage of a three stage network, then $[\frac{3n}{2}]$ is the number of middle-stage switches required for a wide-sense nonblocking switch, where $[x]$ is the largest integer less than or equal to x [68]. If we allow the middle-stage switches to be any dimension $r \times r$ instead of just 2×2, then $[2n - \frac{n}{r}]$ has been shown to be a lower bound on the number of middle-stage switches required for a wide-sense nonblocking network, but this results take no account of packing rule [71]. Yang et. al. in [72] showed that a three stage Clos network is nonblocking under packing strategy is $m \geq \left\lfloor \left(2 - \frac{1}{F_{2r-1}}\right) n \right\rfloor$, where F_{2r-1} is the Fibonacci number.

Multi-plane Banyan networks for wide-sense nonblocking condition has also been proposed in [63]. When more than one connection intend to use the same link then a contention arises – this is known as *link blocking.* There is however, another type of blocking in DC-based photonic switching systems. Sometimes, all the links along the path of the new connection are available, but adding the connection will violate the specified *crosstalk constraint* along the path of the new connection or an existing connection. Under such condition new connection will still be blocked. This is termed in the paper [61, 63] as *crosstalk blocking.* In paper [63] they have proposed how many copies of Banyan networks are required to make the target network wide-sense nonblocking for a specified crosstalk constraint.If c is crosstalk constraint and p the required number of planes, then $N \times N$ Multi-plane wide-sense nonblocking network $B(p, c)$, when $1 \leq c < \log_2 N$, is:

$$p \geq \begin{cases} \sqrt{2N} - 1 & \text{if } \log_2 N \text{ odd} \\ \frac{3}{2}\sqrt{N} - 1 & \text{if } \log_2 N \text{ even} \end{cases} \tag{3.9}$$

It has the same routing algorithm problem as we have discussed for strictly nonblocking multi-plane Banyan networks.

Crossbar networks

The optical crossbar networks is sometimes mistakenly referred to as strictly nonblocking because of the simplicity of the routing algorithm that guarantees nonblocking operation. If we connect input i to output j by routing horizontally in row i to column j, then vertically to the output, we are guaranteed that any idle input can connect to any idle output. An example of 4×4 crossbar switch made from directional couplers is shown in Figure 3.7 [56]. If we let:

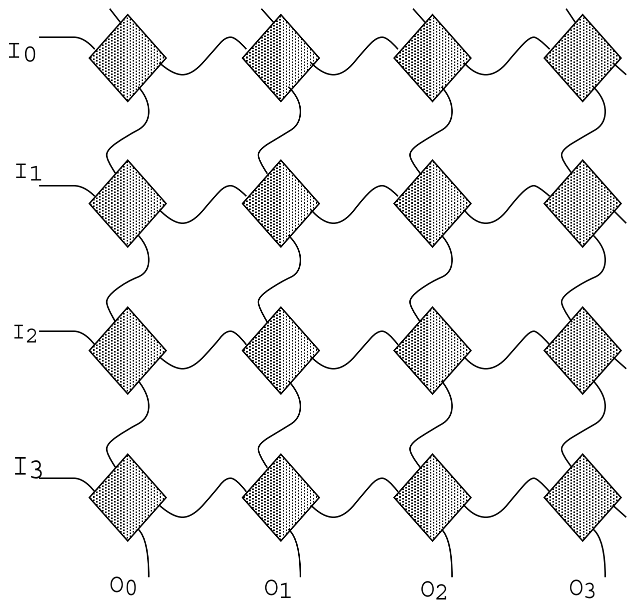

Figure 3.7: 4×4 crossbar switch networks with directional couplers.

L_F = Loss at fiber-waveguide interface

L_C = Loss suffered traversing a directional coupler and its connecting waveguides

L_T = Total loss

all in decibels, then the worst-case fiber-to-fiber loss in an $N \times M$ crossbar network made from directional couplers is just

$$L_T = 2L_F + (N + M - 1)L_C$$

Since loss from fiber-waveguide interface is constant, then for large network

$$L_T = (N + M - 1)L_C \tag{3.10}$$

Again for a square network, where $M = N$,

$$L_T = (2N - 1)L_C \tag{3.11}$$

To calculate the worst-case crosstalk in a crossbar network we select the signal path that intersects the most other paths in a fully loaded network. The path most likely to have the highest cross talk in the crossbar is from input I_0 to output O_0 as shown in Figure 3.7. Since all intersections of signal and noise paths occur in the first column, each noise path has experienced no coupler attenuation before intersecting the signal path. The signal path,however has experienced one coupler attenuation before intersecting the first noise path, two attenuations before intersecting the second noise path, and so on. If we let the power entering any input be P_{IN} and the power leaving any output be P_{OUT}, then the signal path output power is $P_{OUT} = P_{IN}(l_C^N)$. The crosstalk power entering the signal from the input just below the top input and and propagating with the signal to the leftmost output will be $P_{OUT,1} = P_{IN}(x_C)l_C^{(N-1)}$. In general, input i will contribute crosstalk power

$$P_{OUT,i} = P_{IN}(x_C)l_C^{(N-i)} \tag{3.12}$$

The total crosstalk will then be the sum of all noise path inputs and will be

$$P_{OUT,crosstalk} = P_{IN} \sum_{i=1}^{N-i} (x_C)l_C^{(N-i)} \tag{3.13}$$

which can be reduced to closed form

$$P_{OUT,crosstalk} = P_{IN}(x_C)l_C^N \left[\frac{1 - l_C^{1-N}}{l_C - 1}\right] \tag{3.14}$$

The switching elements those contributes to the crosstalk is termed as *crosstalk SEs*. It is notable that the crosstalk is proportional to the number of crosstalk *SE*s along the path of a connection. Thus for having an idea about the crosstalk and for comparison we can use the following equation

$$S_{N\times M} = min(N, M) - 1 \tag{3.15}$$

for an $N \times M$ crossbar network, where $S_{N\times M}$ is the maximum crosstalk in a connection.

The size of the switch network is limited by the signal to crosstalk ratio, SXR, which is defined as $10 \log_{10}(P_{OUT,signal}/P_{OUT,crosstalk})$, and thereby,

$$SXR = 10 \log_{10} \left[\frac{1}{x_C \left[\frac{1-l_C^{(1-N)}}{l_C - 1}\right]}\right]$$

or

$$SXR = -X_C - 10 \log_{10} \left[\frac{1 - 10^{(1-N)L_C/10}}{10^{L_C/10} - 1}\right] dB \tag{3.16}$$

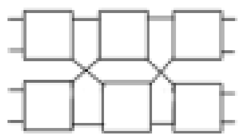

Figure 3.8: A 4×4 Benes network

For example, let the loss per coupler be $L_C = -0.5$ dB and the crosstalk per coupler be $X_C = -30$ dB, then a 16×16 crossbar switch will have an SXR = 13.7 dB. For 32×32 crossbar switch the signal-to-crosstalk ration is 4.99 dB, which is not acceptable.

Crossbar networks have high path dependency. The minimum length of a connection is 1 *SE* and the maximum length of a connection is $N + M - 1$. Thus, path dependency,

$$P_D = N + M - 2$$

3.1.3 Rearrangeably Nonblocking Networks

In this class of networks any input can be connected to any free output, but one or more existing connections may have to be rerouted to established the path. This kind networks usually not suitable for all-optical communication networks, because it requires that packets be of same length and synchronized to one another. As we do not have optical memory synchronization in the optical domain is very difficult. However, once the optical memory is available then we can use this class of nonblocking networks in the optical cross-connect. Most widely used rearrangeably nonblocking network is the Benes network [68] as shown in Figure 3.8. Yang et. al. in [3] presents that two plane of Benes network in unison can be used as a first-order-corsstalk free rearrangeably nonblocking optical network. It has $2\log_2 N - 1$ stages between input and output. So, the loss is almost double of that of a Banyan network. The routing algorithm is also complex and consumes time in the $O(N\log_2 N)$. Jiang et. al. in [73, 74, 75, 76] presented some results on first-order-crosstalk- free vertically stacked multi-plane $\log_2 N$ networks for rearrangeably nonblocking condition. They presented the number of planes required for constructing such a network as given bellow:

$$p \geq \begin{cases} \sqrt{N} & \text{if } \log_2 N \text{ even} \\ \sqrt{2N} & \text{if } \log_2 N \text{ odd} \end{cases}$$

The switch complexity is in the order of $O(N\sqrt{N}\log_2 N)$. This complexity is considerably higher than that of a rearrangeably nonblocking Benes networks. In [73] authors used Benes networks instead of Banyan networks and eliminated the redundancy of switches in the networks for Banyan type. This vertically stacked Benes networks use K copy of $\frac{2N}{K} \times \frac{2N}{K}$ Benes network. K is given by

$$K = 2^{\lfloor (n-m+1)/2 \rfloor}$$

where $n = \log_2 N$ and $m \leq n-1$. This is the best known result in terms of switch count for a rearrangeably nonblocking networks.

3.1.4 Blocking Networks

There are some class of networks in which a new connection may not be established even the destination is free. These networks are called *Blocking networks*. Banyan-type (in other words, $\log_2 N$) [69] networks are an example of this kind. These networks fully connected, i.e. any output can be reached from any input. The example of first-order-crosstalk-free Banyan network is not found in the literature.

3.2 Routing Strategies

The extraction of header from optical signal is not as simple as that of electronic signal. For recognizing a header optical signal first needs to be converted into electronic signal. This conversion is costly in terms of power. Complete self-routing technique is not also suitable because of delay in switching and storage at every stage of switches a signal has to pass through. That is why practically all optical switches uses crossbar networks with centralized routing algorithm. Other than scaling problem with the crossbar networks, it has also problem with computation complexity. Because of complete centralized nature, routing a permutation requires time $O(N)$. Crossbar networks can be self-routing for all permutations but it requires the header size of $O(N)$. Moreover, the network uses a global reset signal to all switches. The means, all of the packets must be buffered by the interfacing hardware, and simultaneously sourced into the network with their first bit synchronized [77]. Non-equal path lengths require extra circuitry to handle the variable delay and signal loss. The clearing of the network may require a total of $N + M - 1$ bit periods for a packet that is routed from the topmost input to the rightmost output port (see Figure 3.7).

The other major candidate for nonblocking optical switch networks is vertically stacked multi-plane Banyan networks. Although networks in [61, 63] are nonblocking they don't have necessary routing algorithms. As soon as a request arrives, a strictly nonblocking network should be able to route the signal to the right plane of Banyan network. But these networks cannot do that. Number of planes in the architecture ensures that there is a plane that contains the path for this request. But for choosing the plane by simple hunting algorithm requires at least $O(\sqrt{2N}\log_2 N)$ computing complexity. Thus a permutation consumes $O(N\sqrt{2N}\log_2 N)$ times to be routed through the network if the control is centralized.

Let us consider that input line has $1 \times p$ switch and each output has $p \times 1$ combiner (Figure 3.9(a)). Every input is connected to p planes. The output i of the first input

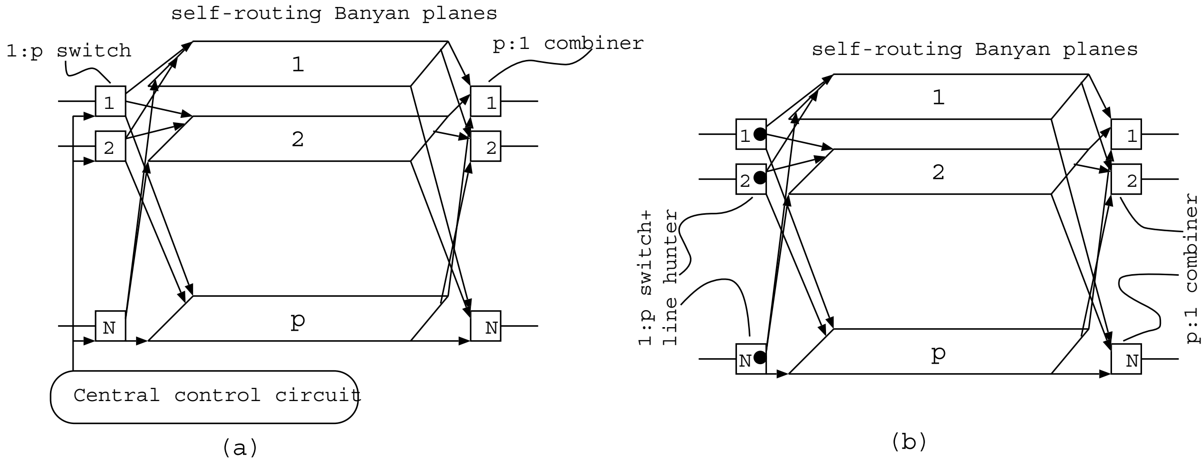

Figure 3.9: Multi-plane Banyan networks. (a) Centralized control. (b) Control distributed to every input line.

switch is connected to the first input of ith Banyan network. The output i of the second input switch is connected to the second input of the ith Banyan network. A central controller reads the input request and decides which plane the signal will be sent to. Then the controller generates an appropriate control signal to that input switch so that the input switch can setup itself accordingly. If input i is routed to the plane (Banyan network) j then ith inputs of all other $p-1$ Banyan networks remain idle. For establishing a connection without disturbing existing connections, controller has to choose a plane (by some order/priority) and check if the required path is free or not, and if it is free the controller then sends a control signal to the corresponding input switch.

Let us consider that each input has $1 \times p$ switch along with a line hunting circuit and each output has $p \times 1$ switch (Figure 3.9(b)). As soon as a request arrives at input i, hunting circuit of that input switch hunts for a plane through which the input can be routed. If another request for at input j arrives at the same time, there can be a contention between hunting. Both hunting circuit may want to choose the same plane. If one succeed by random then the other input has to go for hunting again. This hunting process will also be time-consuming because it may have to wait for a busy response from the last stage of the Banyan network in a plane. Hunting process consumes time at in the order of $O(\sqrt{2N}\log_2 N)$.

If we consider that each input has a $1 \times p$ splitter and each output has $p \times 1$ combiner then signal loss will increase to $O(1/N)$. Besides that, the hardware cost of input/output switches along with hunting circuits is a huge overhead, and can make the practical implementation of the switch difficult.

3.3 Summary

To design optical networks, we need to address other problems in addition to non-blocking, such as signal loss and crosstalk caused by two signals passing through the same switching element. Crossbar and Clos networks are the most widely used non-blocking networks in conventional electronic communication systems. The crossbar network suffers from huge signal loss and crosstalk [1] and therefore cannot be directly employed in optical networks [56, 57]. The Clos network uses the crossbar as building block for the nonblocking property. The Clos network has only three stages, so signal loss is bounded in this regard. However, the crossbar building block in the Clos network still results in large signal loss and crosstalk.

Optical crosstalk occurs when two optical paths (channels) carrying signals interact with each other. There are two ways in which optical paths can interact in a planar switching network. First, two optical channels on different waveguides cross each other in order to obtain a particular topology. We call this a *channel crossover*. Alternatively, two paths sharing a switching element will experience some undesired coupling from one path to the other. This is called *switch crossover* [58]. Experimental results reported in [59] showed that it is possible to make crosstalk from passive intersections of optical waveguides negligible. So, many researchers studied how crosstalk caused by switch crossover can be reduced [56, 57, 58, 60, 61, 62, 63, 64, 65]. Some of them used dilation of Banyan and Benes networks to reduce crosstalk. A double crossbar has been proposed for a strictly nonblocking and zero crosstalk network [64] with increased signal loss ($2N$) and increased number of switching elements ($2N^2$). A Spanke's network [65] has zero first-order crosstalk with a reduced signal loss ($2\log_2 N$), but it requires $2N(N-1)$ switching elements for an $N \times N$ strictly nonblocking network. The Spanke's network lacks of customization capability so that hardware cost cannot be traded off even when the crosstalk and loss requirements are not stringent. In [61, 63] multi-plane Banyan architecture were proposed that have much lower crosstalk, signal loss and switch complexity. However, it is still not known how the signal will be routed in the right plane.

The centralized crossbar networks require computation complexity in the $O(N)$. Conversely, self-routing crossbar networks require header of the size of $O(N)$.

Chapter 4

A New Nonblocking Optical Switching System

4.1 Introduction

Advances in electro-optic technologies have made optical communications a desirable networking choice to meet the increasing demands of high-performance computing and communication applications. Since such applications require a high data transmission rate as well as low error rate and low delay, no rearrangement of the states of the switching elements in optical networks is desirable, making nonblocking switches increasingly important for optical networks. With each circuit having such a high capacity and revenue-earning potential, high priority will be given to reduce circuit connection losses. In non-blocking networks, of course, connection losses during circuit setup due to blocking, or because of interruption when connections are rearranged, are both eliminated [55]. Moreover, if traffic arrives asynchronously at the input ports then the switching network is advantageously nonblocking in order to handle the traffic efficiently. In such cases, packets at each input port can instantly be delivered to their destination ports if the destination ports are free, and rearrangement of states of the internal switching elements will thus be the lowest. So, non-blocking switching provides a promising technology for the development of all-optical networks.

In chapter 3 we have discussed the problems with designing optical switch networks. Considering all aspects we propose a new switch architecture that has the low loss and crosstalk property similar to the Banyan networks and can be strictly nonblocking like double crossbar or Spanke's network. It has one more advantage that it can be customized in terms of crosstalk and loss with hardware cost. The switch network incorporates the concept of independent building blocks.

4.2 Preliminaries

We shall use the term *switching element* or *SE* for short for $1\times2, 2\times2$ and 2×1 types of optical switches. We consider a *directional coupler* or similar devices as switching elements. When a small $m \times n$ network is used as a building block of a large network, we use the term $m \times n$ switch rather than $m \times n$ network. We also use *switch* and *switching element* interchangeably.

We consider the *switch count* as the representative measure for the hardware cost. It is the total number of switching elements required in the network. The *maximum signal loss*, is given by the maximum number of *SE*s on a signal path. The *maximum crosstalk*, is given by the maximum number of crosstalk *SE*s on a signal path, where a crosstalk *SE*, denoted by *CSE*, is an *SE* that carries signals at both of its two inputs at the same time.

For an $N\times N$ optical switching network, where N represents the number of inputs and outputs of the network, we denote its total number of *SE*s by T_N, its maximum signal loss by S_N and its maximum crosstalk by C_N.

4.2.1 Crossbar Network

An $N \times M$ optical crossbar network requires $T_N = NM$ switching elements. Figure 4.1 shows a crossbar network for N=M=4.

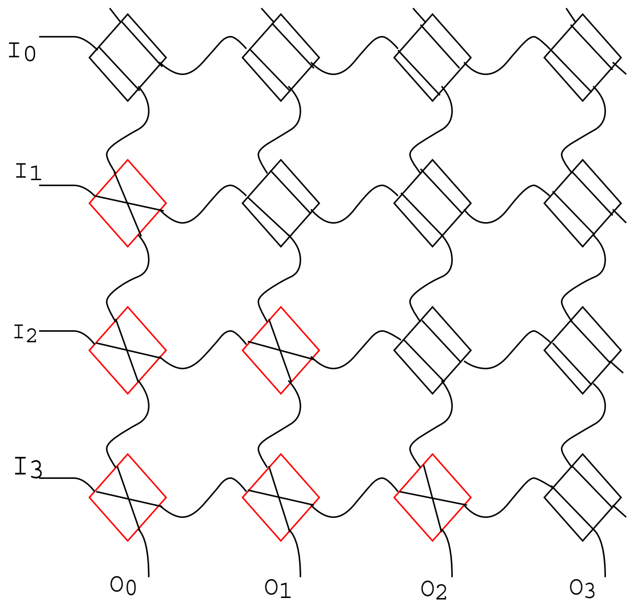

Figure 4.1: A 4×4 crossbar network with crosstalk *SE*s on a signal path

Clearly we can obtain from Figure 4.1:

$$S_N = N + M - 1, \tag{4.1}$$

$$C_N = \min(N, M) - 1. \tag{4.2}$$

For a square crossbar network (i.e. N=M), C_N = N-1.

4.2.2 Clos Network

The Clos network has three stages and its connection pattern is shown in Figure 4.2. Let p be the number of inputs of each input switch, q be the number of middle stage switches and r the number of input (output) switches. Each input switch has p inputs and q outputs. For $N \times N$ networks, the number of input (output) switches is $r = N/p$. The number of middle stage switches is q and each of them is a $r\times$ r switch.

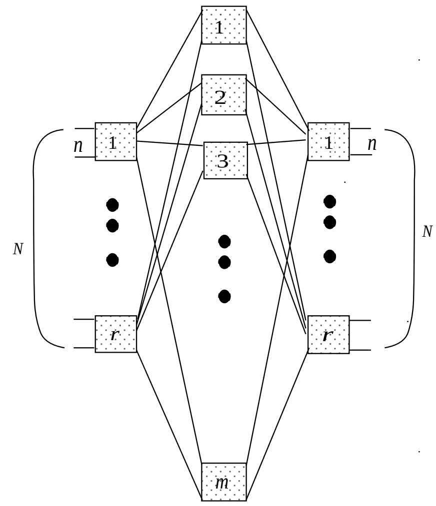

Figure 4.2: A 3-stage Clos network

The total number of *SE*s of the Clos network is

$$T_N = 2pqr + qr^2. \tag{4.3}$$

The Clos network reduces the total number of switching elements required in a crossbar when N>25 and the optimum value is achieved when $N = p^2$. Again, to be nonblocking, the number of middle stage switches should satisfy $q = 2p$-1 [57]. So we can rewrite equation (4.3) as,

$$\begin{aligned} T_N &= (2p-1)(2pr+r^2) \\ &= 3p^2(2p-1). \end{aligned} \tag{4.4}$$

The maximum signal loss and crosstalk can be obtained directly from equations (4.1) and (4.2), respectively:

$$
\begin{aligned}
S_N &= (p + 2p - 1) - 1 + 2r - 1 + (2p - 1 + p) - 1 \\
&= 6p + 2r - 5 = 8p - 5, && (4.5) \\
C_N &= p - 1 + r - 1 + p - 1 = 2p + r - 3 = 3(p - 1). && (4.6)
\end{aligned}
$$

4.3 A New Switch Architecture

Lemma 1 *An $N \times N$ nonblocking network can be built by shuffling the outputs of two nonblocking switches of size $\frac{N}{2} \times N$ to the inputs of N switches of size 2×1.*

Figure 4.3 illustrates an $N \times N$ nonblocking network constructed by Lemma 1.

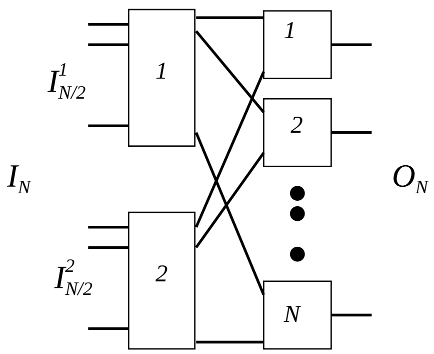

Figure 4.3: An $N \times N$ nonblocking network with two $\frac{N}{2} \times N$ nonblocking switches connected with N *SE*s

Proof Let $I^1_{N/2} = \{1, 2, \ldots, \frac{N}{2}\}$ and $I^2_{N/2} = \{\frac{N}{2} + 1, \frac{N}{2} + 2, \ldots, N\}$ be the input sets of input switches 1 and 2, respectively. Let $Q^1_{N/2} = Q^2_{N/2} = \{1, 2, \ldots, p, \ldots, N\}$ be the output sets of input switches 1 and 2, respectively. Let I_N be the set of inputs of the $N \times N$ network. Then, any input $i \in I_N$ can be connected at any time to either $Q^1_{N/2}$ or $Q^2_{N/2}$. Let O_N be the set of output switches that represents the output as each output switch has one output connection. So, O_N = {1,2,...,N}. The connection pattern between outputs of input switches and inputs of output switches is a shuffle-exchange.

As input switches are non-blocking and have $N/2$ inputs and N outputs, any input can reach any of its N outputs. So, at most $N/2$ of N outputs of an input switch can be busy. Again, any of the N output stage switches can be reached from two input switches by two different links. Each output switches can be connected to only one input at any time. So, it is impossible for two inputs to occupy the same output switch simultaneously.

When N-1 connections are already established, there are N-1 output switches busy through N-1 inputs. Suppose that only the i-th input and the j-th output are free and it is required to connect the i-th input to the j-th output which is connected to the j-th output switch. The j-th switch has two input links that are free. Assume that these two links are connected to the p-th output of each of the input switches 1 and 2, respectively. As switches 1 and 2 are non-blocking, the i-th input can reach the p-th output of its switch. So, input i can be connected to output j without disturbing others. □

From Lemma 1, a new architecture for an $\frac{N}{2} \times N$ non-blocking switch is required. Figure 4.4 shows this architecture. An input switch is a 1×2 switching element and the two output switches are $\frac{N}{2} \times \frac{N}{2}$ nonblocking switches.

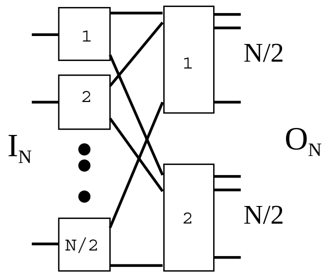

Figure 4.4: An $\frac{N}{2} \times N$ non-blocking switch constructed by N *SE*s shuffled with two $\frac{N}{2} \times \frac{N}{2}$ nonblocking switches

Lemma 2 *An* $\frac{N}{2} \times N$ *nonblocking network can be built using N/2 building blocks of 1×2 switches and two* $\frac{N}{2} \times \frac{N}{2}$ *nonblocking switches.*

Proof Let $I_N = \{1, 2, \ldots, \frac{N}{2}\}$ be the set of inputs, and $O_N = \{1,2,\ldots, \frac{N}{2}, \frac{N}{2}+1,\ldots,N\}$ be the set of outputs. Let Q be the set of outputs of the input switches and P be the set of inputs of the output switches. For any $q \in Q$ and $p \in P$, mapping from Q to P is a function

$$f : q \in Q \rightarrow (p, p + \frac{N}{2}) \in P.$$

Any input switch I_i, i=1,2,..., N/2, has one input and two outputs. So, input i is connected to input switch I_i. There are two output switches, each having $N/2$ inputs and $N/2$ outputs. Input switches are connected to two output switches in the shuffle exchange pattern. Each input has disjoint links to reach two output switches. So, any input can reach the output switches without disturbing other connections. As output switches are nonblocking it holds that once an input from the input stage gets connected to the input of the output switches, it can reach the output without any blocking. □

Figure 4.5 shows an $N \times N$ network using $\frac{N}{2} \times \frac{N}{2}$ switches as building block by applying Lemmas 1 and 2 recursively. We call this method the *recursively nonblocking construction.*

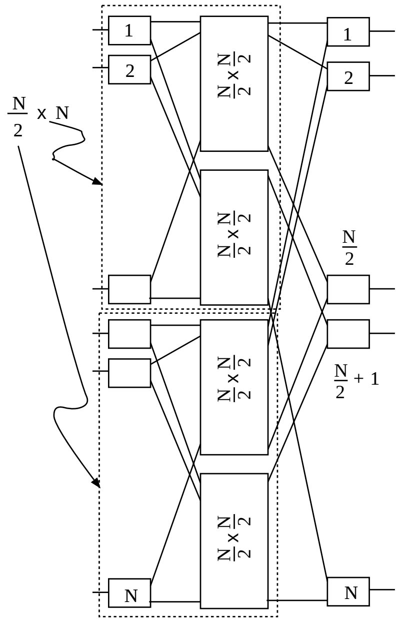

Figure 4.5: An $N \times N$ non-blocking network using the proposed architecture

Let RN(N, m) denote an $N \times N$ network constructed by a recursively nonblocking construction of building blocks of $m \times m$ switches with T_m switches, S_m maximum signal loss and C_m maximum crosstalk. The following theorem depicts the properties of RN(N, m):

Theorem 1 *RN(N, m) is a strictly nonblocking network and its total number of switches, maximum signal loss and maximum crosstalk are given by the following equations, respectively:*

$$T_N = 4^{\log_2(\frac{N}{m})} T_m + 2N(2^{\log_2(\frac{N}{m})} - 1), \quad (4.7)$$

$$S_N = S_m + 2\log_2\left(\frac{N}{m}\right), \quad (4.8)$$

$$C_N = C_m. \quad (4.9)$$

Proof

Since RN(N, m) is obtained by the recursively (strictly) nonblocking construction by applying Lemmas 1 and 2, the resulting network itself must be strictly nonblocking.

To work out T_N, we get by applying recursively nonblocking construction as shown in Figure 4.5

$$T_N = 4(T_{\frac{N}{2}} + \frac{N}{2}).$$

Solving the above recursion results in equation (4.7):

$$T_N = 4(4(4(\cdots 4(T_m + m) \cdots + \frac{N}{8}) + \frac{N}{4}) + \frac{N}{2})$$

$$
\begin{aligned}
&= 4^{\log_2(\frac{N}{m})}T_m + 4^{\log_2(\frac{N}{m})}m + \frac{\log_2(\frac{N}{m})}{4}2m + \frac{4^{\log_2(\frac{N}{m})}}{4^2}4m + \cdots + 8N + 4N + 2N \\
&= 4^{\log_2(\frac{N}{m})}T_m + \frac{N^2}{m^2}m + \frac{N^2}{4m^2}2m + \frac{N^2}{4^2m^2}4m + \cdots + 8N + 4N + 2N \\
&= 4^{\log_2(\frac{N}{m})}T_m + 2N(\frac{N}{2m} + \frac{N}{4m} + \frac{N}{8m} + \cdots + 4 + 2 + 1) \\
&= 4^{\log_2(\frac{N}{m})}T_m + 2N(2^{\log_2(\frac{N}{m})} - 1).
\end{aligned}
$$

To obtain equation (4.8), from Figure 4.5 we have for RN(N, m),

$$
\begin{aligned}
S_N &= S_{\frac{N}{2}} + 2 \\
&= (S_{\frac{N}{4}} + 2) + 2 \\
&= (\cdots(S_m + 2) + \cdots 2) + 2 \\
&= S_m + 2\log_2\left(\frac{N}{m}\right).
\end{aligned}
$$

Since all paths contain the same number of switches, the maximum signal loss is S_N.

For obtaining crosstalk C_N in RN(N, m), we point out that by definition a switch produces crosstalk when it carries two signals through its two ports and the crosstalk of a network is the number of crosstalk *SE*s (*CSE*s) in a signal path. Therefore from Figure 4.5 we have:

$$C_N = C_m.$$

That is, only the building block contributes crosstalk to the network since all other switching elements are either 1×2 or 2×1 switches. Therefore equation (4.9) holds. This completes the proof. □

4.4 Two Examples

We shall note that although RN(N, m) is itself strictly nonblocking, to some degree it also inherits the blocking property from its building block. Any $m \times m$ network can be used as the building block for designing an $N \times N$ network using our architecture. In this section, we show two implementations of our network, RN$(8, 4)$ and RN$(8, 2)$, using a 4×4 switch and a 2×2 switch as the building block, respectively.

4.4.1 RN(N, 4) Network

In the first example, we use m=4 and the 4×4 wide-sense nonblocking Benes network [68] as building block. Figure 4.6 shows a 8×8 network using 4×4 switches as the building block.

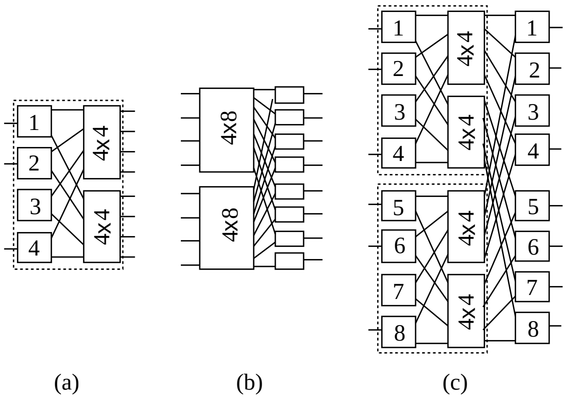

Figure 4.6: (a) A 4×8 network with 4×4 switches. (b) RN$(8, 4)$: 8×8 network using 4×8 switches. (c) Detailed connection pattern of (b).

So, for the $N \times N$ network equations (4.7), (4.8) and (4.9) can be rewritten as:

$$T_N = 4^{\log_2(\frac{N}{4})} T_4 + 2N(2^{\log_2(\frac{N}{4})} - 1) = \frac{N^2}{16} T_4 + 2N(\frac{N}{4} - 1), \tag{4.10}$$

$$S_N = S_4 + 2\log_2\left(\frac{N}{4}\right) = S_4 + 2\log_2 N - 4, \tag{4.11}$$

$$C_N = 4. \tag{4.12}$$

Benes [68] recognized the following structure composed of eight 2×2 switches as a 4×4 wide-sense non-blocking switch. He mentioned that if some states of the switch are avoided, it will behave like a non-blocking switch in the wide-sense. Smyth [55] also showed that it is nonblocking in the wide-sense. In Chapter 5, we will discuss and present necessary algorithm for setting up connections in this switch in detail. Figure 4.7 shows the 4×4 wide-sense nonblocking (hereafter WSNB) switching structure.

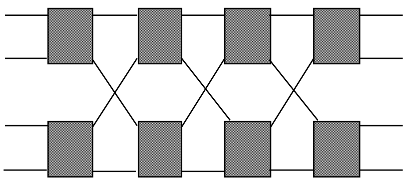

Figure 4.7: A 4×4 wide sense nonblocking switch network composed of eight 2×2 optical switches

We use this switch as the building block in our example. Since $T_m = T_4 = 8$, $S_m = S_4 = 4$, and $C_m = C_4 = 4$, equations (4.10), (4.11) and (4.12) for RN(N,4) can thus be written as

$$T_N = \frac{N^2}{16} 8 + 2N(\frac{N}{4} - 1) = \frac{N^2}{2} + \frac{N^2}{2} - 2N = N^2 - 2N = O(N^2), \tag{4.13}$$

$$S_N = 4 + 2\log_2 N - 4 = 2\log_2 N = O(\log_2 N), \tag{4.14}$$

$$C_N = C_m = 4 = \text{constant}. \tag{4.15}$$

4.4.2 RN(N, 2) Network

In the second example, we consider a 2×2 optical switch (e.g. directional coupler) as the building block. Here $T_2 = S_2 = C_2 = 1$. Figure 4.8 shows an 8×8 network using 2×2 switches as building block, i.e. RN(8, 2).

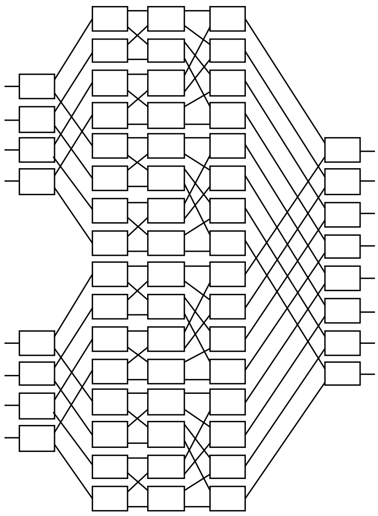

Figure 4.8: An 8×8 strictly nonblocking switch using 2×2 switches as building block

The total number of switches in RN(N, 2) is,

$$T_N = 4^{\log_2(\frac{N}{2})}1 + 2N(2^{\log_2(\frac{N}{2})} - 1) = \frac{N^2}{4} + 2N(\frac{N}{2} - 1) = 1.25N^2 - 2N. \tag{4.16}$$

The *maximum signal loss* for such a network is

$$S_N = 1 + 2\log_2\left(\frac{N}{2}\right) = 1 + 2\log_2 N - 2\log_2 2 = 2\log_2 N - 1. \tag{4.17}$$

By equation (4.9), $C_N = C_2 = 1$.

It is clear that, though $RN(N, 2)$ uses slightly more switches than $RN(N, 4)$, its crosstalk and signal loss are considerably reduced.

4.5 Generalization of RN(N,m) Networks

High cost of optical switches is often a matter of concern for constructing any optical switch networks. To reduce the switch count of a network, strictly nonblocking Clos networks are used. We have discussed necessary conditions for an optimized Clos network in the previous chapter. However, Clos architecture is not an independent architecture. Clos network is constructed using other strictly nonblocking switch as the building blocks.

Usually crossbar networks are used as the building blocks of Clos network. We have seen in Chapter 3, Clos requires non- square size of switches as the building block. But $RN(N, m)$ networks is always square in size, and also constructed from square size of building blocks. To use this network in Clos architecture we have modified the RN(N,m) and proposed a more general switch architecture named as *Generalized Recursive Networks.*

In this architecture, any $M \times N$ nonblocking switch network can be built with building blocks of given size $m \times n$, where $\log_2\left(\frac{M}{m}\right)$ and $\log_2\left(\frac{N}{n}\right)$ are integers. We show that the proposed network is selfrouting for all $N!$ permutations and the propagation delay is $O(\log_2 N)$. We also show that both $RN(N, m)$ and Spanke's networks are special cases of this network.

4.5.1 Optical Crossbar and Clos Networks with Building Blocks

Given a building block of size $n \times m$ and $N \times M$ crossbar optical switch network can be constructed as shown in Figure 4.9 if N, m, n are even numbers, and M and N are integer multiples of m and n respectively. Let $T_{N\times M}$ be the total number of switches required to construct the network, $S_{N\times M}$ be the maximum signal loss and $C_{N\times M}$ be maximum crosstalk. Then these parameters of the crossbar network are given by,

$$
\begin{aligned}
T_{N\times M} &= \frac{4MN}{mn}, &(4.18)\\
S_{N\times M} &= \left(\frac{2N}{n} + \frac{2M}{m} - 1\right) S_{n\times m}, &(4.19)\\
C_{N\times m} &= \{min\left(\frac{2M}{m}, \frac{2N}{n}\right) - 1\} C_{n\times m}, &(4.20)
\end{aligned}
$$

where $S_{n\times m}$ and $C_{n\times m}$ are the maximum signal loss and the maximum crosstalk of the building block respectively.

When 2×2 directional couplers (*SE*s) are considered as the building blocks then equations (4.18), (4.19), (4.20) turns into,

$$
\begin{aligned}
T_{N\times M} &= NM, &(4.21)\\
S_{N\times M} &= N + M - 1, &(4.22)\\
C_{N\times M} &= \min(N, M) - 1. &(4.23)
\end{aligned}
$$

For square network, where $N = M$, $T_{N\times N} = T_N = N^2$. Similar is true for other suffices. Figure 4.9 turns similar to Figure 3.7.

Clos network is a three-stage nonblocking switch network. Crossbar is widely used as the building block of Clos network since crossbar network can be non-square as well as nonblocking. Thus Clos networks inherit the problems of high crosstalk and high loss of building block crossbar networks.

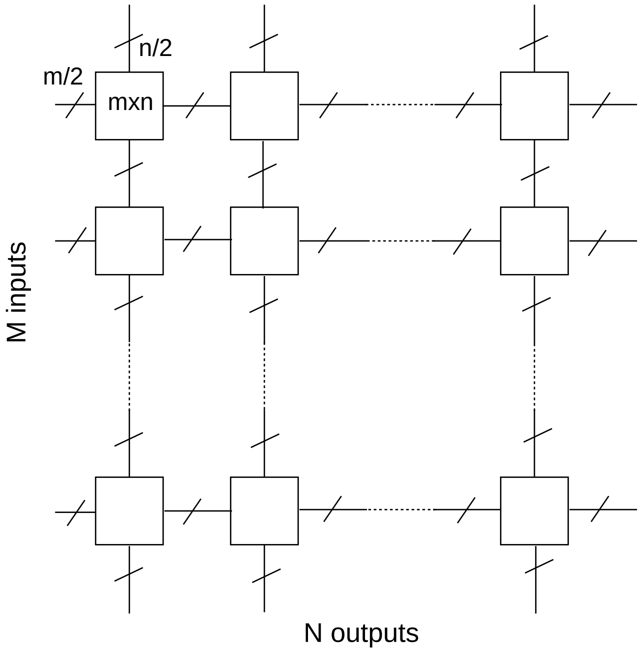

Figure 4.9: Optical crossbar network with building blocks

For $N \times N$ nonblocking Clos network, let p is the number of inputs (outputs) of each input (output) switch, q is the number of middle stage switches, r is the number of input (output) switches and $q = 2p-1$ then, $T_{p\times(2p-1)}$ is the switch count of each input switch, $T_{r\times r}$ is the switch count of each middle stage switch and $T_{(2p-1)\times n}$ is the switch count of each output switch. Since the switch count, loss and crosstalk for input switches and output switches are the same for the same type of building blocks we get equations (4.24),(4.25),(4.26).

$$T_{N\times N}\ (orT_N) = 2rT_{p\times 2p} + (2p-1)T_{r\times r}, \tag{4.24}$$

$$S_{N\times N}\ (orS_N) = 2S_{p\times(2p-1)} + S_{r\times r}, \tag{4.25}$$

$$C_{N\times N}\ (orC_N) = 2C_{p\times(2p-1)} + C_{r\times r}, \tag{4.26}$$

where $S_{p\times(2p-1)}$ is the maximum signal loss of each input and output switches, and $S_{r\times r}$ is the maximum signal loss of each middle switches. Similarly, $C_{p\times(2p-1)}$ is the maximum crosstalk of each input and output switches, and $C_{r\times r}$ is the maximum crosstalk of each middle switches.

If we consider crossbar switches as building blocks for the Clos networks then equations (4.24),(4.25),(4.26) turns into equations (4.4),(4.5),(4.6).

4.5.2 Generalized Recursive Networks (GRN)

Our objective is to construct a nonblocking switch network of size $N \times M$, with building blocks of size $n \times m$ where $\log_2\left(\frac{N}{n}\right)$ and $\log_2\left(\frac{M}{m}\right)$ are integers.

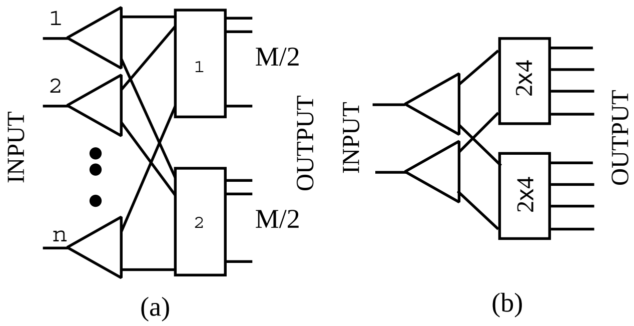

Figure 4.10: (a) $n \times M$ GRN: two $n \times \frac{M}{2}$ nonblocking switches are connected with n switching elements in shuffle-exchange fashion. (b) An example of $n \times M$ GRN where $n = 2$ and $M = 8$.

Lemma 3 *An $n \times M$ GRN is defined as a nonblocking switch network consisting of 2 building blocks of $n \times \frac{M}{2}$ nonblocking switches connected in shuffle-exchange fashion with n 1×2 switching elements. If the size of the building block is $n \times m$, then the number of building blocks required is $\frac{M}{m}$ and the number of switching elements required at the input side is $m\left(\frac{N}{n} - 1\right)$.*

Figure 4.10 shows an example of the $n \times M$ network.

Proof If an input is free, it means both of its output links to output switches are free. So, a free input can always reach both the output switches. Since output switches are nonblocking, the free input can reach the free output without disturbing other connections.

If $T_{n\times M}$ is the switch count of the $n \times M$ network and $T_{n\times \frac{M}{2}}$ is the switch count of the $n \times \frac{M}{2}$ network then from Figure 4.10 we can write,

$$\begin{aligned} T_{n\times M} &= n + 2T_{n\times\frac{M}{2}} \\ &= n + 2(n + \ldots + 2(n + 2T_{n\times m})\ldots) \\ &= n\left(\frac{M}{m} - 1\right) + \frac{M}{m}T_{n\times m}, \end{aligned} \tag{4.27}$$

where $T_{n\times m}$ represents the switch count. Here $n\left(\frac{M}{m} - 1\right)$ is the total number of input stage switches and $\frac{M}{m}$ is the total number of building blocks required for the $T_{n\times M}$ network. □

Lemma 4 *An $N \times m$ GRN is defined as a nonblocking switch network consisting of m switching elements connected with 2 building blocks of $\frac{N}{2} \times m$ nonblocking switches in a shuffle-exchange fashion. If the size of the building blocks is $n \times m$ then the number of building blocks required is $\frac{N}{n}$ and the number of switching elements required is $m\left(\frac{N}{n} - 1\right)$.*

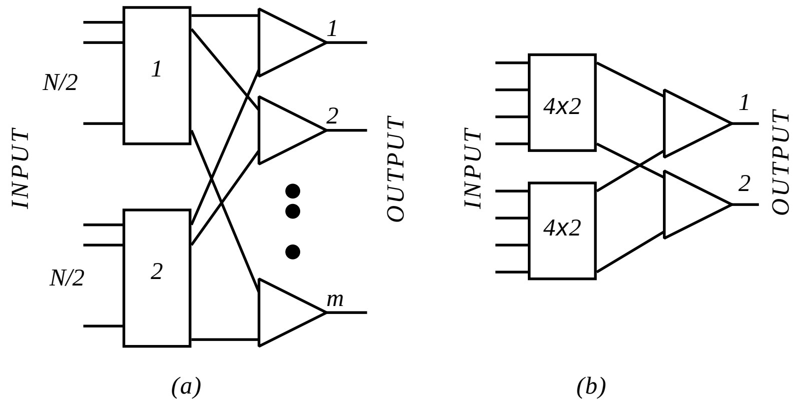

Figure 4.11: (a) $N \times m$ GRN: two $\dfrac{N}{2} \times m$ nonblocking switches are connected with m switching elements in shuffle-exchange fashion. (b) An example of $N \times m$ GRN where $N = 8$ and $m = 2$.

Figure 4.11 shows the construction of an $N \times m$ GRN with an example.

Proof With the same argument as in Lemma 3, we can prove that this network will be nonblocking. Let $T_{N\times m}$ be the switch count of $N \times m$ network and $T_{\frac{N}{2}\times m}$ be the same for $\dfrac{N}{2} \times m$ network, then from the symmetry of Figure 4.11 we can write,

$$\begin{aligned} T_{N\times m} &= m + 2T_{\frac{N}{2}\times m} \\ &= m + 2(m + \ldots + 2(m + 2T_{n\times m})\ldots) \\ &= m\left(\frac{N}{n} - 1\right) + \frac{N}{n}T_{n\times m}. \end{aligned} \tag{4.28}$$

Here $m\left(\dfrac{N}{n} - 1\right)$ is the total number of output stage switches and $\dfrac{N}{n}$ is the total number of building blocks required for the $T_{N\times m}$ network. □

To construct an $N \times M$ GRN with building blocks of $n \times m$ nonblocking switches, first we use Lemma 3 to make a $n \times M$ GRN, then we use Lemma 4 considering this $n \times M$ network as the building block. The total number of switches required for such a non-square nonblocking network is given in Theorem 2.

Theorem 2 *$N \times M$ GRN, constructed from building blocks of $n \times m$ strictly nonblocking switches, is a strictly nonblocking network and the switch count ($T_{N\times M}$), maximum signal loss ($S_{N\times M}$) and maximum crosstalk ($C_{N\times M}$) are given by following equations respectively:*

(a) $T_{N\times M} = \left(\dfrac{MN}{m} + \dfrac{MN}{n} - N - M\right) + \dfrac{MN}{mn}T_{n\times m}$, where $\dfrac{MN}{mn}$ represents the total total number of building blocks of size $n \times m$ and $\left(\dfrac{MN}{m} + \dfrac{MN}{n} - N - M\right)$ represents the total number of switching elements. $T_{n\times m}$ is the switch count of the building block.

(b) $S_{N\times M} = \log_2\left(\frac{M}{m}\right) + \log_2\left(\frac{N}{n}\right) + S_{n\times m}$*, where* $S_{n\times m}$ *is the maximum signal loss of the building block* $n\times m$*.*

(c) $C_{N\times M} = C_{n\times m}$*, where* $C_{n\times m}$ *is the maximum crosstalk of the building block* $n\times m$*.*

Proof To construct an $N\times M$ GRN, first we use Lemma 3 to make a $n\times M$ GRN from $n\times m$ switches. Since $n\times m$ is strictly nonblocking, the $n\times M$ is also a strictly nonblocking network. Next we use Lemma 4 considering the $n\times M$ network as the building block and construct the $N\times M$ GRN. Since $n\times M$ is a strictly nonblocking network, the $N\times M$ network is also strictly nonblocking. So, from the symmetry of construction we can write,

$$\begin{aligned} T_{N\times M} &= M + 2T_{\frac{N}{2}\times M} \\ &= M\left(\frac{N}{n}-1\right) + \frac{N}{n}T_{n\times M}. \end{aligned} \tag{4.29}$$

Now putting the value of $T_{n\times M}$ from equation (4.27) we get,

$$T_{N\times M} = \left(\frac{MN}{m} + \frac{MN}{n} - N - M\right) + \frac{MN}{mn}. \tag{4.30}$$

Here $\left(\frac{MN}{m} + \frac{MN}{n} - N - M\right)$ is the total number of *SE*s and $\frac{MN}{mn}$ is the total number of building blocks of size $n\times m$ in the switch network.

A signal has to cross $\log_2\left(\frac{M}{m}\right)$ input-stage switches, $\log_2\left(\frac{N}{n}\right)$ output-stage switches and only one building block. If $S_{n\times m}$ is the maximum signal loss of the building block, then

$$S_{N\times M} = \log_2\left(\frac{M}{m}\right) + \log_2\left(\frac{N}{n}\right) + S_{n\times m}.$$

The only possible elements that contribute crosstalk are the building blocks. If $C_{n\times m}$ is the maximum crosstalk of a building block, then $C_{N\times M} = C_{n\times m}$. □

4.5.3 Two Special Cases of GRN

In this section we show that $RN(N,m)$ and Spanke's network are two special cases of GRN. The expression of the switch count for an $RN(N,m)$ network given in equation (4.7) can be rewritten as

$$T_N = \frac{N^2}{m^2}T_m + 2N\left(\frac{N}{m}-1\right).$$

Let us consider a GRN where $M = N$ and $m = n$. With this consideration equation (4.30) becomes as follows:

$$T_{N\times N} = \frac{N^2}{m^2}T_{m\times m} + 2N\left(\frac{N}{m}-1\right).$$

Since T_m and $T_{m\times m}$ the same building block, GRN and $RN(N,m)$ have the same number of switches when $N = M$ and $n = m$. It is also easy to check that the maximum signal loss

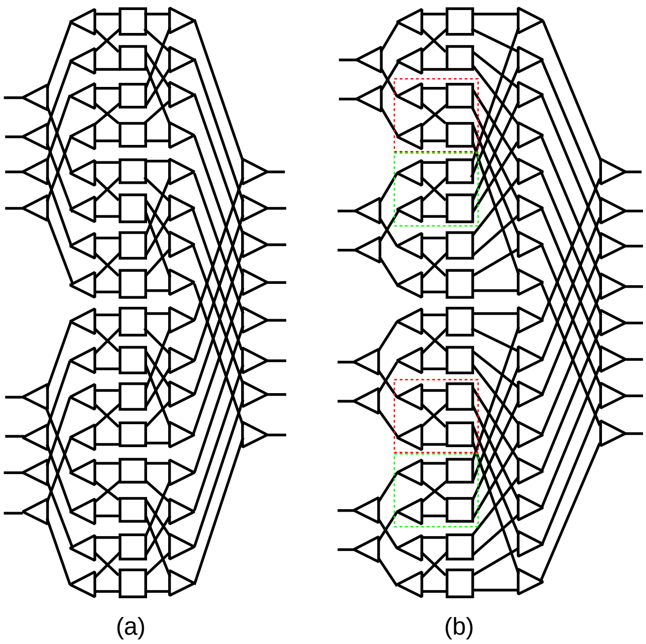

Figure 4.12: Shapes of GRN and RN(N,m) networks.

and maximum crosstalk of the above GRN are also the same as those of $RN(N, m)$. The shape of these two networks have been shown in Figure 4.12. The shapes look different because of their differences in iteration (recursion) sequence.

Figure 4.13(a) shows a 4×4 GRN network with 2×2 switch as the building block. According to Lemma 3, if $m = 2$ and $n = 2$, then an $n \times m$ GRN can be constructed as shown in Figure 4.13(b) using only 1×2 and 2×1 switches. Replacing each 2×2 switch in Figure 4.13(a) with such a 2×2 GRN we get Figure 4.13(c), which is a Spanke's network. The total number of switching elements required for this network is $2N^2 - 2N$ which is the same as a Spanke's network [78].

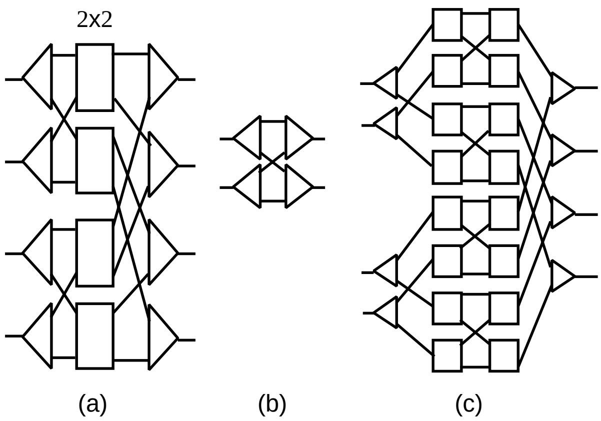

Figure 4.13: (a) 4×4 GRN (b) 2×2 GRN. (c) 4×4 Spanke's network. No crosstalk *SE*s along a signal path.

4.5.4 GRN in Clos networks

GRN can be a good candidate for building blocks in Clos networks. The resulting Clos network will then have smaller switch count, lower signal loss and lower crosstalk. The size of each input (or output) switch is $p \times q$ (or $q \times p$) and the size of each middle switch is $r \times r$. Clos network is nonblocking and has minimum crosspoints on two conditions:

(a) $N = p^2$ i.e $r = p$ and

(b) $q = 2p - 1$

But the number of inputs or outputs of a GRN can only be a power of 2. So, each input (or output) switch is an $p \times 2p$ (or $2p \times p$) GRN and each middle switch is an $p \times p$ GRN. Let us term a GRN network with $n \times m$ as $GRN(n \times m)$. Then the switch count for $p \times 2p$ GRN with $n \times m$ building block is,

$$T_{p\times 2p,GRN(n\times m)} = \frac{2p^2}{n} + \frac{2p^2}{m} + \frac{2p^2}{mn} - 3p.$$

For $n = m$, if we term the GRN as $GRNm$[1], then the switch count is,

$$T_{p\times 2p,GRNm} = \frac{4p^2}{m} + \frac{2p^2}{m^2} - 3p. \tag{4.31}$$

Similarly, the switch count of a $p \times p$ $GRN(m)$ network is,

$$T_{p\times p,GRNm} = \frac{2p^2}{m} + \frac{2p^2}{m^2} - 2p. \tag{4.32}$$

We refer a Clos-GRNm network as $C - GRNm$ and thus the switch count of such a C-GRNm networks is obtained from equation (4.24) as,

$$T_{N,C-GRNm} = \frac{12p^3}{m} + \frac{6p^3}{m^2} - \frac{2p^2}{m} - \frac{p^2}{m^2} - 10p^2 + 2p. \tag{4.33}$$

The maximum signal loss of Clos-GRN networks is obtained from equation 4.25 as follows:

$$\begin{aligned} S_{N,C-GRNm} &= 2(\log_2\left(\frac{p}{m}\right) + \log_2\left(\frac{2p}{m}\right) + S_m) + (2\log_2\left(\frac{p}{m}\right) + S_m) \\ &= 4\log_2\left(\frac{p}{m}\right) + 2\log_2\left(\frac{2p}{m}\right) + 3S_m \end{aligned} \tag{4.34}$$

The maximum crosstalk of a Clos-GRN network, $C_{N,C-GRN(m)}$, is determined by the following equation:

$$C_{N,C-GRNm} = 3C_m \tag{4.35}$$

[1] $GRNm$ is the short form of $GRN(m \times m)$

Chapter 5

Building Block Structure for GRN

The building block plays an important role in GRN networks. We can use any networks as building block but the target GRN will then inherit the properties from the building block. If we use a blocking network as the building block then the resulting GRN will be a blocking network. Understanding this reality we have proposed two wide-sense nonblocking (WSNB) networks as building block. WSNB switch has always lower switch count. So the hardware cost is lower than that of strictly nonblocking networks. On the other hand WSNB switch has higher computation complexity. That is why a building block should be of small size with reasonably faster connection setup speed. Our proposed two networks consist of the fewest known optical switching elements. They have their own routing algorithms.

5.1 3×3 Wise-sense Nonblocking Networks

Initially the 3×3 wide-sense nonblocking networks was proposed for for survivability of self-healing ring networks [79]. The author presented the necessary switching algorithm along with circuit diagram. For the brevity of our discussion we redefine the *Wide Sense Non -Blocking* switch.

Definition 2 *Let the switch has N ($N \geq 3$) inputs and outputs. If r ($2 \leq r \leq N$) inputs and outputs agree to interchange their interconnections (routes), and for setting up connections if they do not interrupt traffic through any of the rest ($N - r$) routes, then the switch is said to be a wide sense non-blocking switch.*

A 2×2 optical switch is inherently a non-blocking switch. But when $N > 2$ then the design of the switch with minimum number of 2×2 switch needs special attention to make it non-blocking.

5.1.1 Properties of 3x3 Nonblocking Optical Switches

A 3×3 switch has six possible states as shown in Figure 5.1. Such a WSNB switch must have the following properties:

1. All six possible states are achievable and
2. For transitions from one state to any other state where a route has to be preserved, the traffic through the unchanged route must not be interrupted, e.g. during the transition from state **a** to state **c** the traffic between input port *2* and output port *2* must not be interrupted.

The six different states are represented as **a** (*11 22 33*), **b** (*11 23 32*), **c** (*13 22 31*), **d** (*12 21 33*), **e** (*12 23 31*) and **f** (*13 21 32*). First digit represents the input ports and second digits represent output ports (Figure 5.1) i.e., *12* means input port *1* is connected to output port *2*.

5.1.2 State Transitions

From Figure 5.1 we see that although every states may have transitions to five other states, only three of them require to have a route preservation; such as from state **a** to states **b**, **c** and **d** require preservation of routes *11, 22* and *33* respectively. Figure 5.2 is the transition diagram of all states keeping a route preserved. Nodes **a, b, c, d, e** and **f** represent six different states of a 3×3 switch. Links among them represent transitions to other states and integer numbers beside the links represent the routes to be preserved for that transition.

5.1.3 Structure of the 3x3 (WSNB) Switch

Figure 5.3 represents the proposed 3×3 wide-sense nonblocking switch which is comprised of four 2×2 optical switches (or *SE*s). Each switching element has two status — *cross* and *bar* — as well as two states. State *11 22* is established by *Bar* status. State *12 21* is established by *Cross* status. The controller sends signal to the switching elements

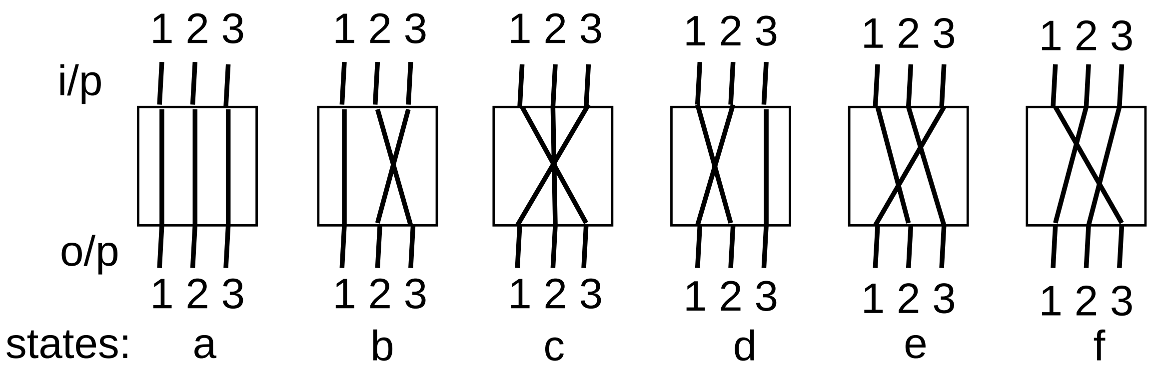

Figure 5.1: Six different states a, b, c, d, e and f

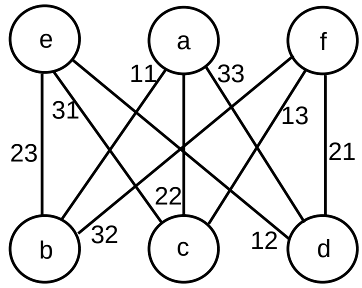

Figure 5.2: Six states showing the three transitions where a route has to be preserved

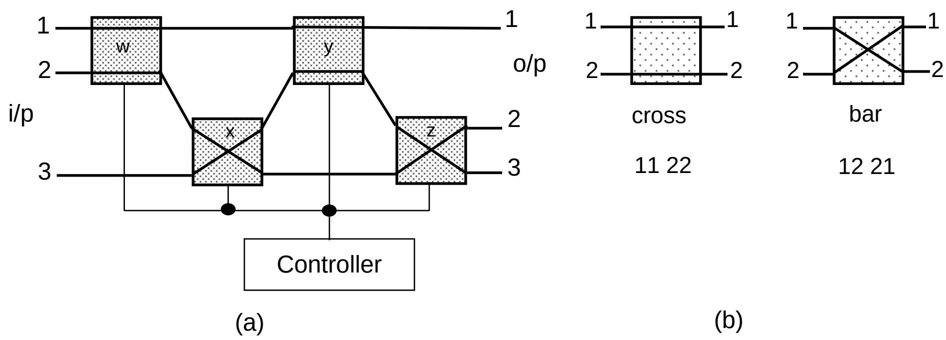

Figure 5.3: (a) Structure of the 3 × 3 WSNB optical switch with 4 *SE*s. (b) Two status' and corresponding states of a switching element(*SE*).

to change their status. The controller must maintain an algorithm described later in this section to setup the status of four switches so that they satisfy the second (WSNB) condition.

Table I: 16 possible status-combinations of 6 different states

States	Status-combinations	Binary code w x y z
a	**A**	0101
	A′	1010
	A″	0000
b	**B**	1011
	B′	0100
	B″	0001
c	**C**	1110
	C′	0111
d	**D**	1101
	D′	0010
	D″	1000
e	**E**	1111
	E′	0110
f	**F**	1100
	F′	0011
	F″	1001

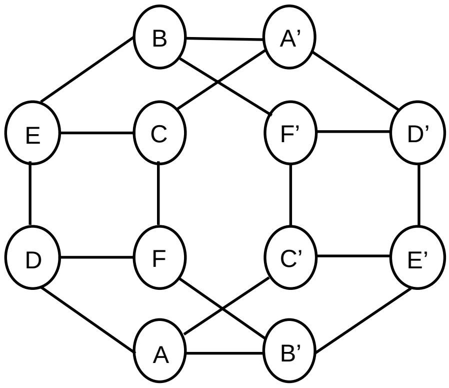

Figure 5.4: The 12 combinations where every state has two possible combinations. The line joining the nodes shows the preferred transitions that will not interrupt the preserved route.

5.1.4 State Representation

Four switching elements altogether in the 3×3 WSNB switch can generate 16 different status-combinations (or combinations) as shown in Table I. However, if we choose more than six combinations to generate the required six states, it is possible to have all the transitions without interrupting the traffic through the preserved route.

A careful study indicates that if we choose six combinations **A** through **F** as well as the other six combinations $\mathbf{A'}$ through $\mathbf{F'}$ to generate the six states so that every state has two status-combinations each, we can have all the transitions satisfying the second condition described earlier. In this case every state will be generated in two different ways (**A** or $\mathbf{A'}, \mathbf{B}$ or $\mathbf{B'}$ etc.). The *present status-combination* of a state will determine which *next status-combination* to choose as the next state from those two combinations for smooth transition. The twelve combinations and their transition sequence are summarized in the Figure 5.4. Each node represents a state of the switch (3×3 WSNB) and equivalent status-combination (as labelled in Table II). A link between two nodes represents their valid transition from one state to other state preserving a route. For example, node **A** and $\mathbf{B'}$ and the link between them represent that if the system is in state **a** with status-combination **A**, then to go to state **b**, the system has to choose status-combination $\mathbf{B'}$; not **B**. Since all six states are interconnected by two hexagon in Figure 5.4, their nonblocking transition is ensured.

5.1.5 State Transition Algorithm

We describe here the algorithm for selecting a particular status- combination to go to the *next state* from the *present state.*

Assumptions:

StateIdx[] is an array that contains six states of the 3×3 WSNB switch.

MainCom[] is an array that contains six non-prime status-combinations corresponding to six different states of the switch.

PrimCom[] is an array that contains six prime status-combinations corresponding to six different states of the switch.

NextState is a variable that contains next state of the switch to be changed to.

NextStatus is a temporary variable that contains the status-combination corresponding to the next state of the switch.

PresentState is a variable that contains the present state of the switch.

PresentStatus is a temporary variable that contains the status-combination corresponding to present state of the switch.

The system is initialized to state *11 22 33* with status-combination **a**. When a new request arrives the requested state is saved in *NextState* variable. Then following algorithm is executed in the control circuit.

Algorithm:

1. Find the status-combination in *MainCom[]* corresponding to *NextState* and save it to *Nextstatus*.

2. If *NextStatus* does not differ with *PresentStatus* in only *1* bit position, find the status-combination in *PrimCom[]* corresponding to *NextStat* and save it to *NextStatus*.

3. Change the state of the switch to the *NextState* with the status-combination *NextStatus*.

4. PresentState := NextState, PresentStatus := NextStatus.

From Table II and Figire 5.4 we see every valid transition i.e. a transition satisfying the second condition, has the code difference of its two combinations in only 1 bit position. If the system is in state **a** with combination **A**(**0101**), then to go state **b** it will choose combination $\mathbf{B'}$(**0100**). We see **A**(**0101**) and $\mathbf{B'}$(**0100**) differs in only 1 bit position (in the least significant bit position). So, before every transition the system first compares the present state's code with the codes of two possible combinations of the target (next) state and choose the combination that differs in only one bit position.

5.2 4×4 Wise-sense Nonblocking Networks

V. E. Bene represented a structure for only 4×4 switch using fewest number of 2×2 switches. In [80] he represented the structure and mentioned that the structure can provide WSNB transition of states if the blocking states are avoided by clever routing algorithm. Figure 4.7 shows the structure of the switch. However, no transition algorithm is available by now. The required constrain or rule that has to be maintained for nonblocking transition is:

Rule 1 Status of the switches must be such that *f(A,B,C,D)*= $A \oplus B + C \oplus D$, where *A, B, C, D* are the status's (*cross* or *bar*) of switches *3, 4, 5* and *6* respectively. *1* represents a cross and *0* represents a bar.

A 4x4 wide sense non blocking switch must satisfy following two conditions:

1. It must have $4! = 24$ different states.
2. It must be able to rearrange the interconnections between any two pair of i/o without interrupting other two routes.

First condition could easily be achieved as there are $8! = 256$ status-combinations of the given 4×4 structure. But the second condition is very restrictive. The best possible way to satisfy the 2nd condition is to find free switch(es) that are not involved in preserved routes and to see if the required state(s) is achievable by changing its status. If we maintain any of Rule 1 then there will always be at least one free switch to change. C.J. Smith [55] has given a way to proof that the switch is wide-sense nonblocking. But here we give a more easy explanation for the switch of being nonblocking.

Explanation:

All four routes intersected each other in different switches. Any one route intersected all other routes and the route intersected another route at least once along the path. So, changing the status of only one switch along a route will interchange the destinations of two routes involved in the switch. All other routes will be uninterrupted. The new state must maintain these characteristics of the switch and it is only possible when the middle switch obeys the rules mentioned above. It is notable that the switch can have as many as six different states keeping one particular route preserved ($(4-1)! = 6$). In the worst case the switch can preserve two routes at the same time. Keeping any two routes preserved the switch can have as many as six different states, because ($^4C_2 = 6$). That is why the routing algorithm must ensure that any time any two routes do not cover all eight switches. Otherwise, preserving those two paths, the switch cannot go to a new state. The structure can be divided into two parts by an imaginary line between two rows. So, only possible way to cover all switches by any two routes is if the middle two switches, those

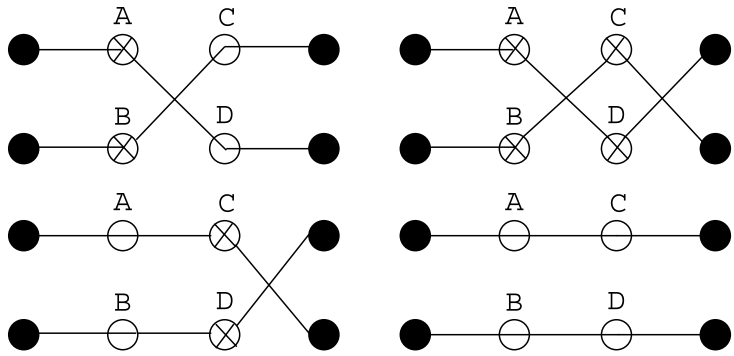

Figure 5.5: Four situations in which the switch can plunge into a blocking state

are opposite to each other in position (in the same column), are in the same sate. The four possible situation in which blocking can arise is depicted in Figure 5.5. All cross dots represents switches in cross position, all blank dots represents switches in bar position and all black dots represent switches in don't care position. Link represents signal path. It is clear that all eight switches are involved in the following four cases. These four cases can be avoided by the Rule 1. For explaining the rule we define some terms:

Definition 3 *The structure is defined by a set* $\mathcal{A}$=*{1,2,3,4,5,6,7,8}. Elements of* $\mathcal{A}$ *are all* 2×2 *switches in the structure.*

Definition 4 *A route is defined by the route-set. A Route-set* $\mathcal{R}_i$ *is defined as the set whose elements are the switches involved in carrying signal on input port i (*$1 \leq i \leq 4$*).*

Definition 5 *A particular state of the switch is represented by sets* $\mathcal{R}_1, \mathcal{R}_2, \mathcal{R}_3$ *and* $\mathcal{R}_4$*.*

For example the state *11 22 33 44* of the 4×4 WSNB is represented as:

$\mathcal{R}_1 = 1, 3, 6, 7$; switches carry input signal at port *1*

$\mathcal{R}_2 = 1, 4, 5, 7$; switches carry input signal at port *2*

$\mathcal{R}_3 = 2, 3, 5, 8$; switches carry input signal at port *3*

$\mathcal{R}_4 = 2, 4, 6, 8$; switches carry input signal at port *4*

Definition 6 $\mathcal{F}_{ij}$ *is a set of switches those are common to routes* ip *or* qj *where* $1 \leq i, j, p, q \leq 4$.

This set will never be empty since each route has intersected any other route at least once (and at most twice). So there must be one or two elements in the set $\mathcal{F}_{ij}$. Changing the status of a switch from this set satisfying Rule 1 provides a new nonblocking state of the structure that contains the new route ij.

We notice the following characteristics:

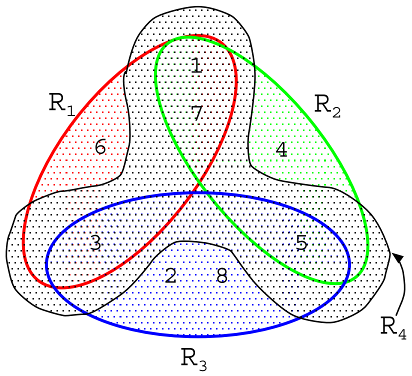

Figure 5.6: Venn diagram representing the 4x4 switch structure

1. $\mathcal{R}_i$ has always four elements. $\mathcal{R}_i \cup \mathcal{R}_j \cup \mathcal{R}_k = \mathcal{A}$; where $i \neq j \neq k,\ 1 \leq i, j, k \leq 4$.

2. $\mathcal{F}_{ij} = \mathcal{R}_i \cap \mathcal{R}_j$; where $i \neq j$.

3. Complement of the union of any two Route-sets is equal to the intersection of another two Route-sets. Mathematically, $\overline{\mathcal{R}_i \cup \mathcal{R}_j} = \mathcal{R}_k \cap \mathcal{R}_l$ where $i \neq j \neq k \neq l$, $1 \leq i, j, k, l \leq 4$. For example, $\overline{\mathcal{R}_1 \cup \mathcal{R}_2} = \mathcal{R}_3 \cap \mathcal{R}_4$.

4. Changing the status of a switch M of set $\mathcal{F}_{ij}$ provides transition to a new state of the 4×4 switch. It affects only two routes $\mathcal{R}_i$ and $\mathcal{R}_j$ those have M as one of their element. $\mathcal{R}_{i,new} = \{\mathcal{R}_M(i)\} \cup \{\mathcal{R}_{M+}(j)\}$,
$\mathcal{R}_{j,new} = \{\mathcal{R}_M(j)\} \cup \{\mathcal{R}_{M+}(i)\}$; Where $\mathcal{R}_M(i)$ represents the set of all elements up to M in $\mathcal{R}_i$ and $\mathcal{R}_{M+}(i)$ represents the set of all elements after M in $\mathcal{R}_k$; similar for $\mathcal{R}_j$. All these characteristics are summarized in Figure 5.6.

The initialized state is *11 22 33 44*. Routes $\mathcal{R}_1, \mathcal{R}_2, \mathcal{R}_3$ are represented by three ellipses. Switches outside the shaded area represent $\mathcal{R}_4$. It is clear that switch 1 and 7 involves routes $\mathcal{R}_1$ and $\mathcal{R}_2$ which is represented by overlapping of ellipses $\mathcal{R}_1$ and $\mathcal{R}_2$ in the Figure 5.6. Similarly looking at the figure we can say switch 3 involves routes $\mathcal{R}_1$ and $\mathcal{R}_3$, switch 6 involves routes $\mathcal{R}_1$ and $\mathcal{R}_4$ etc. We can check if a particular state is non-blocking or not in paper pencil using above diagram.

5.2.1 Transition Algorithm

State *11 22 33 44* is initialized with the status-combination as shown in Figure 5.7(a). If ij is a new route to be establish, then $\mathcal{F}_{ij}$ is the set of switches those are common to routes ip and qj. So, $\mathcal{F}_{ij} = \{x, y\} or \{x\}$

1. Find $\mathcal{F}_{ij}$.

1. choose x from $\mathcal{F}_{ij}$.

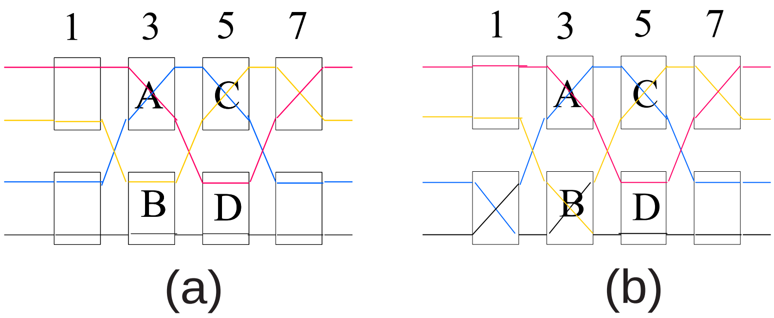

Figure 5.7: Example of state transition

2. (a) if $x \in \{A, B, C, D\}$, then change its state such that Rule 1 holds; otherwise,
   (b) Repeat 2 with y
3. if $x, y \notin \{A, B, C, D\}$ change its state

Example of transition

Let the switch is in initialized state *11 22 33 44*. So, the Route-sets are:

$$\mathcal{R}_{11} = \{1, 3, 6, 7\},$$
$$\mathcal{R}_{22} = \{1, 4, 5, 7\},$$
$$\mathcal{R}_{33} = \{2, 3, 5, 8\},$$
$$\mathcal{R}_{44} = \{2, 4, 6, 8\}.$$

Let a new request *11 24 32 43* arrives. The new route *11* is the same as the old one. So no change takes place in the Route-set $\mathcal{R}_{11}$. The new route *24* is different from the old *22* route. Now, according to algorithm, $\mathcal{F}_{24}$ is determined by comparing Route-sets $\mathcal{R}_{22}$ and $\mathcal{R}_{44}$.

$$\mathcal{F}_{24} = \{4\} \tag{5.1}$$

The status of the switching element 4 is changed (in this case to *cross*)satisfying the Rule 1. New paths established are *24 42* and their corresponding route-sets are:

$$\mathcal{R}_{24} = \{1, 4, 6, 8\},$$
$$\mathcal{R}_{42} = \{2, 4, 5, 7\}.$$

Again, the route *32* in the new request is different from the old state and thereby finds $\mathcal{F}_{32}$ by comparing route-sets $\mathcal{R}_{33}$ and $\mathcal{R}_{42}$ (note route *42* is just established):

$$\mathcal{F}_{32} = \{2, 5\} \tag{5.2}$$

According step 2 in the algorithm we select switching element 2 and check if changing its status violates Rule 1 or not. We see it does not. So the status of switching element 2 is changed and new routes *32 43* are established. Interestingly, switching element 5 could not be chosen as it had violate Rule 1. Next, route *43* in the new request is different from the old one and it had already been established. That's the end of establishing the new request. The state of the WSNB switch is shown in Figure 5.7(b).

5.3 $N \times N$ Wide-Sense Nonblocking Networks

If the building blocks are non blocking and of the size $m \times m$ where $m = 2^k$, then $N \times N$ non blocking switch can be build using those building blocks in the following way. Each column performs partial permutations. It is not known how the middle switch be

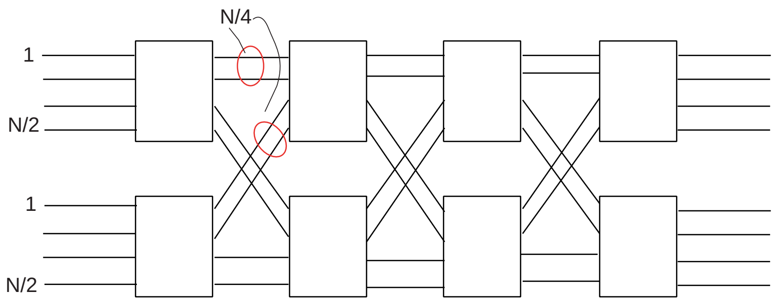

Figure 5.8: Any square size wide-sense nonblocking networks

established to make the switch wide-sense nonblocking. It is an open problem to find out a generalize algorithm for making the switch structure wide-sense nonblocking. However, if we use recursive strategy to build such a WSNB networks, the switch count becomes very large; even higher than crossbar networks.

$$T_N = 8^{\log_2 N - 1} = \frac{N^3}{8}, \tag{5.3}$$

$$S_N = \frac{N^2}{4}, \tag{5.4}$$

$$C_N = \frac{N^2}{4}. \tag{5.5}$$

An 8×8 wide-sense nonblocking networks has the switch count, maximum signal loss and maximum crosstalk as 64, 16 and 16 respectively. Therefore, we say that larger size of wide-sense nonblocking switch constructed in the proposed method cannot give us any benefit.

Chapter 6

Routing in GRN Networks

Self-routing has several advantages over global routing, as the routing time in a self-routing network is the same as the propagation delay in the network. Furthermore, if the address decoding logic at each switch can be kept simple then the hardware cost of a self-routing network will in general be less than that of a network with global routing scheme. Consequently, self-routing reduces the connection complexity for the control lines [81]. Again, as the control function is distributed among different switching modules, the network is less susceptible to faults of a switch. Most of the existing switch networks are not self-routing for all permutation. Banyan and its equivalent networks are self-routing, but they cannot route all N! permutations. Nassimi and Sahni established that many permutations frequently used in parallel computations, which they named class F, can be self-routing through the Benes network [82]. Boppana and Raghevandra showed in [83] that many more permutaions, which they called class L, can also be self-routed by the same network. Barry and Yavuz in [84] showed that Benes network with more than five inputs are not self-routing. They also showed that Clos network whose first stage contains more than two switches are not self-routing. Crossbar network is self-routing for all permutations but it requires the header of size O(N). Moreover, the network uses a global reset signal to all switches. That means, all of the packets must be buffered by the interfacing hardware, and simultaneously sourced into the network with their first bits synchronized with respect to one another [77]. Non-equal path lengths require extra circuitry to handle the variable signal loss and relative delay among paths

We show that the proposed network is self-routing for all N! permutations and the propagation delay is $O(\log_2 N)$.

6.1 Distributed Control Routing

We consider a separate control plane parallel to the optical switch plane as shown in Figure 6.1. The control plane consists of electronic switches. The interconnection pattern of electronic switches in the control plane is the same as that of optical plane. Each

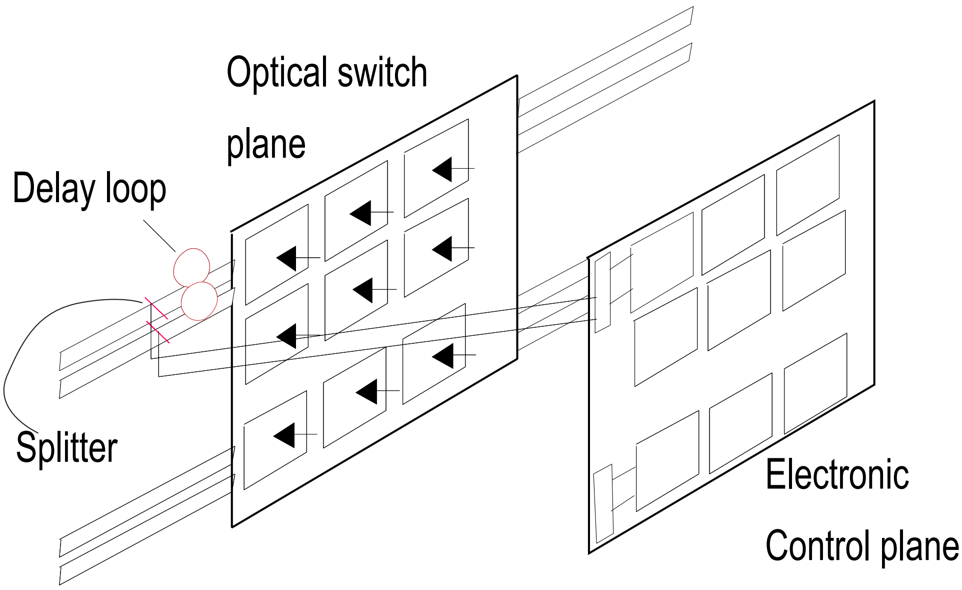

Figure 6.1: Distributed control routing in GRN networks

electronic switch is connected to corresponding optical switches that carries a control signal to the control input of the optical switch.

A portion of light signal is taken away from the input fiber and converted into electronic domain. This electronic signal is sent through the control plane in the self routing fashion. Switches at every stages along the path takes incremental decision about the routing and reaches at the correct output. It is assumed that the control network takes a finite amount of time t_S to establish the route. A fixed delay equal to t_s is inserted in every input to cope with this setup time. The optical signal just passed through the network with this delay. It is also assumed that an acknowledgement from the destination ensures the successful reception of the packet.

6.2 Self-routing in GRN Networks

Figure 6.2 Shows an 8×8 GRN with 2×2 switch as the building block. The column of the building block switches (i.e. 2×2 switches) is called *building-block-stage*. The switches at the left of the *building-block-stage* are called *input stage* switches. Similarly, the switches at the right of the *building-block-stage* are called *output stage* switches.

A signal from an input up to the building-block-stage has paths like a binary tree. Similarly if we track paths of a signal from an output to the building-block-stage, we see that they also form a binary tree. Both these trees have their leaves at the building blocks. Thus we can define following two terms:

Definition 7 *Input tree is the binary tree formed by all possible paths of a signal from an input up to the building-block-stage with the root at the input switch and leaves at the*

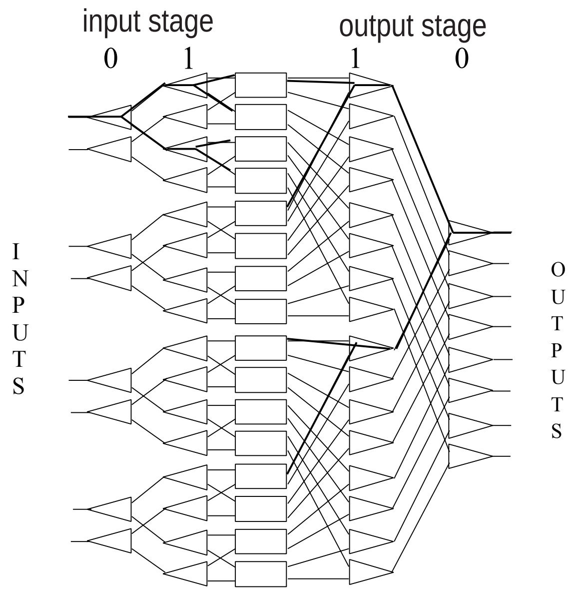

Figure 6.2: Routing in 8×8 GRN with 2×2 switch as the building block.

building blocks.

Definition 8 *Output tree is the binary tree formed by all possible paths of a signal from an output up to the building-block-stage with the root at the output switch and leaves at the building blocks*

In Figure 6.2, both these trees have been shown in thick lines. A signal from an input of the GRN has to cross $\log_2\left(\frac{N}{n}\right)$ switches of the input stage, one building block and $\log_2\left(\frac{M}{m}\right)$ switches of the output stage. Therefore, we divide the whole routing mechanism from an input to an output into three steps:

(a) Routing in the Input Stage

(b) Routing in the Building-block-stage

(c) Routing in the Output Stage

Switches at the input and output stages have the following properties (Figure 6.3):

(i) *Contol_register = 0*, input (output) is connected to output (input) 0.

This state of the switch is called Normal or stable state. The Normal state is decided at the time of manufacturing the optical device.

(ii) *Control_register = 1*, input (output) is connected to output (input) 1.

This state of the switch is called Biased or Quasi-stable state. The optical device remains in this state as long as there is a control potential at its control input.

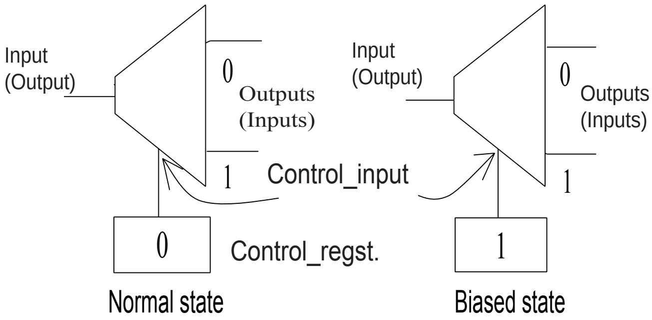

Figure 6.3: Control logic for input and output switches

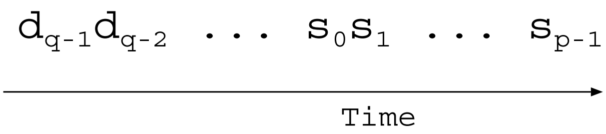

Figure 6.4: Format of the routing tag in the packet header

Let $S = s_{p-1}s_{p-2}\ldots s_0$ be the source address where s_{p-1} is the most significant bit (MSB) and s_0 is the least significant bit (LSB), $D = d_{q-1}d_{q-2}\ldots d_0$ be the destination address where d_{q-1} is the MSB and d_0 is the LSB, and $p = \log_2 M, q = \log_2 N$. The format of the routing tag in the header is shown in Figure 6.4.

6.2.1 Routing Mechanism

We assume that

- Each input and output switches uses 1 bit to decide its state.
- A building block has m inputs and n outputs. Each building block has its own routing strategy. It can route a signal properly with the given source and destination addresses (local to the building block).

Routing in the input-stage

The input switch (the first switch along the signal path) uses the first tag bit arriving at the switch, sets the state of the switch accordingly and sends rest of the tag bits to the next switch along the path up to the building block. Starting from the left, the first $\log_2\left(\frac{N}{n}\right)$ bits are used by the input stage switches, i.e. bit d_{q-1} by *SE* at input stage 0, bit d_{q-2} by *SE* at input stage 1 and so on. Bit $d_{q-\log_2(\frac{N}{n})}$ (i.e. bit $d_{\log n}$) is used by the last *SE* of the input stages. In this way the signal traverse across the input tree from the root to a leaf (the building block). Let **RIS** be the set of bits used for routing in the input stage, then **RIS** $= \{d_{q-1}d_{q-2}\ldots d_{\log n}\}$.

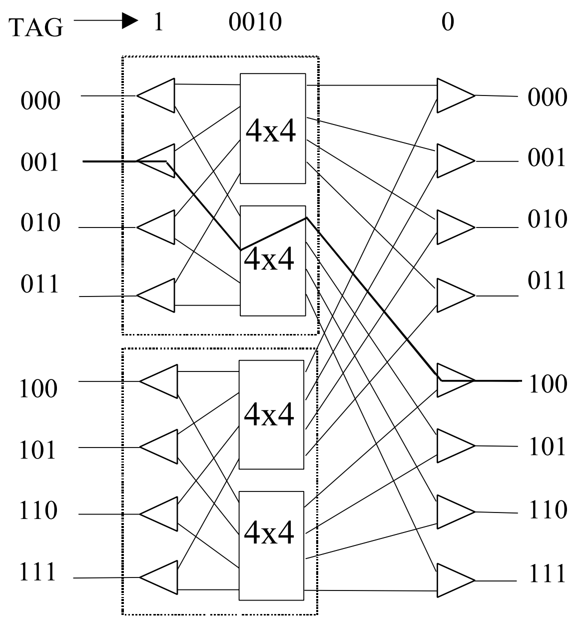

Figure 6.5: Example of self-routing. Input *001* is routed to output *100*

Routing in the Building-block-stage

Bits $d_{\log_2 n-1} \dots d_0 s_0 s_1 \dots s_{\log_2 m-1}$ are used by the building block. Bits $s_{\log_2 m-1} \dots s_1 s_0$ is the source address at the building block, i.e. the signal from the input stage *SE* appears at this input of the building block (i.e. leaf). The building block routes the signal to its output $d_{\log_2 n-1} \dots d_1 d_0$ by its own routing strategy. At this point the signal is at a leaf of the output tree. Let **RBS** be the set of bits used for routing in the building-block-stage, then **RBS** $= \{d_{\log_2 n-1} \dots d_0 s_0 s_1 \dots s_{\log_2 m-1}\}$.

Routing in the output-stage

In this stage the signal is routed from the leaf to the root of the output tree. The last $\log_2 \left(\dfrac{M}{m}\right)$ bit are used by the output stage switches, i.e. bit s_{p-1} is used by the *SE* at output stage 0 (rightmost *SE* of the network), bit s_{p-2} is used by the *SE* at output stage 1 and so on. Bit $s_{p-\log_2(\frac{M}{m})}$ (i.e. bit $s_{\log_2 m}$) is used by the last *SE* of the output stages. The signal from the building block (i.e. leaf) enters into this *SE* of the output stages. Let **ROS** be the set of bits used for routing in the output stages, then **ROS** $= \{s_{\log_2 m} s_{\log_2 m+1} \dots s_{p-1}\}$.

6.2.2 An Example of Self-routing

Figure 6.5 shows an 8×8 GRN with 4×4 non-blocking switch as the building block. Suppose that the signal at input *001* requests to be connected with output *100*. So, the header in the request message has **TAG** = *100100*. Here $m = n = 4, M = N = 8$, thereby

$\log_2\left(\frac{N}{n}\right) = \log_2\left(\frac{M}{m}\right) = 1$. That is, the first (from left) bit, *1*, will be used by the *SE* at the only input stage and the last bit, *0*, will be used by the *SE* at the only output stage. The leaf building block will use the middle 4 bits, *0010*, for its internal routing. The thick line in Figure 6.5 shows the route from input *001* to output *100*.

6.2.3 Size of Routing Tag

Let **TAG** be the set of bits used for routing a signal from an input to an output, then the size of the **TAG** is,

$$\begin{aligned} |TAG| &= |RIS| + |RBS| + |ROS| \\ &= \log_2\left(\frac{N}{n}\right) + (\log_2 m + \log_2 n) + \log_2\left(\frac{M}{m}\right) \\ &= \log_2(MN). \end{aligned} \tag{6.1}$$

For an $N \times N$ network $|TAG| = 2\log_2 N$. Therefore, for an $N \times N$ network the size of the routing tag is of the $O(\log_2 N)$.

Since every path can be routed independently, any permutation can be routed without any conflict in the switches. Even if the routing requests are asynchronous to each other it can be routed to the correct outputs without any conflict in switches. Furthermore, the length of the routing tag is considerably small, $O(\log_2 N)$. So the propagation delay is only $O(\log_2 N)$.

Chapter 7

Performance Evaluation

We consider the following figure of merits to evaluate the performance of the proposed system and compare it with existing ones. However, as all systems are not compatible to each other from all aspects, mainly crossbar and GRN are compared for all figure of merits.

7.1 Figure of Merits

Switch Count is the total number of switching elements (*SEs*) required to build the switching structure. The switch count of an $N \times M$ network is represented by $T_{N \times M}$. When $N = M$, then it is represented by T_N.

Maximum Signal Loss is the maximum loss of optical signal that a path can incur in the network. It is represented by $S_{N \times M}$. When $N = M$, then it is represented by S_N. The amount of loss is directly proportional to the number of *SE*s a signal path has to pass through.

Maximum Crosstalk is the maximum crosstalk that a connection may suffer while passing from input to output of the network. It is represented by $C_{N \times M}$. When $N = M$, then it is represented by C_N. $C_{N \times M}$ is directly proportional to the number of crosstalk *SE*s. Thus, it is also represented in terms of *SE*s.

Signal-to-Crosstalk Ratio is the ratio of the output signal to the crosstalk signal in an output of the switch networks. It is represented by SXR and expressed in dB.

Routing Complexity is a measure for the time to determine the routing decision and setting up switches. It is represented by t_R.

7.2 Evaluation of GRN networks

7.2.1 Switch Count

The switch count of a GRN network of size $N \times M$ depends on the building blocks. From Theorem 2 we get the expression of switch count as follows:

$$T_{N\times M} = \left(\frac{MN}{m} + \frac{MN}{n} - N - M\right) + \frac{MN}{mn} T_{n\times m},$$

where $\frac{MN}{mn}$ represents the total total number of building blocks of size $n \times m$ and $\left(\frac{MN}{m} + \frac{MN}{n} - N - M\right)$ represents the total number of switching elements. Let's consider the 2×2 switch as the building block. Then $m = n = 2$ and $T_{2\times 2} = 1$, so the switch count is

$$T_{N\times M} = MN - N - M + \frac{MN}{4}. \tag{7.1}$$

For a square size of networks, where $N = M$, equation (7.1) turns into equation (4.16):

$$T_N = 1.25N^2 - 2N$$

If we consider 3×3 WSNB switch as the building block, then the switch count of the building block, $T_{3\times 3} = 4$, and thereby the switch count of an $N \times M$ GRN is

$$T_{N\times M} = \frac{10MN}{9} - N - M. \tag{7.2}$$

When $N = M$, equation (7.2) turns into equation (7.3):

$$T_N = \frac{10N^2}{9} - 2N \tag{7.3}$$

If we consider 4×4 WSNB as building blocks then, $T_{4\times 4} = 8$ and the switch count of an $N \times M$ GRN network is

$$T_{N\times M} = MN - N - M. \tag{7.4}$$

when $N = M$ equation (7.4) turns into equation (7.5):

$$T_N = N^2 - 2N \tag{7.5}$$

From the above equations it is evident that the switch complexity of the GRN is $O(N^2)$, similar to that of the optical crossbar networks.

7.2.2 Maximum Signal Loss

Maximum signal loss, S_N (or $S_{N\times M}$), of a switch networks is represented in terms of switching elements that a signal has to pass for reaching an output. The maximum signal loss of GRN networks is given in Theorem 2 as following:

$$S_{N\times M} = \log_2\left(\frac{M}{m}\right) + \log_2\left(\frac{N}{n}\right) + S_{n\times m}, \tag{7.6}$$

where $S_{n\times m}$ is the maximum signal loss of the building block $n \times m$ switch network.

$S_{2\times 2} = 1$ for building blocks of size 2×2,then equation(7.6) becomes

$$S_{N\times M} = \log_2 N + \log_2 M - 1. \tag{7.7}$$

When $N = M$, the maximum signal loss is,

$$S_N = 2\log_2 N - 1. \tag{7.8}$$

For building block of size 3×3, $S_{3\times 3} = 3$, the maximum signal loss is,

$$S_{N\times M} = \log_2 \left(\frac{N}{3}\right) + \log_2 \left(\frac{M}{3}\right) + 3. \tag{7.9}$$

When $N = M$, the maximum signal loss is,

$$S_N = 2\log_2 \left(\frac{N}{3}\right) + 3. \tag{7.10}$$

For building blocks of size 4×4, $S_{4\times 4} = 4$, the maximum signal loss is,

$$S_{N\times m} = \log_2 N + \log_2 M. \tag{7.11}$$

When $N = M$, it is,

$$S_N = 2\log_2 N. \tag{7.12}$$

Table II shows some numerical examples of maximum signal loss of GRN networks. For the brevity of discussion we describe a GRN network constructed with the building block of size $m \times m$ by $GRNm$.

Table II: Numerical examples of S_N of GRN networks

Net size	S_N, GRN2	S_N, GRN3	S_N, GRN4
4	3	-	4
6	-	5	-
8	5	-	6
12	-	7	-
16	7	-	8
24	-	9	-
64	11	-	12
256	31	-	32

7.2.3 Maximum Crosstalk

Maximum crosstalk of GRN networks is represented by the term $S_{N\times M}$ and expressed in terms of *SE*s. Theorem 2 gives the expression of maximum crosstalk as given below:

$$C_{N\times M} = C_{n\times m},$$

where $C_{n\times m}$ is the maximum crosstalk of the building block $n \times m$ switch.

Considering 2×2 as the building block, $C_{2\times 2} = 1$. Thereby, the maximum crosstalk loss of a GRN network with 2×2building block switches is $C_{N\times M} = 1$. For the 3×3 building block switches the GRN has the *maximum crosstalk*, $C_{N\times M} = 3$.

For the 4×4 building block switches the GRN has the *maximum crosstalk*, $C_{N\times M} = 4$. Table III shows some numerical examples of maximum crosstalk of different GRN networks.

Table III: Numerical examples of C_N of GRN networks

Size,N	C_N, GRN2	C_N, GRN3	C_N, GRN4
4	1	-	4
6	-	3	-
8	1	-	4
12	-	3	-
16	1	-	4
24	-	3	-
32	1	-	4
48	-	3	-
64	1	-	4

7.2.4 Signal-to-Crosstalk Ratio

Practically, the signal-to-crosstalk ratio, SXR, limits the size of switch networks. Input-stage-switches in GRN do not add any crosstalk to the signal. The first switch that adds crosstalk to the signal path is the building block. Suppose the building block adds c_m (expressed in ratio) crosstalk to a signal path. All output-stage-switches also add crosstalks to the signal path. In the worst case scenario, every output-stage-switches along the signal path may add second-order crosstalk. Crosstalks of the higher order has little practical significance. We are ignoring those terms. Figure 7.1 gives us a clear idea about the situation. Since all the paths from input to out puts have the same length, loss terms are cancelled out in the calculation. A signal that comes out from a building block has c_m crosstalk. At inputs of the switch of next stage along the connection, there are two signals – one is power signal with c_m crosstalk and the other is only crosstalk c_m signal. Thus the output of this switch will have $c_m + c_m.x_c$ crosstalk. x_c is the crosstalk produced in every switching elements. It is also called as the *Extinction ratio,* X_c.

$$X_c = 10 \ \log_{10} x_c \text{ dB} \tag{7.13}$$

As there are $\log_2\left(\frac{N}{n}\right)$ switches along the connection in the output-stage where n is the size of the input of the building block, we get the following expression for the crosstalk in the output signal:

$$x_{ctalkout} \;\; = \;\; c_m + c_m.x_c + \ldots \text{upto } \log_2(N/n) \text{ terms}$$

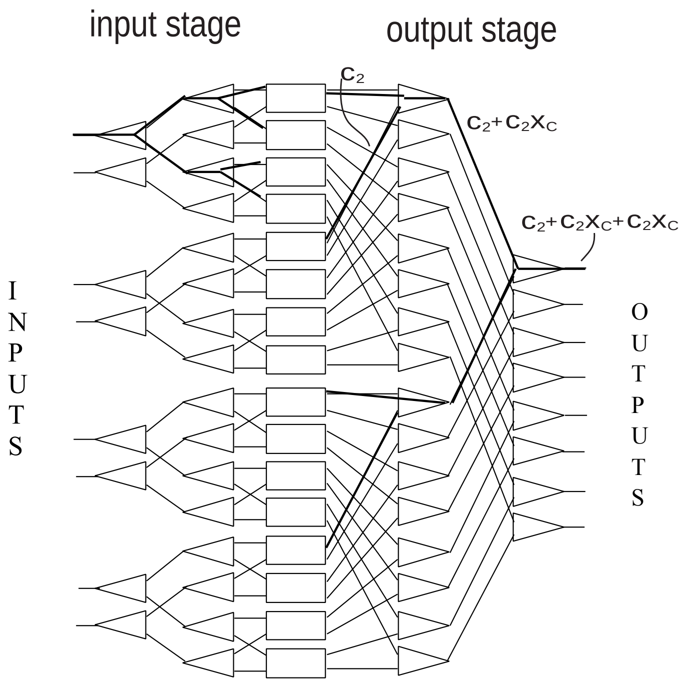

Figure 7.1: Amount of crosstalk signal produced in the signal

$$x_{ctalkout} = c_m(1 + \log_2 \left(\frac{N}{n}\right) x_c) \quad (7.14)$$

Thereby the signal-to-crosstalk ratio is,

$$SXR = 10 \log_{10} \left[\frac{1}{c_m(1 + \log_2 \left(\frac{N}{n}\right) x_c)} \right] \text{dB}. \quad (7.15)$$

Table IV shows some examples of SXR of GRN networks. We consider the extinction ratio, X_c, of a switching element (as well as a 2×2 switch) is -30 dB, i.e $x_c = 0.001$. The crosstalk of a 3×3 WSNB is,

$$c_3 = 3x_c = 0.003.$$

Similarly, the crosstalk for 4×4 WSNB is,

$$c_4 = 4x_c = 0.004.$$

Table IV: Numerical examples of Signal-to-Crosstalk Ratio of GRN networks

Net size	GRN(2)	GRN(3)	GRN(4)
8	29.991	-	-
12	-	25.220	-
16	29.987	-	23.9707
24	-	25.216	-
32	29.983	-	23.966
48	-	25.211	-
64	29.978	-	23.962
256	29.970	-	23.953
1024	29.961	-	23.945

7.2.5 Routing Complexity

A header from the signal is converted into electronic domain. Let us suppose that the time for conversion of an optical bit is t_b, then the time required to convert the header from the signal is,

$$t_C = |TAG| \times t_b.$$

Since the length of the **TAG** is $\log_2 N$, t_C is given by

$$t_C = t_b \times 2\log_2 N. \tag{7.16}$$

The building block has its own control strategy. Our proposed wide-sense nonblocking switches have a centralized control-circuit that sets up connections from inputs to outputs. An $m \times m$ WSNB has computation complexity in the $O(m^2)$. So, 4×4 and 3×3 have routing complexities $O(4^2)$ and $O(3^2)$ respectively. Again the input stage and the output stage have constant computation complexities since all the connections are established independently and they do not depend on the size of the network. That means, the computation complexity for routing signals is constant and the same as that of the building block.

Time required for routing a header from input to an output is comprised of input-stage, building-block-stage and output-stage delays. In every stage the delay is due to setting up an electronic control switch. Let this time is t_E, then the propagation delay of the header, t_D, is

$$t_D = t_E(\log_2\left(\frac{M}{m}\right) + t_m + \log_2\left(\frac{N}{n}\right)),$$

where t_m is the delay for building-block-stage $= O(m^2)$.

For 2×2 building block it is,

$$t_D = t_E(\log_2 M + \log_2 N - 1). \tag{7.17}$$

For 3×3 WSNb as building block, it is,

$$t_D = t_E(\log_2 \left(\frac{M}{3}\right) + 3 + \log_2 \left(\frac{N}{3}\right)). \tag{7.18}$$

For 4×4 as the building block, it is,

$$t_D = t_E(\log_2 N + \log_2 M). \tag{7.19}$$

Thus, if $n << N$ and $N = M$, then the resulting propagation delay of the header is on the order of $O(\log_2 N)$.

The switch setup time, t_{SE}, refers to the time to set up all *SEs* along the path. Header routing does not wait for setting up of the corresponding *SEs*. The propagation of the header from an input to an output completes at least one 1 *SE* setup-time (t_s) earlier than the corresponding optical path is established. Thereby,

$$t_{SE} = t_D + t_s.$$

Since the time for propagation of optical signal is negligible compared to switch setup time, the routing complexity results from the above two factors – computation complexity and the switch setup time, and thereby,

$$\begin{aligned} t_R &= t_C + t_{SE} \\ &= t_C + t_D + t_s \\ &= t_C + t_s + O(\log_2 N) \\ &= t_b(2\log_2 N) + t_E(\log_2 \left(\frac{M}{m}\right) + t_m + \log_2 \left(\frac{N}{n}\right)). \end{aligned} \tag{7.20}$$

Thus the routing complexity is on the order of $O(\log_2 N)$.

7.3 Clos-GRN Networks

We represent a Clos-GRNm networks as C-GRNm in short. Considering a 2×2 switch as the building block of GRN, we get following expressions:

$$T_{p\times 2p} = \frac{5p^2}{2} - 3p \tag{7.21}$$

$$T_{p\times p} = \frac{5p^2}{4} - 2p \tag{7.22}$$

Thereby the switch count of a Clos-GRN2 is as following:

$$T_{N,C-GRN2} = \frac{15p^3}{2} + 2p - \frac{45p^2}{4} \tag{7.23}$$

That means, the switch complexity is $O(N\sqrt{N})$, which is the same as that of a Clos-Crossbar (C-CB) network on the same condition.

Again for a GRN with 3 × 3 as the building block, we get,

$$T_{p\times 2p} = \frac{20p^2}{9} - 3p,$$
$$T_{p\times p} = \frac{10p^2}{9} - 3p,$$

and thus,

$$T_{N,C-GRN3} = \frac{60p^3}{9} - \frac{118p^2}{9} + 3p. \quad (7.24)$$

Similarly, when $n = m = 4$, we get,

$$T_{p\times 2p} = 2p^2 - 3p,$$
$$T_{p\times p} = p^2 - 2p,$$

and using above expressions we get the equation for the switch count of Clos-GRN4 networks as,

$$T_{N,C-GRN4} = 6p^3 - 11p^2 + 2p. \quad (7.25)$$

Table V shows some numerical examples of the switch count, $T_N, C - GRNm$, of Clos-GRN networks.

Table V: Numerical examples of switch count of different Clos-GRN networks

Size, N	C-GRN2	C-GRN3	C-GRN4
9	-	71	-
16	308	-	216
36	-	986	-
64	3136	-	2384
144	-	9668	-
256	27872	-	21792
576	-	84680	-
1024	234304	-	185408

The maximum signal loss of different Clos-GRN networks are obtained from equation (4.34) as follows:

$$S_{N,C-GRN2} = 6\log_2 p - 1 \quad (7.26)$$
$$S_{N,C-GRN3} = 4\log_2\left(\frac{p}{3}\right) + 2\log_2\left(\frac{2p}{3}\right) + 9 \quad (7.27)$$
$$S_{N,C-GRN4} = 6\log_2 p + 2 \quad (7.28)$$

The *maximum crosstalk* of Clos network is given in equation(4.26). If we consider crossbar network as building blocks then equation (4.6) gives the expected result. On the other hand, for a Clos network with GRN as building blocks following are resulting expressions:

$$C_{N,C-GRN2} = 3 \quad (7.29)$$
$$C_{N,C-GRN3} = 9 \quad (7.30)$$
$$C_{N,C-GRN4} = 12 \quad (7.31)$$

The path-dependency of Clos-GRN networks is zero because the constituent GRN networks have zero path-dependencies.

7.4 Comparisons

Table VI shows the comparison of different nonblocking switch networks on switch count. Although the comparison with the multi-plane Banyan networks is not fare because the later does not include the hardware overhead for input/output circuitry in the calculation, we have mentioned its switch count in the table to compare it with that of Clos-GRN networks. $GRN(m)$ means the GRN network with $m \times m$ as the building blocks.

Table VI: Comparison of different switch networks on switch count

Network	T_N	Complexity
Crossbar	N^2	$O(N^2)$
D-crossbar	$2N^2$	$O(N^2)$
M-Banyan (WSNB)	$\frac{N}{2}\log_2 N\sqrt{2N}-1$ if $\log_2 N$ odd $\frac{3N}{4}\log_2 N\sqrt{N}-1$ if $\log_2 N$ even	$O(N\sqrt{N}\log N)$
GRN2	$1.25N^2 - 2N$	$O(N^2)$
GRN3	$\frac{10N^2}{9} - 2N$	$O(N^2)$
GRN4	$N^2 - 2N$	$O(N^2)$
C-GRN2	$\frac{15N\sqrt{N}}{2} - \frac{45N}{4} + 2\sqrt{N}$	$O(N\sqrt{N})$
C-GRN3	$\frac{60N\sqrt{N}}{9} - \frac{118N}{9} + 3\sqrt{N}$	$O(N\sqrt{N})$
C-GRN4	$6N\sqrt{N} - 11N + 2\sqrt{N}$	$O(N\sqrt{N})$

From the table it is evident that the switch complexity of the GRN network is the same as that of other nonblocking networks except the M-Banyan. But the expression of M-Banyan does not include input/output overhead. Clos-GRN networks outperform M-Banyan networks on switch count. Among different GRN configurations, GRN4 has the lowest switch count.

The graph in Figure 7.2 and 7.3 give the comparisons of GRN with other networks on maximum crosstalk and maximum signal loss parameters. In all graphs X-axis represents the size of the networks and the Y-axis represents corresponding performance metrics in terms of SEs. We see the GRN networks are moderate and reasonable on all metrics. The most widely used switch architecture, the crossbar (and Double crossbar) networks have unacceptably high signal loss. Again, GRN, Spanke's and M-Banyan architectures have the same, $O(\log_2 N)$, maximum signal loss. Regarding the crosstalk, although, crossbar, M-Banyan and Spanke's have zero value, but we have seen that crossbar has high signal-to-crosstalk ratio and thereby cannot scale beyond 100×100 networks. Figure 7.4 shows the comparison between C-CB and Clos-GRN networks on switch count. Graph in Figure 7.5 shows how the maximum signal loss and maximum crosstalk changes in Clos-GRN2 and

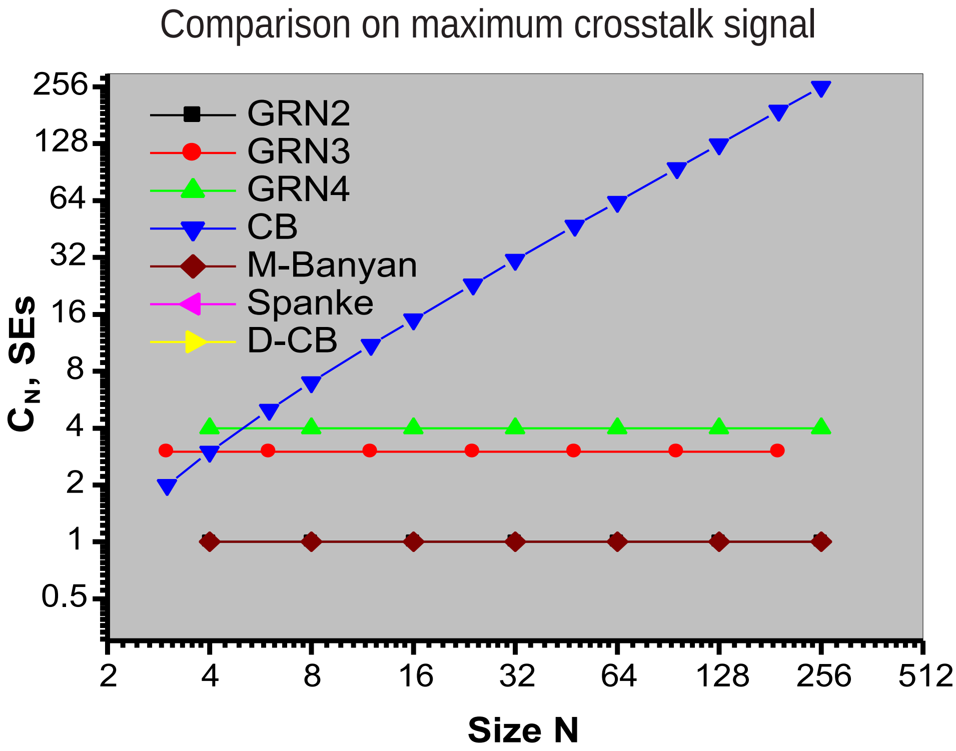

Figure 7.2: Comparison of maximum crosstalks

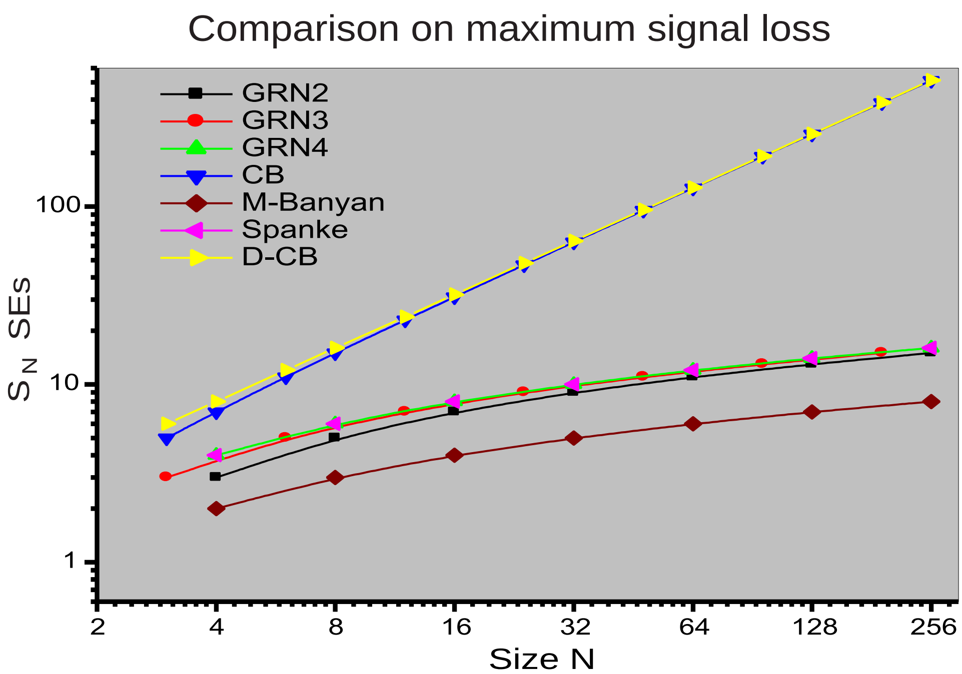

Figure 7.3: Comparison of maximum signal losses

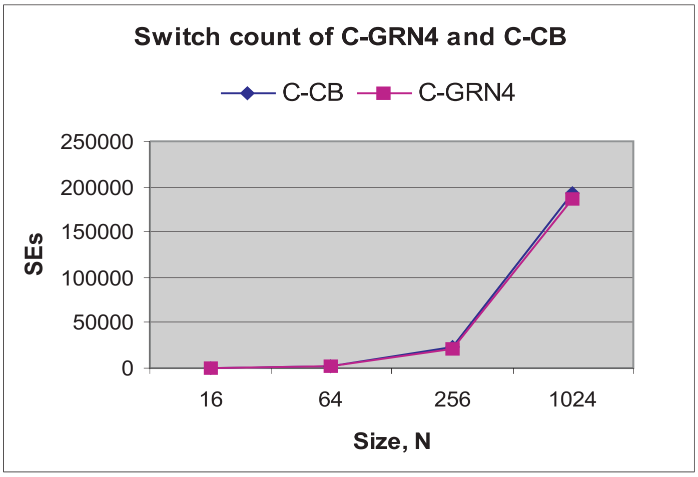

(a)

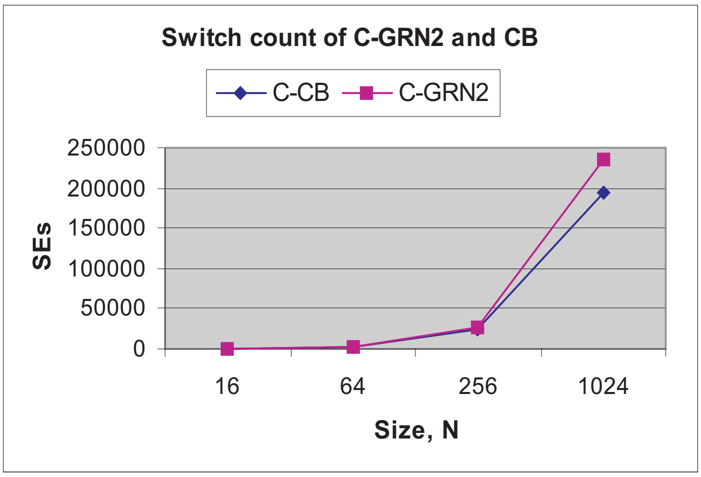

(b)

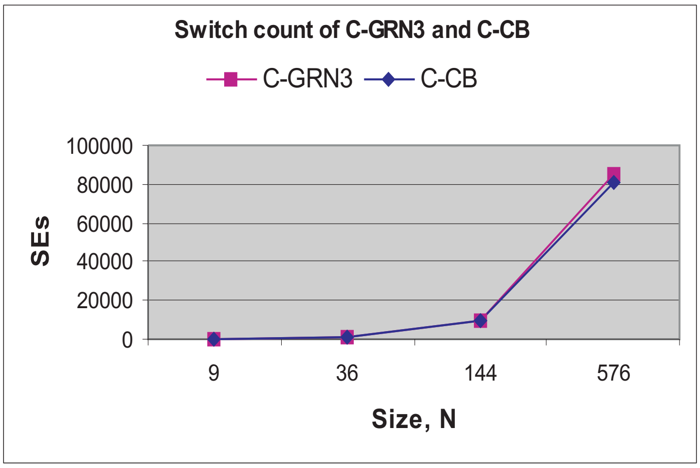

(c)

Figure 7.4: Comparison between C-CB and Clos-GRN on switch count

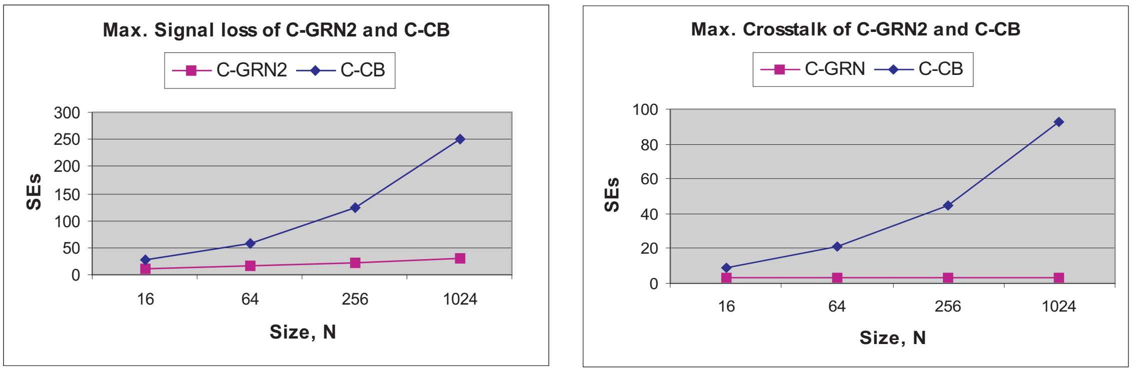

(a) (b)

Figure 7.5: Maximum signal loss and Maximum crosstalk in Clos-GRN2 and Clos-CB networks

Clos-CB networks. Figure 7.6 show the comparison between Clos-GRN3 and Clos-CB networks on Maximum signal loss and Maximum crosstalk. Figure 7.7 shows the compar-

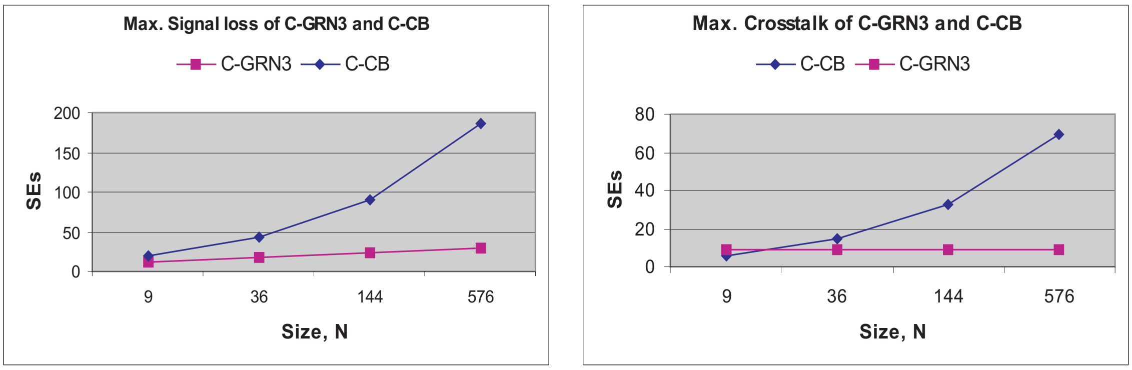

(a) (b)

Figure 7.6: Comparison between Clos-GRN3 and Clos-CB networks on Maximum signal loss and Maximum crosstalk

ison between Clos-GRN4 and Clos-CB on Maximum signal loss and Maximum crosstalks. Among different GRN configuration GRN4 is most promising because they have lowest switch switch count, lowest maximum signal loss and lowest maximum crosstalk. We see from the figure that the signal loss of a path has been significantly reduced in our proposed network. Note that, for a 256×256 network, S_N is equal to 511 in the crossbar network and 16 in GRN4 network. Moreover, S_N is equal to 123 in the Clos network built on crossbars switch and 26 in the Clos-GRN4 network. Figure 7.8 shows how the signal-to-crosstalk ratio varies when the size of a network increases. Crossbar and Double Crossbar optical networks do not scale over 32×32 networks as their Signal-to-Crosstalk Ration falls bellow 10 dB. In this regard Spanke's network shows the best performance. But it has to pay high hardware cost in return. However, we have seen that this Spanke's network is actually a special case of our Generalized Recursive Networks. The M-Banyan

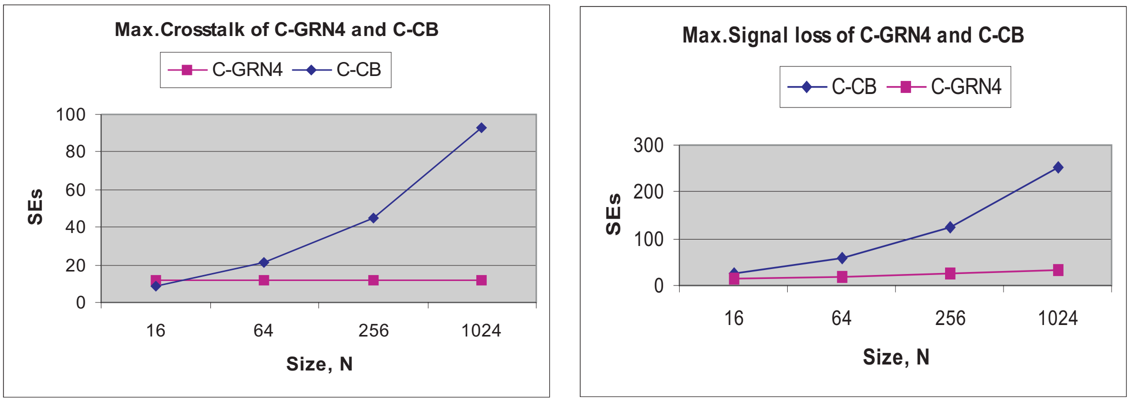

(a) (b)

Figure 7.7: Comparison between Clos-GRN4 and Clos-CB on Maximum signal loss and Maximum crosstalk

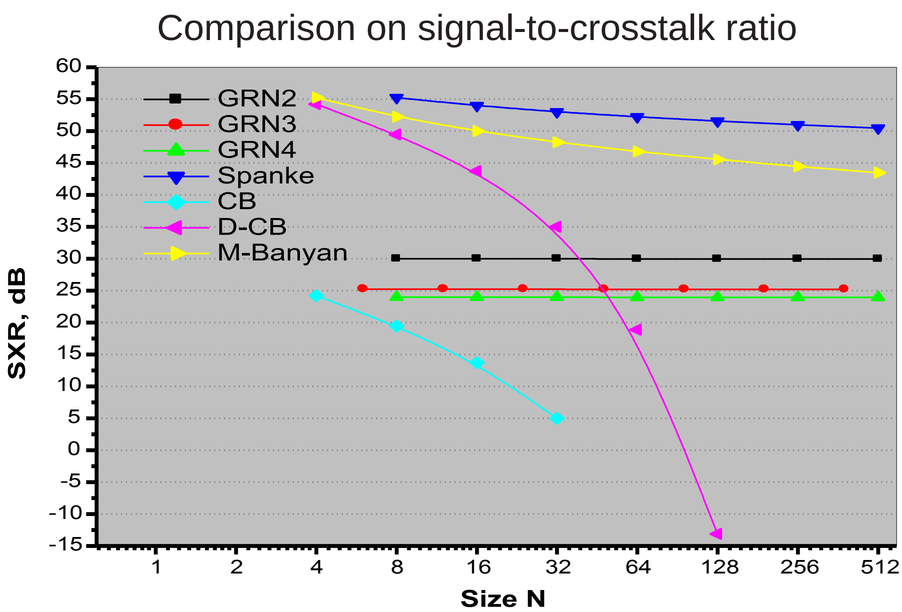

Figure 7.8: Signal-to-crosstalk ratio of different switch networks

networks also shows good performance in this regard. GRN along with M-Banyan and Spanke's networks scale well for large networks with reasonable signal-to-crosstalk ratio.

7.5 Effect of the Size of Building Blocks on GRN Networks

The building blocks that constructed by the recursion technique have very high switch complexity, maximum signal loss, and maximum crosstalk (see equations (5.3), (5.4), and (5.5)). In general, size of building blocks cannot be very large because of the following reasons:

1. Size of a GRN network (N) must be less than or equal to the size of the building

block (n).

2. n cannot be so large (e.g.>> 16) that the crosstalk produced in the building block decreases SXR of the GRN networks less than 11 dB.

3. Since building block has $O(n^2)$ routing complexity, large n may result the routing time prohibitively large. Small size of the building blocks distributes the control over more number of building blocks, and therefore, parallelizes the routing task.

However, we are still investigating a more efficient architecture which can increase the size of the building block.

Chapter 8

Conclusion

8.0.1 Summary

Designing of an all optical crossconnect in a reasonable cost is a longstanding problem. In the heart of the problem is the costly switching system. It needs to be strictly nonblocking (at least in the wide-sense) as well as low cost, low loss and low crosstalk with easy routing algorithm. The system should be customizable on different cost-performance environment. Although switching systems have a long history, the introduction of optical signals as the carrier of information has made the researcher rethink on the architecture of the switching systems. Our survey reveals that merely embedding the optics in the existing switch networks cannot serve the purpose.

Crossbar and Clos networks are the most widely used switch architecture in optical switching system for their easy routing algorithm and non-blocking property. But they have many limitations. The crossbar network suffers from huge signal loss and crosstalk. A switching system with more than 32 ports cannot be employed because of low signal-to-crosstalk ratio. The Clos network uses the crossbar as building block for the nonblocking property. The Clos network has only three stages, so signal loss is bounded in this regard. However, the crossbar building block in the Clos network still results in large signal loss and crosstalk.

Although Double crossbar has zero first-order crosstalk with increased signal loss ($2N$) and increased number of switching elements ($2N^2$), it cannot scale beyond 40 ports. Spanke's networks can be made larger with very good signal-to-crosstalk ratio, but it requires $2N(N-1)$ switching elements for an $N \times N$ strictly nonblocking network. The Spanke's network lacks of customization capability so that hardware cost cannot be traded off even when the crosstalk and loss requirements are not stringent. Multi-plane Banyan architecture were proposed that have much lower crosstalk, signal loss and switch complexity. But input/output overhead and $O(N\sqrt{N}\log_2 N)$ routing complexity makes it difficult to be implemented.

The centralized crossbar networks require computation complexity in the $O(N)$. Conversely, self-routing crossbar networks require header of the size of $O(N)$.

We focused on the core part of the optical networks — the crossconect. We proposed $RN(N, m)$ switch netowrks to be used in the all-optical crossconnet. The networks have been proposed considering all the limitations of directional couplers. Since the switch count is high of the $RN(N, m)$ networks and it is always of square size constructed with square size of building blocks, we proposed more generalized switch structure — *Generalized Recursive Networks.* This network can be used in the Clos network (like crossbar networks) to reduce the switch complexity of the target network.

Since the concept of building block is central to our switching system, we investigated novel building block architectures. We proposed 3×3 and 4×4 wide-sense nonblocking networks along with their transition algorithms as building blocks of GRN networks. These two wide-sense nonblocking networks have so far the fewest switch count. Choosing an appropriate building block we can trade off the hardware cost with signal loss and crosstalk requirements of a network.

We proposed the distributed control routing technique for our switching system. The routing complexity is constant and the same as that of the building blocks. The size of the routing tag is $O(\log)$ unlike $O(N)$ of the crossbar networks.

8.0.2 Discussion

Our proposed switching system includes almost all cherished essence from different existing switching systems. This is the biggest contribution of this thesis. For example, it can be from strictly nonblocking to blocking networks depending on building blocks, and thereby traded off cost with the performance. It can be used in Clos network to reduce the switch complexity, and the resulting Clos network has the lowest switch complexity, $O(N\sqrt{N})$, among all available nonblocking architecture. It has reasonable loss and crosstalk. Loss is not path dependent like crossbar networks. It scales well for a large network like M-Banyna or Spanke. It has very easy, distributed control routing algorithm that has constant complexity (compared to $O(N\sqrt{N}\log_2 N)$). In this regard it is even better than Crossbar and M-Banyan. This networks can readily be implemented.

8.0.3 Further Problems

There are a few more tasks to be done on this topic. Introduction of the multicasting capability in the system in optical domain is yet to be done. Even when the network is fully loaded there are some switches remain idle. So, further reduction of the switch complexity could be possible. The vertically stacked GRN could also result better performance. Removing loopback connections in the switch system can result lower switch count. We have only discussed how the signal is routed through the system. But to make it useful in the multi-hop dynamic network environment it is also necessary to incorporate the ability of modifying header information at the outbound links in the optical domain. This is a major challenging tasks left for future research.

The other open problems in the all-optical photonic networks that this author is actively considering are as follows:

Waveband or single wavelength switching

Although there is no doubt that WDM is necessary to cope with the future demanding bandwidth but there are questions on how the multiple wavelengths will be used to maximize throughput. Each wavelength can be used as an independent channel. In such case the aggregated address overhead will be high. If band of wavelengths are routed simultaneously then this overhead is less, and effective data transfer rate will be higher. But this approach may degrade the flexibility of wavelength usage. Recently, two dimensional (time and space) addressing scheme for identifying a node in the networks using multiple wavelengths for optical packet switching has been proposed in the literature [86]. In this addressing technique K wavelengths are used as address wavelengths out of W available wavelengths and $W - K$ wavelengths are used for sending payload only. These K wavelengths remain idle during the $W - K$ wavelengths send data. The longer the packet size, the longer is this idle period. This reduces effective bandwidth of W wavelength bands. Also the effect of this waveband switching on multicast traffic has not been investigated.

Routing strategy

When a source sends a request, the request information is carried out to the destination through the cross-connect in a packet (or cell). It is very common that the destination will respond to the request of the source in most cases. It does so by sending information in another packet through the cross-connect. These two packets are independent and take different paths in the present system. Since setting up paths consumes time, which is very much comparable to the data transmission time for a large optical network, we can make the second packet (answer of the request) adopt the same path already established from source to destination during request sending. It is possible in the all-optical networks because the switches are clear channel. This will reduce average path setup time. A path will always be established by the source. Destination can reply on the same path but cannot establish the path. Each node has a source and a destination.

Bibliography

[1] T. Chikama, H. Onaka, S. Kuroyanagi, "Photonic networking using optical add drop multiplexers and optical crossconnects", Fujitsu Science and Technology Journal, vol.35, no.1, pp.46-55 (Jan. 1999).

[2] V. R. Chinni et al., "Crosstalk in a lossy directional coupler switch", J. Lightwave Technology, vol.13, no.7, pp.1530-1535 (July 1995).

[3] Y. Yang, J. Wang and Y. Pan, "Permutation capability of optical multistage interconnection networks", Journal of Parallel and Distributed Computing, vol.60, no.1, pp. 72-91 (Jan. 2000).

[4] G. Maier and A. Pattavania, "Design of Photonic rearrangeable networks with zero first-order switching element crosstalk", IEEE Trans. Commun., vol.49, no.7, pp.1268-1279 (July 2001).

[5] D. Li, "Elimination of crosstalk in directional coupler switches", Optical Quantum Electron., vol.25, no.4, pp.255-260 (Apr. 1993).

[6] R. C. Alferness, Guided wave devices for optical communications, IEEE J. of Quantum Electronics, Vol. QE-17, pp.946-959 (1981).

[7] S. K. Korotky, R. C. Alferness, C. H. Joyner, and L.L. Buhl, "14 Gbit/sec optical signal encoding for $\lambda = 1.32 \mu m$ with double pulse drive of a $Ti : LiNbO_3$ waveguid modulator, Electron. letters, No. 20, pp. 132-133 (1984).

[8] V.E. Benes, "Heuristic remarks and mathematical problems regarding the theory of switching systems", Bell System Technical Journal, vol.41, pp. 1201-1247 (1962).

[9] J.W. Goodman, F.J Leonberger, S.-Y.Kung, and R A Athale, "Optical interconnections for VLSI", Proc. IEEE, 72, 850-866 (1984).

[10] M. R. Feldman, S. C. Esener, C. C. Guest, and S. H. Lee, "Comparison between Optical and Electrical Interconnect based on Power and Speed Considerations", Appl. Optics, 27, 1742 - 1751 (1988).

[11] David A. B. Miller, "Physical reasons for optical interconnection", Int. J. Optoelectronics Vol. 11, 155-168 (1997).

[12] D. A. B. Miller and H. M. Ozaktas, "Limit to the Bit Rate Capacity of Electrical Interconnects from the Aspect Ratio of the System Architecture", J. Parallel Dist. Comp. (to be published).

[13] H. M. Ozaktas, “A Physical Approach to Communication Limits in Computation”, Ph.D. Thesis, Stanford University, Stanford, CA (1991).

[14] H. Ozaktas and J. W. Goodman, “The limitations of interconnections in providing communication between an array of points”, Frontiers in Computing Systems Research, Vol. 2, 61-130, Ed: S. K. Tewksbury (Plenum Press, New York, 1991).

[15] B. J.Smith, “Interconnection networks for shared memory parallel computers”, Proc. 2nd Int. Conf. Massively Parallel Processing Using Optical Interconnections (MPPOI’95), 255-256 (IEEE Computer Society Press, Los Alamitos, California).

[16] J. W. Goodman, F. J. Leonberger, S.-Y. Kung, and R. A. Athale, “Optical Interconnections for VLSI Systems”, Proc. IEEE 72, 850 - 866 (1984).

[17] P. J. Delfyett, D. H. Hartman, and S. Z. Ahmad, “Optical Clock Distribution using a Mode-locked Semiconductor Laser Diode System”, J. Lightwave Tech. 9, 1646 - 1649 (1991).

[18] G. D. Boyd, G. Livescu, L. M. F. Chirovsky, and A. L. Lentine, “Modelocked pulse operation of GaAs/AlGaAs field effect transistor self-electrooptic effect device smart pixels and saturation considerations”, Appl. Phys. Lett. 65, 3108-3110 (1994).

[19] G. Livescu, G. D. Boyd, L. M. F. Chirovsky, R. A. Morgan, and T. Mullally, “Picosecond switching of GaAs/AlGaAs smart pixels”, Optics Lett. 19, 2122-2124 (1994).

[20] T. K. Woodward, A. L. Lentine, and L. M. F. Chirovsky, “Experimental sensitivity studies of diode-clamped FET- SEED smart-pixel optical receivers”, IEEE J. Quantum Electron. 30, 2319-2324 (1994).

[21] A. L. Lentine, L. M. F. Chirovsky, and T. K. Woodward, “Optical energy considerations for diode-clamped smart pixel optical receivers”, IEEE J. Quantum Electron. 30, 1167-1171 (1994).

[22] N. S. Patel, K. L. Hall, and K. A. Rauschenbach, “40-Gbit/s cascadable alloptical logic with an ultrafast nonlinear interferometer”, Optics Lett. 21, 1466-8 (1996).

[23] K. H. Ahn, M. Vaziri, B. C. Barnett, G. R. Williams, X. D. Cao, M. N. Islam, B. Malo, K. O. Hill, and D. Q. Chowdhury, “Experimental demonstration of a low-latency fiber soliton logic gate”, J. Lightwave Tech. 14, 1768-75 (1996).

[24] K. H. Brenner and A. Huang, “Optical implementation of the perfect shuffle interconnection”, Appl. Opt. 27, 135-137 (1988).

[25] J. Jahns and M. J. Murdocca, “Crossover networks and their optical implementation”, Appl. Opt. 27, 3155-3164 (1988).

[26] T. J. Cloonan and M. J. Herron, “Optical implementation and performance of one-dimensional and two-dimensional trimmed inverse augmented data manipulator networks for multiprocessor computer-systems”, Opt. Eng. 28, 305-314 (1989).

[27] R. R. Michael, M. P. Christensen, and M. W. Haney, "Experimental evaluation of the 3-D optical shuffle interconnection module of the sliding Banyan architecture", J. Lightwave Tech. 14, 1970-1978 (1996).

[28] D. A. B. Miller, "Optics for low-energy communication inside digital processors: quantum detectors, sources, and modulators as efficient impedance converters", Optics Lett. 14, 146-148, (1989).

[29] A. Krishnamoorthy, A. L. Lentine, K. W. Goossen, J. A. Walker, T. K. Woodward, J. E. Ford, G. F. Aplin, L. A. D'Asaro, S. P. Hui, B. Tseng, R. Leibenguth, D. D. Kossives, D. Dahringer, L. M. F. Chirovsky, and D. A. B. Miller, "3-D Integration of MQW Modulators Over Active Submicron CMOS Circuits: 375 Mb/s Transimpedance Receiver-Transmitter Circuit", IEEE Photonics Tech. Lett. 7, 1288-90 (1995).

[30] A. V. Krishnamoorthy and D. A. B. Miller, "Scaling Optoelectronic-VLSI Circuits into the 21st Century: A Technology Roadmap", IEEE J. Selected Topics in Quantum Electronics 2 , 55-76 (1996).

[31] Kogelnik, H. and R. V. Schmidt, "Switched directional couplers with alternating", IEEE J. Quantum Electron., Vol. QE-12, No.7, 1976, pp.396-401.

[32] R. V. Schmidt and R.C. Alferness, "Directional Coupler Switches, modulators, and filters using alternating $\triangle\beta$ techniques", IEEE Trans. On Citcuits Syst. CAS-26, pp.1099-1108, 1979.

[33] L. McCaughan and G. A. Bogert, "4x4 strictly nonblocking integrated T:LiNbO3 switch array", Conference on Optical fiber communications, San Diego, pp.76-77 (1985).

[34] J.E Watson, "polarization-independent 1x6 optical switch using T:LiNbO3 waveguides", Conf. on Optical fiber communications, San Diego, p.110 (1985).

[35] R. j. simpson, R.H. stolen, F. M. Sears, W. pleibel, J.B. McChesney, and R.E. Howard, "A single-poarization fiber", J. Lightwave Technol., LT-1, pp. 370-373 (1983).

[36] S. Yamada and M. Minakata, "DC drift phenomena in $LiNbO_3$ optical waveguide devices", Japan Journal of App. Physics, Vol.20, pp. 733(1981).

[37] T. Mukai, Y. Yamamoto, and T. Kimura, "S/N and error rate performance in AlGaSa semiconductor laser preamlifier and linear repeater systems", IEEE J. Quantum Electronics, QE-18, pp. 1560-1568 (1982).

[38] Press Release, http://www.genoa.com/news/pr031302.html, Genoa Corporation, USA.

[39] Y. suzuki, T. Ito, and Y. Shibata, "Monolithically intgrated Wavelength Converter: Sagnac Interferometer Integrated with Parallel-Amplifier Structure (SIPAS) and Its Application", IEEE LEOS Newsletter, Vol.16, No.4, pp.11-12 (2002).

[40] J. Leuthold, B. Mikkelsen, R.E. Behringer, G. Raybon, C.H. Joyner, P.A. Besse, "Photonic Technology Letters", vol. 13, no. 8, pp. 860-862 (2001).

[41] Krishnan Padmanbhan and Arun N. Netravali, " Dialated networks for photonic switching", IEEE Transaction on Communications, Vol. COM-35, NO. 12, Dec. 1987, pp. 1357-1365.

[42] G.A Bogert, "$Ti : LiNbO_3$ intersecting waveguides", Electronics Letters, Dec. 1987, pp. 817-818.

[43] R.A. spanke, " Architecture for large nonblocking optical space switches", IEEE Journal of Quantum Electronics, QE-22, pp.964-967 (1986).

[44] M. Kondo, N. Takado, K. Komatsu, and Y. Ohata, "32 switch-elements integrated low-crosstalk Ti:$LiNbO_3$ optical matrix switch", Proceedings of IOOC-ECOC'85, Venice, Italy, Oct. 1985, pp 361-364.

[45] Hiroaki Harai and Naoya Wada, "Photonic Packet Forwarding in A Multi-Wavelength Label Switching Node", Communications Research Laboratory, Koganei-shi, Tokyo 184-8795, Japan, Email: harai@crl.go.jp, http://www.crl.go.jp/jt/a113/.

[46] N. Chandhok et al. "IP over optical networks: A summary of Issues", internet draft, work in progress, July 2000.

[47] Brinkman, M.J. and G.J. sonek, "Low powe response of all-optical crossbar networks in quantum well heterostructures," Applied Optics, Vol.31, No. 3, pp. 338-349 (1992).

[48] Langer, D.W., M. Chen, H. Lee, and M. Chimielowski, "Quantum well structures for intergrated opto-electronics," Proc. SPIE Digital Optical Computing II, Vol. 1215, pp. 243-251 (1990).

[49] C. Baack and G. Walf, "Photonics in future telecommunications," proc. IEEE, Vol. 81, No. 11, pp. 1624-1631 (1993).

[50] H.H. Witte, "Comparison of a novel photonic frequency based switching network with similar architechtures," IEICE Trans. Commun. Vol. E77-B, no. 2, pp. 147-154 (1994).

[51] T. Matsumoto, M. Jinni, K. kimura, and. K. Noguchi, "Studies on optical digiatal cross-connect systems for very-high-speed optical communication networks," Proc. ICC'94, New orleans, LA, pp. 1060-1065 (April 1994).

[52] K.Y. Eng, M.A. Santoro, T.K. Koch, J. Stone, and W.W. Snell, " Star-couppleer-based optical cross-connect switch experiments withntunablwe receivers," IEEE J. Selcted Areas in Comm., Vol.8, pp. 1026-1031 (Aug 1990).

[53] C.A. Brackett, "Dense wavelength dividsion multiplexing networks: principle and applications," IEEE J. Selected Areas in Comm., Vol.8, pp.948-964 (aug 1990).

[54] Y. Tada, N. Shibata, O. Ishida, K. Nosu, and H. Ishii, “Optical cross-connect confguration based on FDM technologies,” Proc. ICC’92, Chicago, June 1992, pp. 1588-1592.

[55] C. J. Smyth, “Nonblocking photonic switch networks,” *IEEE Journal on Selected Areas in Communications*, Vol.6, No.7, Aug. 1988, pp. 1052-1062.

[56] H. S. Hinton, “ A nonblocking optical interconnection network using directional couplers,” *Proceedings of IEEE Globecom’84*, Atlanta, GA, Nov. 1984, Vol.2, pp. 885-889.

[57] H. S. Hinton, “An introduction to photonic switching fabrics”, *Plenum publishing co.*, 1993, pp. 83-158.

[58] K. Padmanabhan and A. Netravali, “Dilated networks for photonic switching”, IEEE Trans. Commun., vol.COM-35, pp.1357-1365 (Dec. 1987).

[59] G.A Bogert, “Ti:$LiNbO_3$ intersecting waveguides”, *Electronics Letters,* Dec. 1987, pp. 817-818.

[60] Andrzej Jajszczyk, “A Class of directional-coupler-based photonic switching networks”, *IEEE Transactions on Communications*, Vol. 41, No. 4, April 1993, pp. 599-603.

[61] M.M.Vaez and C.-T Lea, “Strictly nonblocking directional-coupler-based switching networks under crosstalk constraint”, IEEE Trans. Communication., vol.48, no.2, pp.3160323 (Feb. 2000).

[62] T.-S. Wong and C.-T. Lea, “Crosstalk reduction through wavelength assignment in WDM photonic switching networks”, IEEE Trans. Commun., vol.49, no.7, pp.1280-1287 (July 2001).

[63] M. Mehdi Vaez and Chin-Tau Lea, “Wide-sense nonblocking Banyan-type switching systems based on directional couplers”, *IEEE Transactions on Communications*, Vol. 16, No. 7, July 1998, pp. 1327-1332.

[64] M. Kondo, N. Takado, K. Komatsu, and Y. Ohata, “32 switch-elements integrated low-crosstalk Ti:$LiNbO_3$ optical matrix switch”, *Proceedings of IOOC-ECOC’85*, Venice, Italy, Oct. 1985, pp 361-364.

[65] R.A. Spanke, “Architectures for guided-wave optical switching systems”, *IEEE Communications Magazine*, Vol. 25, No. 5, May 1987, pp. 42-28.

[66] C.-T. Lea, “Muti-log2N networks and their applications in high speed electronic and photonic switching systems,” IEEE Trans. Commun., vol.38, pp.1740-1749, Oct. 1990.

[67] J.Hui, Switching and Traffic Theory for Integrated Broadband Network. Boston, MA: Kluwer Academic,1990.

[68] V.E.Benes, Mathematical Theory of Connecting Networks and Telephone Traffic. New York: Acaddemic,1965.

[69] G.R.Goke and G.J. Lipovski, "Banyan networks for partitioning multiprocessor systems", Proc. 1st Annu. Symp. Comp. Architecture, pp.21-28 (1973).

[70] C. Clos, "A study of non-blocking switching networks", Bell System Technical Journal, vol.32, pp.406-424 (1953).

[71] D.G. Smith and M.M. Rahmnekhan, "Wide-sense non-blocking networks, and some packing algorithms," proc. 1976 int. Teletraffic conference, pp.542-1–542-4.

[72] Yuanyuan Yang and Jianchao Wang, " Wide-sense nonblocking Clos networks under packing strategy," IEEE Transactions on Computers, Vol.48, No.3, pp.256-284 (1999)

[73] X. Jiang, H. Shen, Md. Mamun-ur-R. Khandker, S. Horiguchi, "A new Scheme to Realize Crosstalk-free Permutation in Vertically Stacked Optical MINs", Photonic Network Communications, vol.5, no.1, pp.89-102, Jan.2003.

[74] X.Jiang, Md.Mamuan-ur-R. Khandker, S. Horiguchi, "Nonblocking Optical MINs under crosstalk-free permutations", 2001 IEEE Workshop on High Performance Switching and Routing, May 2001, Dallas, USA.

[75] X.Jiang, Md.Mamuan-ur-R. Khandker, S. Horiguchi, "Upperbound for Blocking Probabilities of a Clsaa of Optical MINs under Crosstalk-free Permutations", 2001 IEEE Workshop on High Performance Switching and Routing, May 2001, Dallas, USA.

[76] X.Jiang, H. Shen, Md. Mamun-ur-R. Khandker, S. Horiguchi, "Permutation in Rearrangeable Nonblocking Optical MINs with Zero First-order Switching-Element-Crosstalk", 2002 IEEE Workshop on High Performance Switching and Routing, May 2002, Kobe, Japan.

[77] H. S. Hinton, "An introduction to photonic switching fabrics", Plenum publishing co., 1993, pp. 432-435.

[78] R. A. Spanke, "Archetcture for Large Nonblocking Optical Space Switches," IEEE Journal of Quantum Electronics, Vol. QE-22, No. 6, 1986, pp. 964-967.

[79] Md.Mamuan-ur-R. Khandker, S. Horiguchi, "3x3 Wide sense Non-blocking Optical Switch for WDM Self-healing Ring Networks," International Conference on Electrical and Computer Engineering ICECE 2001, January 2001, Bangladesh.

[80] V. E. Benese et. al., "Wide-Sense Nonblocking Network made of sqaure switches," Electronics Letters, Vol. 17, No. 19, 1981, pp. 697.

[81] David M. Koppelman and A. Yavuz Oruc, 1989 Int'l Confe. on Parall. Processing, Pennsylvania State University Press, USA, 1(1989), 288-295.

[82] D. Nassimi and S. Sahni, IEEE Trans. on Computers, C-30(May 1981), 157-161.

[83] R. Boppana and C. S. Raghevandra, Proceed. of Int'l. Confe. on Parall. Processing, St. Charles, IL., 1(Aug. 1988), 196-200.

[84] Barry G. Douglas and A Yavu Oru, IEEE Trans. on Commun., 41/1(1993), 121-124.

[85] Gambini, P. et al., “Transparent optical packet switching: Network architecture and demonstrations in the KEOPS project,” IEEE Journal on Selected Areas in Communications, vol.16, no.7, pp.1245-59, 1998.

[86] Wada, N., Harai, H., Chujo, W., “Multi-hop, 40 Gbit/s variable length photonic packet routing based on multi-wavelength label switching, waveband routing and label swapping,” Optical Fiber Communication Conference and Exhibit, 2002. OFC ’02, California, USA, pp. 216- 217, (Mar 2002).

Publications

Journal Papers

[1] Md.Mamun-ur-R. Khandker, X.Jiang, S. Horiguchi and H. Shen, "Generalized Recursive Network: A New Architecture for Self-Routing Non-blocking Optical Switch Networks", Optics Communication, vol.208, no.4-6, pp.299-308,July 2002.

[2] Md.Mamun-ur-R. Khandker, X.Jiang, H. Shen and S. Horiguchi, "A New Architecture for Optical Switching Networks", Photonic Network Communications, vol.3, no.4, pp.393-400, Oct.2001.

[3] X. Jiang, H. Shen, Md. Mamun-ur-R. Khandker, S. Horiguchi, "A new Scheme to Realize Crosstalk-free Permutation in Vertically Stacked Optical MINs", Photonic Network Communications, vol.5, no.1, pp.89-102, Jan.2003.

[4] X. Jiang, H. Shen, Md. Mamun-ur-R. Khandker, S. Horiguchi, "Blocking Behavior of Crosstalk-free Optical Banyan Networks on Vertical Stacking," Accepted in IEEE/ACM Transactions on Networking for publication in December, 2003.

Refereed Conference Proceedings

[5] Md.Mamun-ur-R. Khandker, X.Jiang, S. Horiguchi and H. Shen, "Generalized Recursive Network: A New Architecture for Non-blocking Optical Multistage Interconnection Networks", 2002 IEEE Workshop on High Performance Switching and Routing, May 2002, Kobe, Japan.

[6] Md.Mamun-ur-R. Khandker, X.Jiang, S. Horiguchi and H. Shen, "A new self-routing Optical MIN", High Performance Computing Asia'2001, May 2001, Queensland, Autralia.

[7] Md.Mamun-ur-R. Khandker, S. Horiguchi, "3x3 Wide sense Non-blocking Optical Switch for WDM Self-healing Ring Networks", International Conference on Electrical and Computer Engineering ICECE 2001, January 2001, Bangladesh.

[8] X.Jiang, Md.Mamun-ur-R. Khandker, S. Horiguchi, "Nonblocking Optical MINs under crosstalk-free permutations", 2001 IEEE Workshop on High Performance Switching and Routing, May 2001, Dallas, USA.

[9] X.Jiang, Md.Mamun-ur-R. Khandker, S. Horiguchi, "Upperbound for Blocking Probabilities of a Clsaa of Optical MINs under Crosstalk-free Permutations", 2001 IEEE Workshop on High Performance Switching and Routing, May 2001, Dallas, USA.

[10] X.Jiang, H. Shen, Md. Mamun-ur-R. Khandker, S. Horiguchi, "Permutation in Rearrangeable Nonblocking Optical MINs with Zero First-order Switching-Element-Crosstalk", 2002 IEEE Workshop on High Performance Switching and Routing, May 2002, Kobe, Japan.

Non-refereed Conference Proceedings

[11] Md.Mamun-ur-R. Khandker, X.Jiang, S. Horiguchi, "New Nonblocking Optical Switch Networks", Proc. of the 1st Workshop on International Joint Research: parallel computing, data mining and optical networks, March 7, 2001, JAIST, Japan.

[12] X.Jiang, Md. Mamun-ur-R. Khandker, S. Horiguchi, "Blocking behavior of a Class of Optical Multistage Interconnection Networks under Crosstalk-free Constraint", Proc. of the 1st Workshop on International Joint Research: parallel computing, data mining and optical networks, March 7, 2001, JAIST, Japan.